SOLAR POWER SATELLITE

SYSTEM DEFINITION STUDY

Solid State SPS Analysis

Boeing Aerospace Company
P. O. Box 3999
Seattle, Wash. 98124

Contract
NAS9-15636

June, 1980
D180-25969-4

FINAL REPORT FOR PHASE III, DECEMBER 1979—MAY 1980

VOLUME 4

Prepared for

LYNDON B. JOHNSON SPACE CENTER
HOUSTON, TEXAS 77098

1. Report No.	2. Government Accession No.	3. Recipient's Catalog No.
4. Title and Subtitle SOLAR POWER SATELLITE SYSTEM DEFINITION STUDY, PHASE III, FINAL REPORT VOL. 4 - SOLID STATE SPS ANALYSIS		**5. Report Date** June 1980
		6. Performing Organization Code
7. Author(s)		**8. Performing Organization Report No.** D180-25969-4
		10. Work Unit No.
9. Performing Organization Name and Address Boeing Aerospace Company P. O. Box 3999 Seattle, Washington 98124		
		11. Contract or Grant No. NAS9-16536
		13. Type of Report and Period Covered Final Report, Dec. '79 - May 1980
12. Sponsoring Agency Name and Address National Aeronautics and Space Administration Lyndon B. Johnson Space Center Houston, Texas 77058 (Harold Benson, Technical Monitor)		
		14. Sponsoring Agency Code

15. Supplementary Notes

16. Abstract

This document contains the analysis of the solid state solar power satellite option that was analyzed in the Phase III Solar Power Satellite System Definition Study.

17. Key Words (Suggested by Author(s)) SOLAR POWER SATELLITE (SPS) SPACE POWER SYSTEM SOLID STATE SPS	**18. Distribution Statement**		
19. Security Classif. (of this report) UNCLASSIFIED	**20. Security Classif. (of this page)** U	**21. No. of Pages**	**22. Price**

JSC Form 1424 (Rev Nov 75)

NASA JSC

FOREWORD

The SPS System Definition Study was initiated in June of 1978. Phase I of this effort was completed in December of 1978 and was reported in seven volumes (Boeing document number D180-25037-1 through -7). Phase II of this study was completed in December of 1979 and was completed in five volumes (Boeing document number D180-25461-1 through -5). The Phase III of this study was initiated in January of 1980 and is concluded with this set of study results published in five volumes (Boeing document number D180-25969-1 through -5):

    Volume 1 - Executive Summary
    Volume 2 - Final Briefing
    Volume 3 - Laser SPS Analysis
    Volume 4 - Solid State SPS Analysis
    Volume 5 - Space Transportation Analysis

These studies are a part of an overall SPS evaluation effort sponsored by the U. S. Department of Energy (DOE) and the National Aeronautics and Space Administration (NASA).

This series of contractual studies were performed by the Large Space Systems Group of the Boeing Aerospace Company (Gordon Woodcock, Study Manager). The study was managed by the Lynden B. Johnson Space Center. The Contracting Officer is David Bruce. The Contracting Officer's Representative and the study technical manager is Tony Redding.

The subcontractors on this study were the Grumman Aerospace Company (Ron McCaffrey, Study Manager) and Math Sciences Northwest (Dr. Robert Taussig, Study Manager).

TABLE OF CONTENTS

LIST OF ABBREVIATIONS AND ACRONYMNS

Units of Measurement

micron	-	1/1000 millimeter
mil	-	1/1000 inch
ps	-	picoseconds (10^{-12} seconds)
MT	-	metric tons
KT	-	kilotonnes (metric)
M	-	millions of dollars
B	-	billions of dollars

Descriptors

SPS	-	Solar Power Satellite
MPTS	-	Microwave Power Transmission System
FET	-	Field Effect Transistor
GaAs FET	-	Gallium Arsenide Field Effect Transistor
CW	-	Continuous Wave
DC	-	Direct Current
AC	-	Alternating Current
RF	-	Radio Frequency
EBS	-	Electron Bombarded Semiconductors
IMPATT	-	Impact Avalanche Transit Time
BARITT	-	Barrier Ionization Transit Time
TRAPATT	-	Trapped Plasma Avlanche Transit Time
E-Beam	-	Electron Beam
IC	-	Integrated Circuit
I^2R	-	(Electrical Current)^2 x (Resistance)
CL	-	Center of (Lift) Force
CG	-	Center of Gravity
MTBF	-	Mean Time Before Failure

Materials

Al	-	Aluminum
Al_2O_3	-	Alumina
BeO	-	Beryllium Oxide
Cu	-	Copper
GaAs	-	Gallium Arsenide
InP	-	Indium Phosphide
Si	-	Silicon

SOLID STATE TRANSMITTER FOR SOLAR POWER SATELLITE
SYSTEMS ANALYSIS AND SYSTEM DESCRIPTION

1.0 BACKGROUND

1.1 Introduction

Solid state SPS transmitters and satellites were investigated by the SPS Systems Studies beginning in 1978. The reasoning behind the investigation was that solid state systems excel in low failure rates and may be competitive in power output per unit cost. The early analyses were generally parametric in nature, and indicated that solid state transmitters could be attractive for SPS's in the 2500 megawatt class if certain problems could be solved.

There are three main problems that must be solved to make solid state transmitters practical for SPS use. The first is the low voltage of the solid state devices themselves. Early investigations eliminated the few hybrid kinds of devices that can operate at relatively high voltage from consideration because of efficiency limits, and converged on Gallium Arsenide FET's (GaAsFETS) as the most promising devices, because they hold promise of reaching higher efficiencies at SPS frequencies than other devices for which appreciable practical experience exists. GaAsFETS operate at roughly 15 volts, with efficiencies (dc to rf) of 72% demonstrated in the laboratory. (The parametric studies used estimates for conversion efficiency of 80% as reasonable extrapolations of present experience.) The distribution of dc electric power on the SPS must be done at several kilovolts to avoid excessive conductor mass and high resistive losses in the power conductors.

The second problem is the temperature limitations of solid state devices. Operating temperatures allowable for GaAsFET's consistent with long life are limited to 125 degrees C or less, limiting the waste heat rejection power/area of the transmitting antenna to approximately $1.5 \, \text{kw m}^{-2}$. By comparison, the reference (Klystron) system rejects $5.5 \, \text{kw m}^{-2}$ of heat at over 300 degrees C. As a result, with a conventional 10-step 9.54 db Gaussian taper solid state systems are limited to power levels in the 2500 megawatt range. Also, careful attention must be given to the thermal paths in the detail design of power transmitting elements in order to minimize the temperature drop from devices to heat rejection surfaces so as to maximize the effective heat rejection surface temperature.

The third problem is the low power of the solid state amplifiers. Although 15 watt GaAsFET's have been made[1] RCA has estimated that for efficient devices the output per device will be on the order of five watts. The power is limited by the very small dimension of the active area in the GaAsFET chip. Even in 5-watt devices, large numbers of channels are operated in parallel. The power level per antenna element (i.e., dipole) required on a 2.5 gigawatt SPS is greater—ten to twenty watts. Thus combining of outputs of individual amplifiers in antenna elements is likely to be required. Conventional combining schemes incur additional losses on the order of 10%. A lossless combiner is an important need.

---

[1] Fukuta, Takashi, Suzuki and Suyama, "4 GHz 15 W Power GaAs MESFET," IEEE Trans. Electron Devices ED-25, HG, June 1978, pp. 559-563.

Design and technology work conducted during Phase II of the present study developed an approach to solving these problems. An antenna element design was developed that could combine amplifier outputs with low loss, provide good thermal paths, radiate heat from both faces of the transmitter and be compatible with series-parallel connection of the dc power supplies of the amplifiers that allowed the antenna subarrays to be fed at +/- 2 kV for an effective power distribution voltage of 4 kV. Analysis of a satellite employing these antenna elements showed promise but identified two significant problems. First, the power distribution voltage resulted in losses of roughly 30% even when mass optimized. Secondly, some difficulties were identified with the means of integrating phase feed networks and power supplies.

1.2 Problem Statement

The present study phase included a task to resolve those issues exposed by prior work. Principal attention was to be directed to design details of the transmitter, with secondary emphasis on defining the operational aspects of the solid state system including its construction in space and any differences in transportation operations. The technology program conducted on the antenna element itself led to several design modifications that needed to be reflected in the SPS definition.

1.3 Configuration Overview

The configuration that evolved from Phase III of this study is shown on Figure 1.3-1. It uses the same solar array blanket and bay size as a reference SPS with a pentahedral (instead of hexahedral) bay structure and has a 1.42 km diameter transmitting array with a 10-step 9.54 db quantized Gaussian taper. The transmitting array is connected to the main satellite via one rotary joint and 6 actively controlled linear actuators with large flex cables that conduct power at 8.64 kV. Because of the lower dc-rf efficiency of the solid state amplifiers, 9 solar array bays instead of the 8 of half a reference SPS are required.

The quantization hierarchy for the transmitting antenna is shown on Figures 1.3-2 and 1.3-3. The 10 steps of the transmitting array taper are synthesized from 10.73 m subarrays which each consist of 324 panels. The panels are made of 64 cavity combiner radiator modules or 48 dipole radiator modules, depending on whether they are located on a subarray on the inner or outer set of rings. Table 1.3-1 explains the number types and characteristics of the modules at each taper step.

Differences between this configuration and that at the end of Phase II are that the power bussing is done at 8.64 kV instead of 5.5 kV on a completely redesigned power bussing network. This cuts conductor I^2R and solar array mismatch losses significantly, weighs less and allows the use of a solar array that is 9 bays instead of 11 bays long. Also the solid state power modules were redesigned to provide grounded cover sheets at some mass penalty. Finally, the construction base required for assembly of 10 Gw SPS grid power per year was defined by Grumman under subcontract.
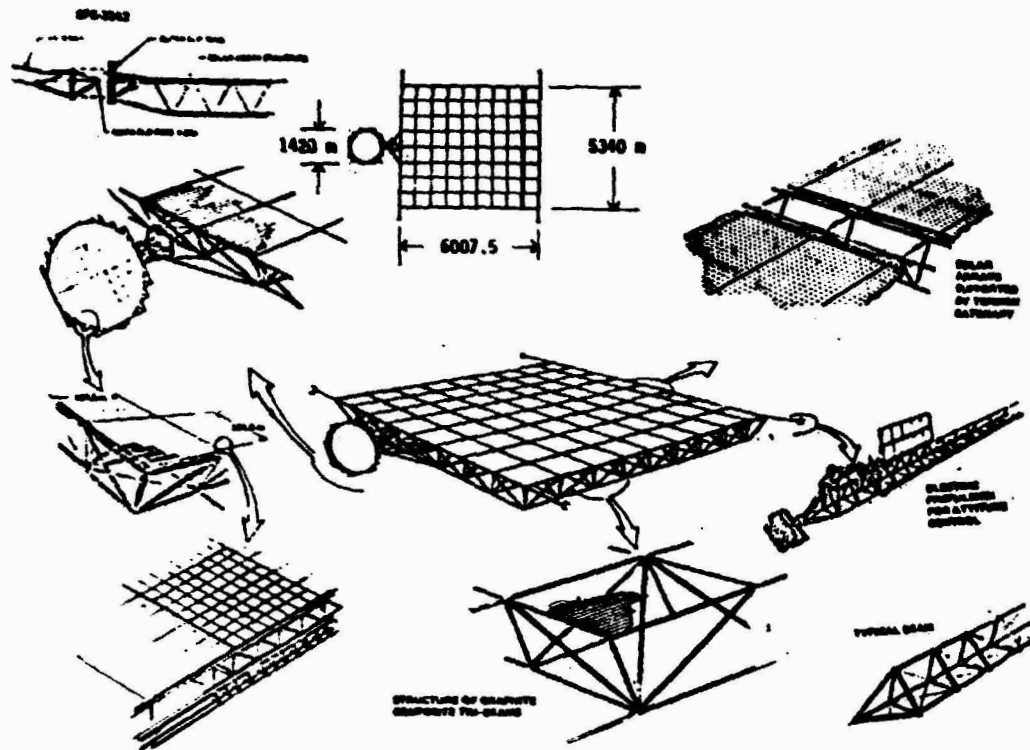
ORIGINAL PAGE IS
OF POOR QUALITY

1420 m
5340 m
6007.5

Figure 1.3-1. 2.5 GW Solid State SPS Configuration

TRANSMITTING ANTENNA
CENTRAL RING SUBARRAY
PANEL
CAVITY MODULE
(18 PANELS)²
(4.8 λ)²
(.6 λ)²
1
2
3
10
(4.8 λ)²
(.6 λ) x (.8 λ)
1.42 KM
DIAMETER
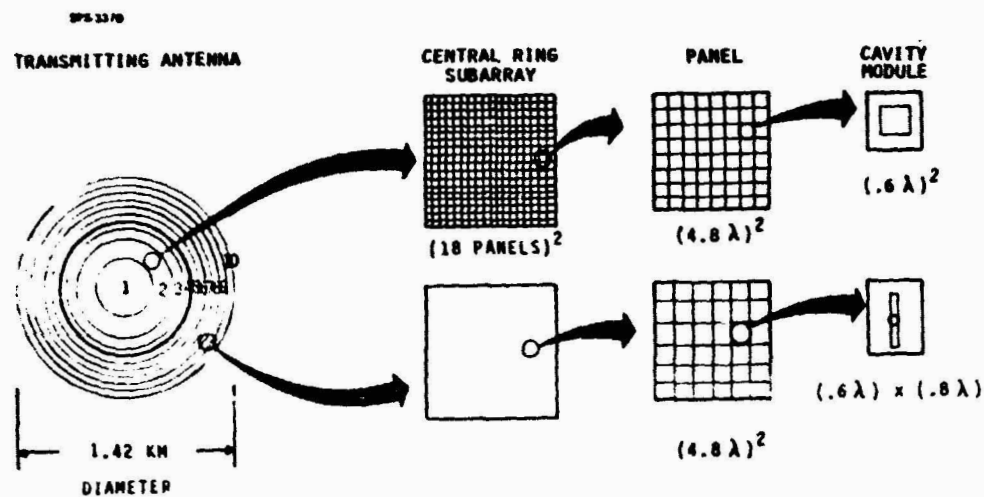
Figure 1.3-2. Solid State Transmitting Antenna Quantization Hierarchy

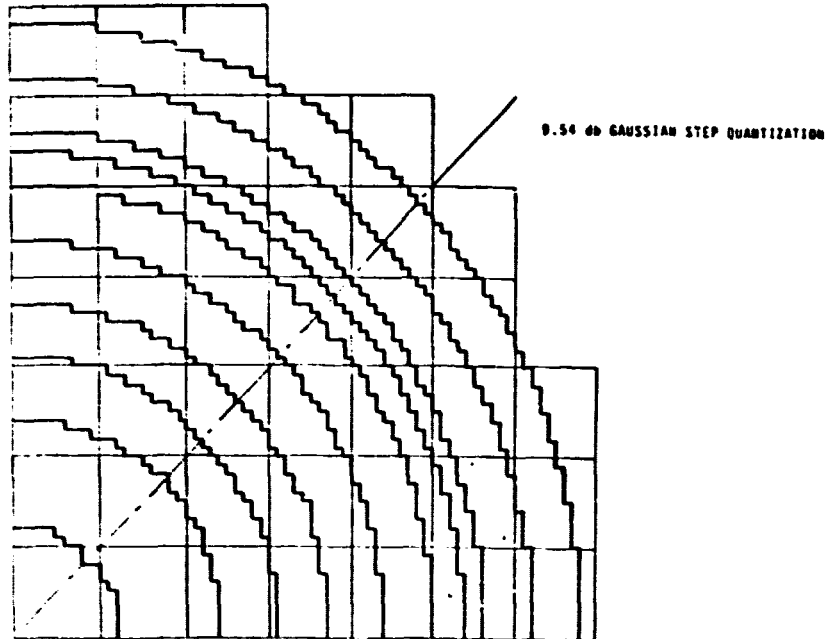SPS-3288

□ 18.43 m x 18.43 m

9.54 db GAUSSIAN STEP QUANTIZATION

Figure 1.3-3. 2.5 GW Solid State SPS Transmitting Antenna

Table 1.3-1 Solid State Transmitting Antenna Quantization

STEP	NUMBER OF SUBARRAYS	MODULE TYPE	MODULE POWER (W)	$(P/A)_{RF}$ (kWm^{-2})	RADIATED STEP POWER (MW)	STEP MASS (T)
1	472	High Power 4-FET, Cavity Radiator (6.73 kgm^{-2})	28.7	5.50	282.4	345.6
2	1392	"	24.0	4.45	673.9	1019.1
3	1208	Reduced Power 4-FET Cavity Radiator (6.46 kgm^{-2})	19.2	3.56	467.8	848.9
4	1296	"	16.0	2.97	418.7	910.8
5	1764	2-FET Cavity Radiator (5.50 kgm^{-2})	12.8	2.37	455	1055.4
6	1860	2-FET Dipole (2.69 kgm^{-2})	12.8	1.78	360.2	544.3
7	1136	"	9.6	1.33	164.4	332.4
8	840	"	8.5	1.18	107.8	245.8
9	2208	1-FET Dipole (2.06 kgm^{-2})	6.4	.89	213.8	646.1
10	2476	"	4.3	.59	158.9	724.6
TOTALS	14652					6673.0

4

2.0 SOLID STATE MICROWAVE POWER TRANSMISSION SYSTEMS

2.1 Solid State Microwave Power Amplifier Technology

Currently a wide variety of solid state devices suitable for use as microwave amplifiers exist. These include bipolar and field effect transistors, many types of two-terminal devices (tunnel, Gunn, IMPATT, BARITT and TRAPATT diodes) and electron bombarded semiconductors (EBS). (EBS have been included as being solid state since the electron beam only supplies a small control current, with the bulk of the supply current staying in the semiconductor.) For those active devices with over two terminals, there are several classes of circuit configurations that the active devices may be used in. Finally, there is a growing number of commonly used solid state materials out of which components may be fabricated, using several types of process at each step of the fabrication.

State of the art power-added efficiency, gain and single device power as a function of frequency for various types of CW microwave output solid state devices are shown on Figures 2.1-1 through 2.1-3. As technology evolves the curves will move towards the upper right-hand corners of the graphs.

Given the results of Figure 2.1-1, it would appear that there is no hope of achieving efficient solid state DC-microwave conversion in the near future. All the two terminal devices have efficiencies less than .36, which is so low as to make their use for SPS impractical. Most of the three terminal devices are not much better. However, in the case of three-terminal devices, the classes of amplifiers presently used (Classes A and B for GaAs FETs and Class C for bipolar transistor amplifiers) inherently limit their efficiency. Other classes of amplifiers, summarized on Figure 2.1-4, can have efficiencies approaching unity.

In fact, to achieve the desired efficiencies of .8 or greater requires that the devices be used in "switched mode" types of amplifiers, which attain high efficiency by minimizing the I-V product time integral over the operating cycle. This generally require device switching times about a factor of ten less than the RF period. Experimental amplifiers with efficiencies of over 90% have been built at frequencies above 100 MHz. NASA-sponsored microwave amplifier studies have recently been initiated to determine the feasibility of high efficiency at microwave frequencies and have achieved efficiencies of .72 at 2.45 GHz.

Because of the many high frequency components in the waveforms characteristics of fast switches, efficient switching amplification devices must have large bandwidths. This leads to different device noise properties than those at the narrowband SPS reference system klystron tubes. While the switching amplifiers do have frequency selective output circuits that transform the switched waveform into a sine wave, these will not be nearly as selective as a 5-cavity klystron. However, the solid state design will benefit due to its small module size giving a larger ground footprint for noise and harmonics than that of the larger klystron module.

Achieved device gains vs frequency are shown on Figure 2.1-2. There is a striking difference between small-signal and power gain for FETs. At the SPS frequency of 2.5 GHz bipolars have about 8 db gain while GaAs FETs yield around 10 db. In general, GaAs FETs have several db more gain than bipolars throughout the spectrum. As for the other devices, IMPATTs can have gains of over 20 db and electron beam semiconductors are projected to yield about 20 db. The low gain of Static Induction Transistors (SITs) at 1 GHz eliminates them from consideration at present, although they appear to have great potential for further development due to their high power bandwidth product.
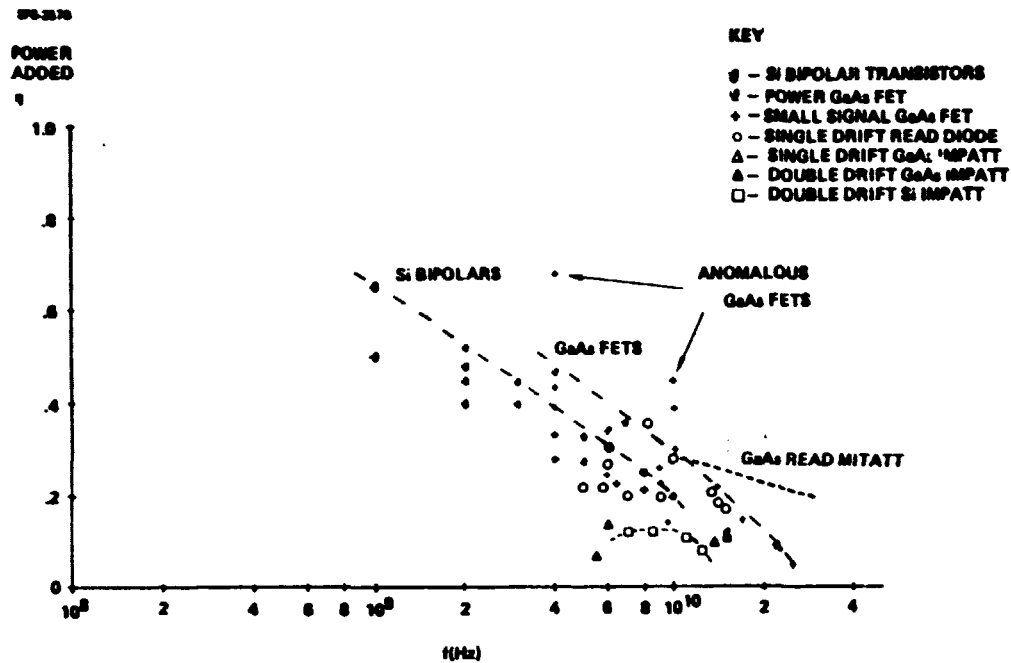
5

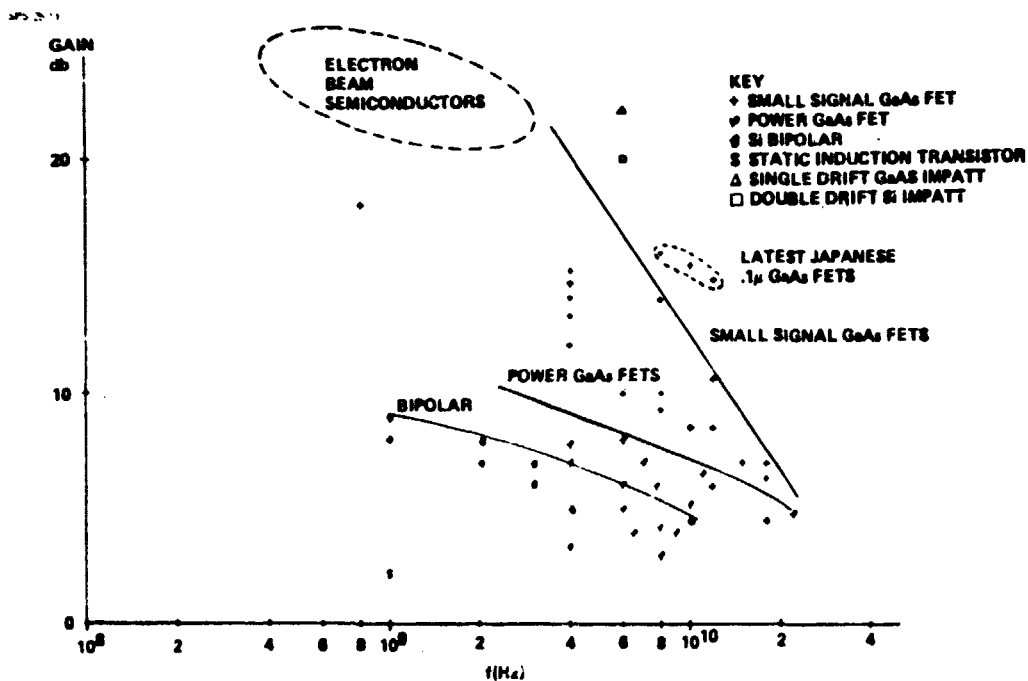Figure 2.1-1. CW Solid State Device Efficiency vs Frequency—1978

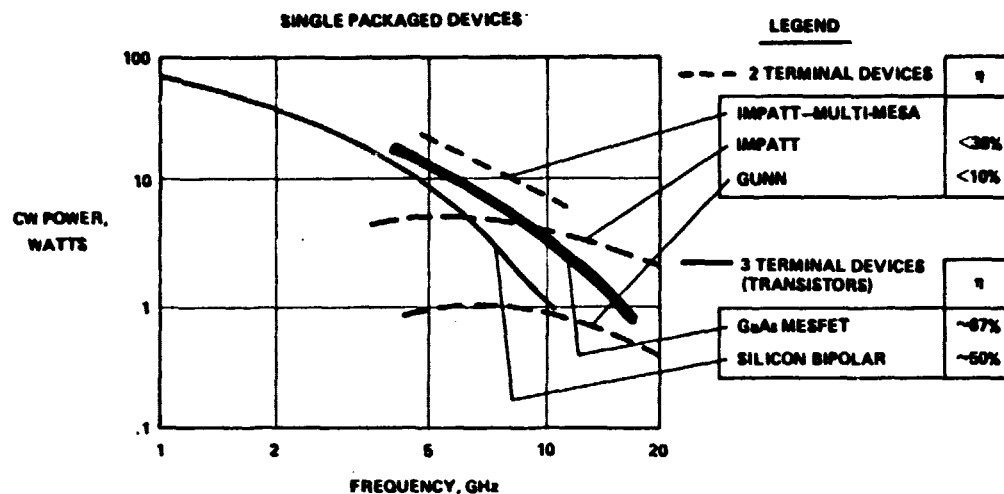Figure 2.1-2. Solid State Device Gain vs Frequency—1978

6

Figure 2.1-3. Solid State CW Power vs Frequency—1978

	Amplifier Class	Maximum Power-added Efficiency for Sine Wave Output	Typical Efficiency Values Achieved	@ Frequency	Duty Cycle at Maximum Efficiency	Active Device Saturated ?	Active Device Cut Off ?
	A	.5	.3	@ 4 GHz	1.0	No	No
	B	.785	.5	@ 4 GHz	.5	No	Yes
	C (Unsaturated)	.896	.6	@ 2.5 GHz	.3	No	Yes
Switched Mode Amplifiers	D	1.0	.9	@ 10 MHz	.5	Yes	Yes
	E	1.0	.9	@100 MHz	.5	Yes	Yes
	F	1.0	.9	@ 10 MHz	.5	Yes	Yes
	S	1.0	.8	@ 100 KHz	Variable ≫ :	Yes	Yes
	Multivoltage	1.0	.8	@ 10 MHz	Variable	Yes	Yes
	G	.818	.7	@ 100 KHz	Variable	Yes	Yes

Figure 2.1-4. Characteristics of Various Amplifier Classes

The power per device is an important SPS parameter since the number of devices which can be efficiently combined in a module is limited by circuit losses and the power per module determines the RF power density per unit transmitting array area. The single device power chart (Figure 2.1-3) shows that silicon bipolar transistors, GaAs FETs and multi-mesa IMPATTs can all handle powers above 10 watts, which is an adequate power level for SPS application. Of the devices considered here, only E-beam semiconductor devices are capable of generating a power level of 100 watts per device which would be adequate for one device per radiating element. For the other devices, power combining will be necessary.

The fundamental failure modes in semiconductor devices are wearout failure modes that tend to be concentrated at surfaces, both internal and exposed, and are generally electrochemical in origin. In the case of the internal surfaces, transport of species to and away from interfaces eventually degrades contacts. In the case of external surfaces, impurities can come in from outside to form compounds and high electric fields can cause breakdown.

EBS cathodes presently have an expected mean lifetime of 2×10^5 hours, over an order of magnitude less than that required for a 30-year satellite, so they appear unsuitable. The two remaining solid state amplifier candidates are GaAs FETs and Si bipolar transistors. Si bipolar lifetimes are limited by electromigration of emitter finger metallizations due to localized high current densities. This gives relatively sudden and complete hard (open or short circuit) failures, whereas GaAs FETs seem to suffer from contact degradation which decreases performance gradually.

Of the three terminal devices, GaAs Field Effect Transistors (FETs) and silicon bipolar transistors provide approximately equal power capability at 2.45 GHz and appear potentially feasible for SPS use. GaAs FETs were selected as the preferred DC-RF conversion devices because they have higher gain than silicon bipolars, higher power added efficiencies, roughly equal power capabilities at 2.5 GHz and lower device metallization current densities leading to better expected reliabilities. However, progress on silicon microwave bipolars is still continuing to advance and they should be viewed as a viable alternative to GaAs FETs.

GaAs FETs for SPS application could be fabricated separately and mounted in hybrid fashion or combined with other components on larger GaAs chips in integrated circuits. The latter alternative is preferred because of its significantly lower costs in mass production, although it does entail somewhat more development. For conservatism and in consideration of the fact that efficient "switched mode" amplifiers require gain at frequencies higher than the fundamental, the maximum single device powers in the solid state baseline design satellite were chosen to be 7.5 watts. For devices like this, a reasonable operating voltage is 15 volts.

A small signal GaAs FET lifetime versus temperature curve is shown on Figure 2.1-5. There is currently no lifetime data on power GaAs FETs in the literature. When it appears, it is likely to be somewhat worse than Figure 2.1-5, but Figure 2.1-5 probably represents lifetimes achievable with development of the relatively new GaAs FET technology. It should be noted that solid state devices fail with log-normal statistics, not the exponential failure rates commonly used as a conservative engineering approximation.

At times less than the mean time to failure the log normal failure rates have significantly less failure than the exponential failure curve. However, even in this case for the SPS failure criterion of loss of 2% the transmitting array with no maintenance, the mean time to failure required for the device is about a factor of ten more than the SPS life. Thus the average junction temperature for SPS GaAs FETs should be no higher than 140°C.

8

Figure 2.1-6 shows current and projected GaAs FET costs with an estimated 70% production rate improvement curve (i.e., units produced at the rate of 2n per year cost 70% as much as units produced at the rate of n per year). For the anticipated projected rates, the cost per unit power for GaAs FETs are nearly the same as the projected cost per unit power for klystrons. In practice, integrated circuits with several stages of driver amplifiers and other circuitry will be incorporated with the power amplifier. Since production costs are roughly equivalent to chip size and the output FET is anticipated to use approximately 70% of the total semiconductor area, the above cost estimates are adequate to first order.

2.2 Solid State Power Combining Modules

The previous Boeing solid state MPTS concept is described in Boeing document D180-25461-5. Here, the central unit of DC-RF power conversion is the power-combining module/antenna which combines the output of four solid state amplifiers to coherently drive two radiating slots. This module represents a dc load of about 30 W at 15 V.

The fundamental grouping of modules in the central 5 rings of the transmitting antenna is a square array of 64 modules, shown in Figure 2.2-1. These are dc connected as eight parallel strings of eight modules, connected in series to drop 120 V. Three hundred twenty-four panels are arranged in turn into a square subarray with a design operating voltage of 2160 volts. Previously each subarray had a complement on the other side of ground so that the dc power transmission was accomplished at 4320 V. For the present design the base output voltage has been doubled to 8640 V, necessitating quad series subarrays.

The reference phase distribution to the panel consists of a network, shown in Figure 2, which splits the incoming reference phase signal into 64 equal length arms which feed the modules. The relationship between this network and the panel can be appreciated by overlaying Figure 2.2-1 with Figure 2.2-2.

The concept of the power combining module has been fundamentally validated by Fitzsimmons[2]. In this work, two slots were driven by one amplifier at each end. The coupling of each amplifier to the slot was accomplished by the stripline feed shown in Figure 2.2-3. The two slots were electromagnetically coupled through a backing can, as shown in Figure 2.2-4. When driven by four solid state amplifiers this module exhibited an increase in gain over its passive gain of within 0.1 db of the measured amplifier gain.

Although a successful scheme for rf power combination, the Fitzsimmons module as tested is not ideally suited to the series stacking of modules implicit in the Boeing concept. The fundamental shortcoming lies in the fact that the stripline slot feed of the present design utilizes the module face as stripline ground (see Figures 2.2-5). Unfortunately, electrostatic considerations dictate that the module face must sit at satellite ground. This leads to a problem in coupling the local amplifier rf ground to the satellite (stripline) ground.

A potential means of coupling the satellite and local grounds would be through the capacitance between the bottom of the power amplifier and the aluminum baseplate. Due to the combined constraints of dc standoff and thermal conductivity, the dielectric configuration of this capacitor would be such that a capacitive reactance of tens of ohms would be incurred at 2.45 GHz. Consequently this solution is deemed unattractive. A similar problem would arise at the amplifier input where the local amplifier rf ground must be coupled to the phase distribution system if the phase distribution network is at satellite ground.

---

[2]G. Fitzsimmons, SPS Solid State Antenna Power Combiner, Final Report under Contract NAS9-15636A (1980).   9
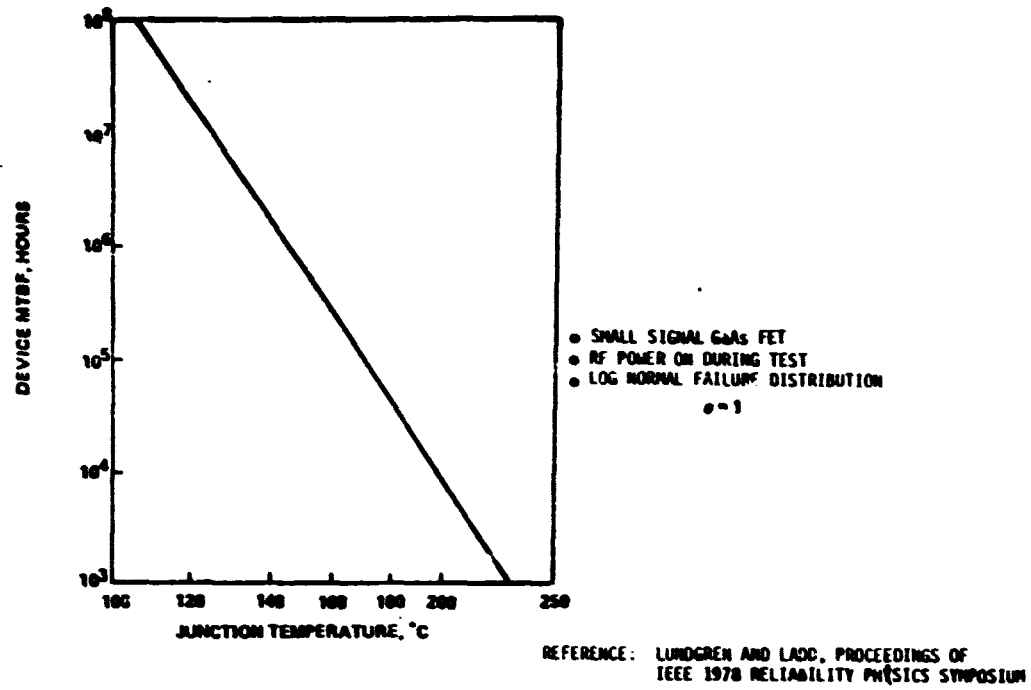
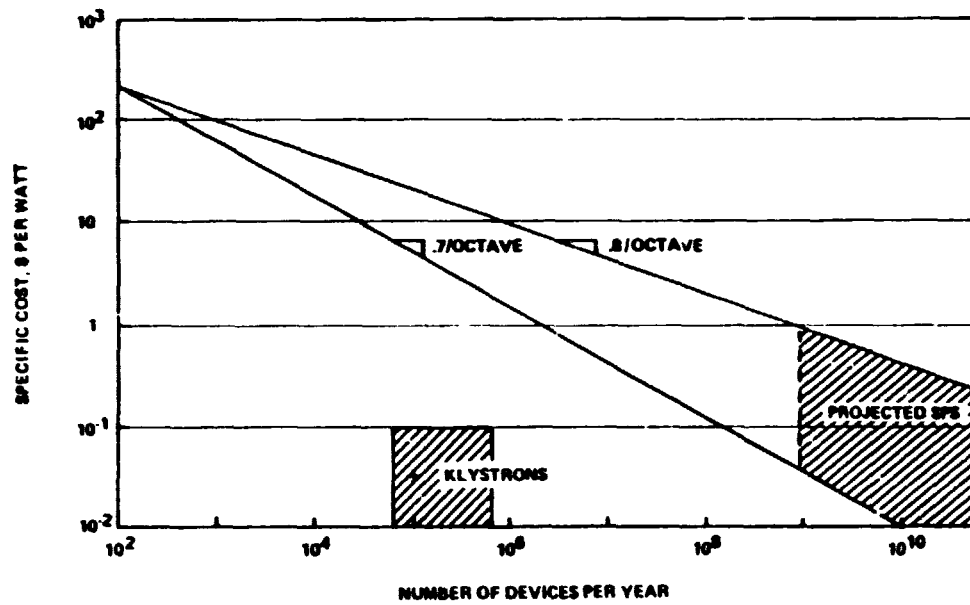Figure 2.1-5. Small Signal GaAs FET Lifetime vs Junction Temperature

Figure 2.1-6. Projected GaAs FET Costs
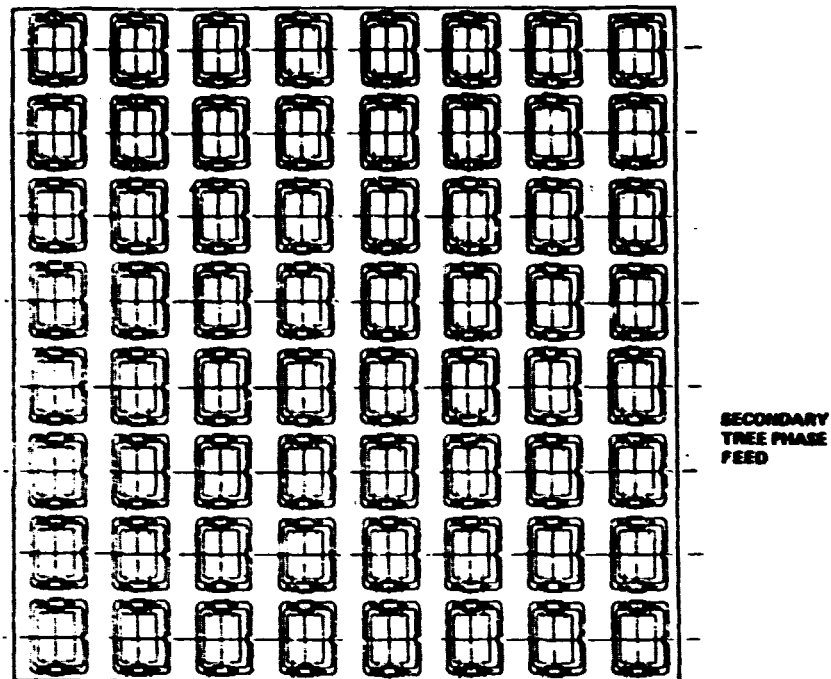
Figure 2.2-1. 64-Module Panel Layout

SECONDARY
TREE PHASE
FEED

PRIMARY
TREE PHASE
FEED

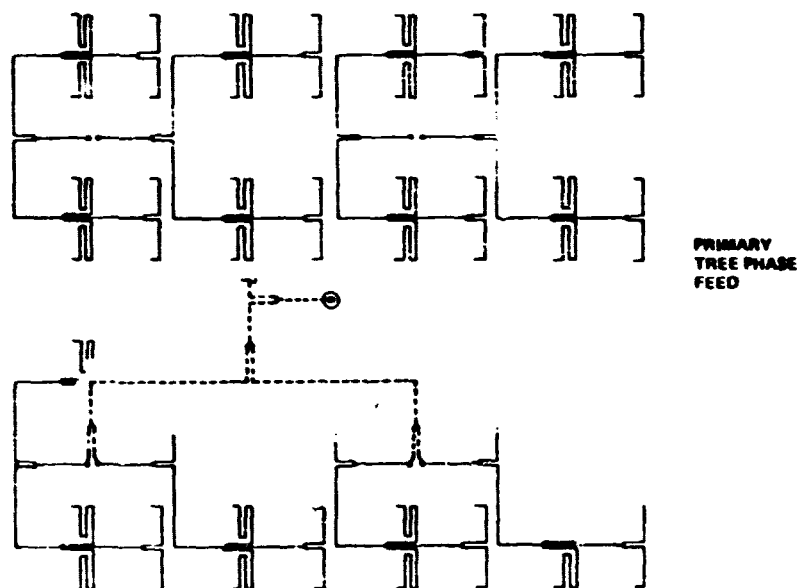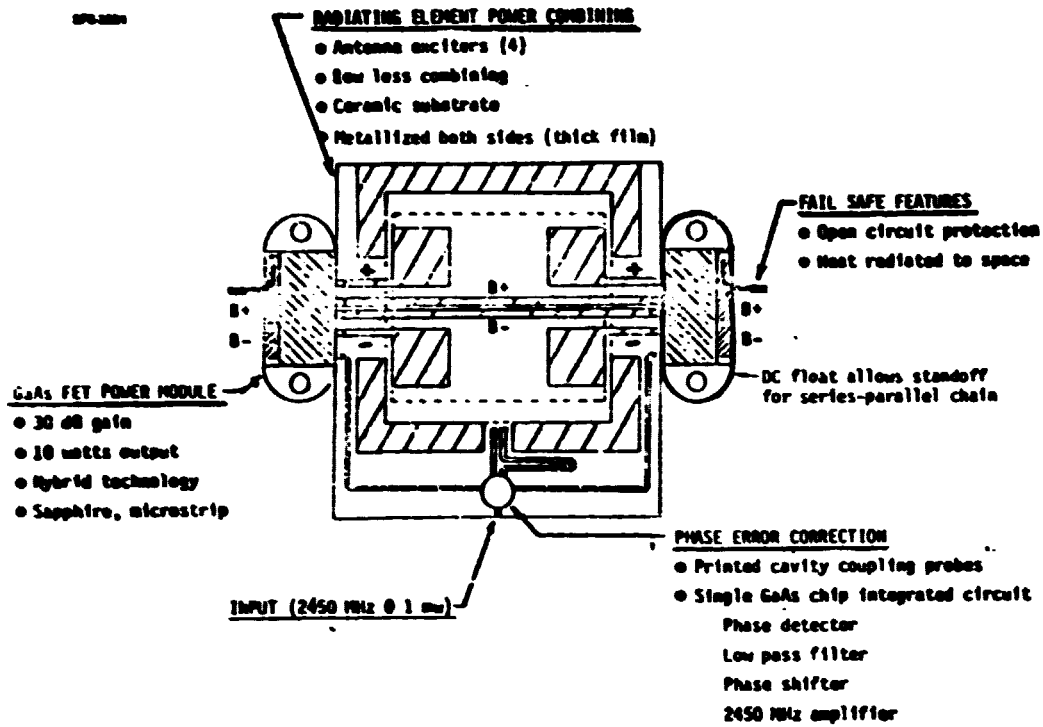*Figure 2.2-2. Antenna Panel Reference Phase Distribution Network*

Figure 2.2-3. Solid-State Power Module Concept (20 Watts)

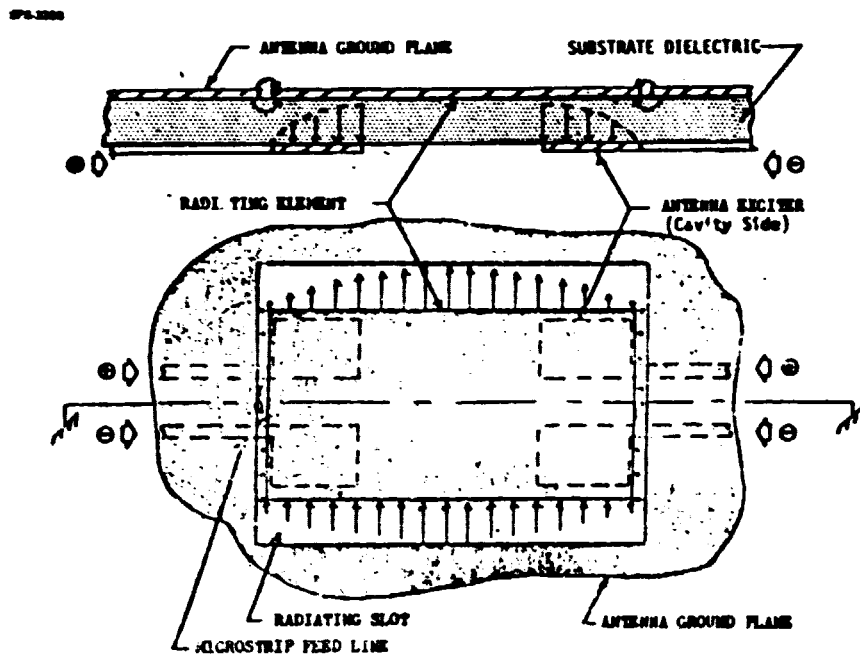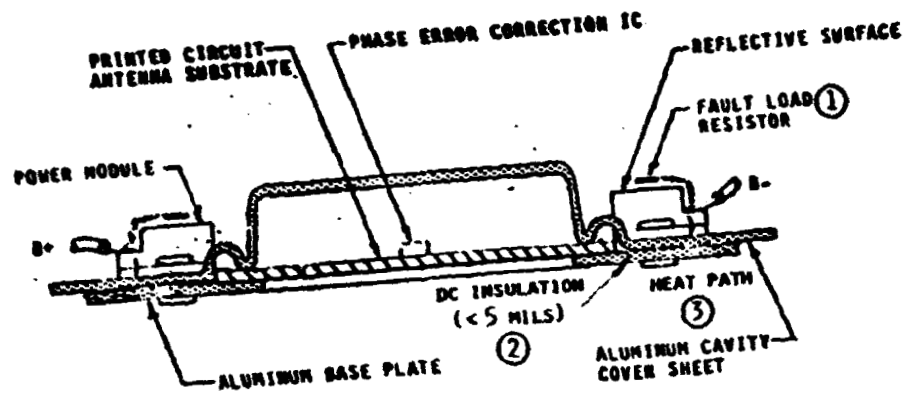*Figure 2.2-4. Four Feed Power Combining Microstrip Antenna*

Figure 2.2-5. Solid-State Power Module Cross Section

The present exercise is intended to refine the existing design. As such, the resulting design has been somewhat constrained, and may not represent the best overall approach. Nevertheless, it is felt that the design proposed here does solve the most serious problem of the existing concept, that of adequate rf coupling and dc isolation, as well as offering other advantages to be enumerated.

The panel proposed here is depicted in Figures 2.2-6 and 2.2-7. Its major elements may be identified as: 1) the face sheet, 2) the power modules, 3) the back sheet, 4) the stripline phase feed network, 5) the fault load resistors, 6) the dc wiring, and 7) the top sheet. A description of the system, through descriptions of these components, follows.

The entire panel is constructed upon the face sheet which is stamped to provide its shape and to punch out the radiating slots. As presently conceived this sheet would consist of 20 mil aluminum but 10 mil stock may be allowable. In either case this sheet would be bonded to the back sheet. In this process, it may be desirable to mask off the area on which the substrate is to be mounted.

The power amplifier module is based upon a dielectric substrate on which are deposited two integrated power amplifiers, and their phase sampling and comparison circuitry. Coupling loops are provided for rf input and output. The input inductive coupling occurs between the overlap of the amplifier module input coupling loop, and the phase distribution coupling loop shown in Figure 2.2-8. The output coupling is also accomplished inductively by the output coupling loops, which induce currents in the periphery of the slot.

The substrate also acts as a dielectric load for the radiating slots, and as a spreader and transmitter of power amplifier waste heat. The suggested substrate material is BeO, due to its adequate dielectric and excellent thermal properties. It is anticipated that a 40 mil thickness of this material will standoff 10 kV dc with a temperature drop of less than 1°C at the anticipated heat loads.

The power amplifier section of the power module would be potted for protection and for dc isolation. The potting material would also serve as mechanical support for the dc terminals, which would be of the crimp variety.

The back sheet consists primarily of the combiner module shield cans. Like the face sheet, it is stamped out of 10-20 mil aluminum. It is relieved to fit around and over the power-module dielectric slots. It is plated and tinned on the front side where it contacts the face sheet so that the two can be soldered together. The solder joint provides the requisite rf communication between the face sheet and the shield can portion of the back sheet.

The reference phase distribution architecture is essentially that of D180-25461-5, but the feed network shown in Figure 2.2-2 is rotated by 90° with respect to the panel from its original orientation. Also, each module is fed at two points instead of one as before. As presently conceived, this network will take the form of a stripline. Because the coupling to the modules is inductive and requires no direct connection, the stripline could be glued into place. To prevent charge buildup, a conducting adhesive should be used on runs remote to the coupling regions.

The dc power wiring utilizes #16 Cu wire, crimped to posts in the module top.

The entire assembly is stiffened by the top sheet which is adhesively bonded to the backs of the shield cans. The intended top sheet is 10-20 mil Al. It may be cut away over the majority of the shield can to minimize weight.

FAULT LOAD RESISTORS

CAVITY COVERS

PHASE DISTRIBUTION STRIPLINE

INSULATORS

DC POWER FEEDERS

POWER AMPLIFIERS &
RADIATOR COUPLERS

RADIATOR FACE
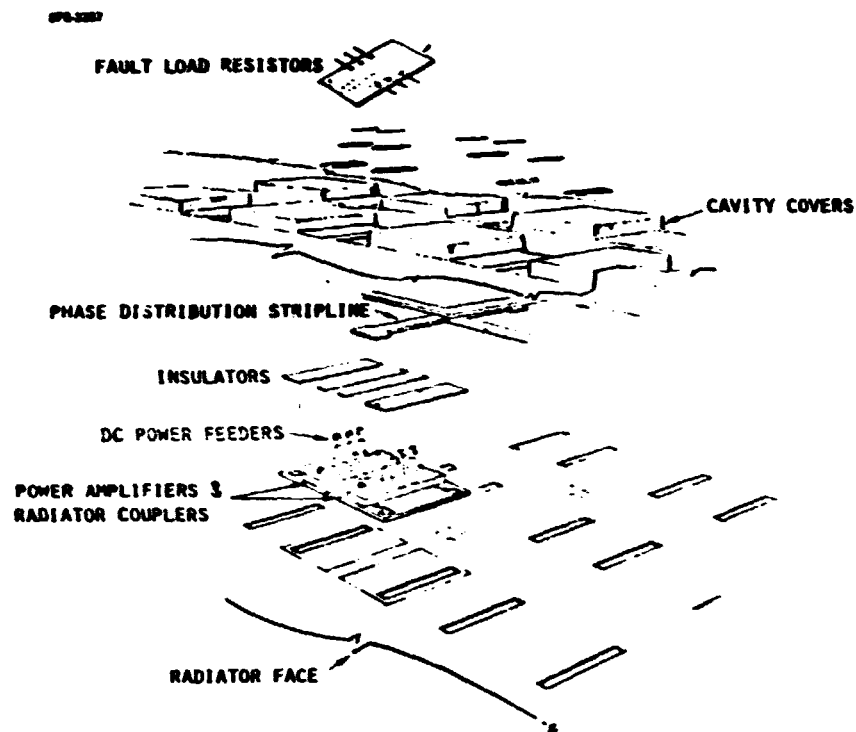
Figure 2.2-6. Revised Solid State Cavity Radiator Module - Exploded View

CERAMIC COATED .020 AL.

.050 RIVET
TERMINAL PIGTAIL

SHOWN AS
CRIMPED

SKETCH NOT TO SCALE

CERAMIC COATED AL. (.020)

TYPICAL SLOT TERMINAL,
BEFORE BENDING

0   1"

Figure 2.2-7. Solid-State Module Cross-Section with Fault Resistor Detail

15

Figure 2.2-8. Bottom View of Phase Distribution Network Coupling Loops

The fault load resistors (4 per module) are printed on their own thermal radiator, as shown on Figures 2.2-9 and 2.2-10. This is suspended between terminal posts from the power module which protrude through holes in the top sheet as shown.

While this design retains the essence of the original architecture, it differs from its predecessor in several important ways.

1.   The rf coupling to the amplifier at both input and output is inductive.

2.   The amplifier substrate doubles as the radiating slot dielectric.

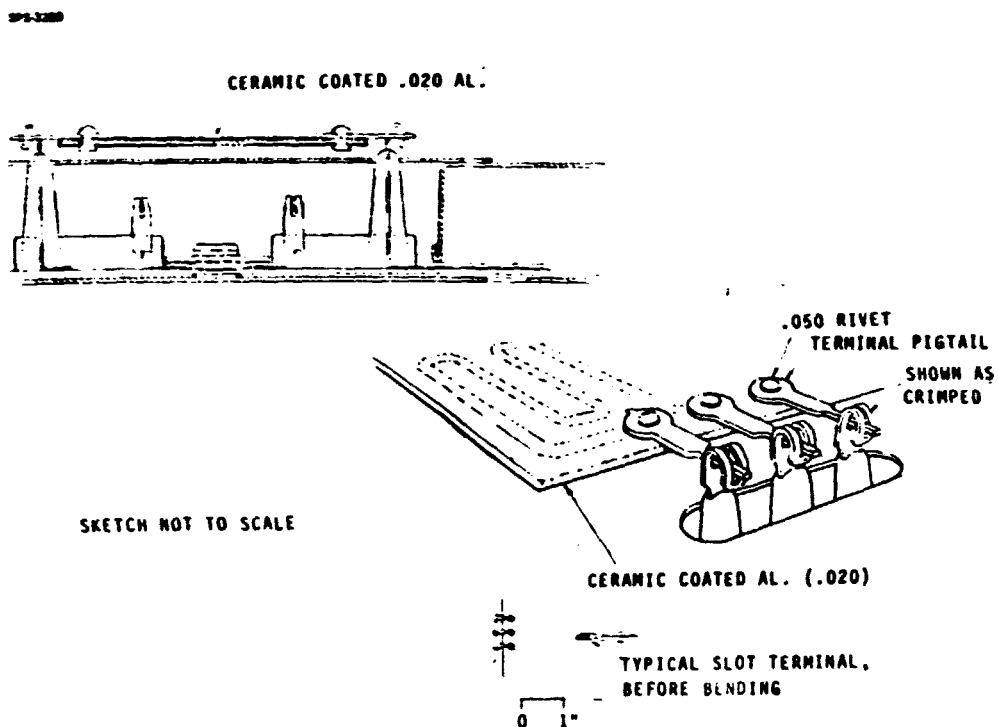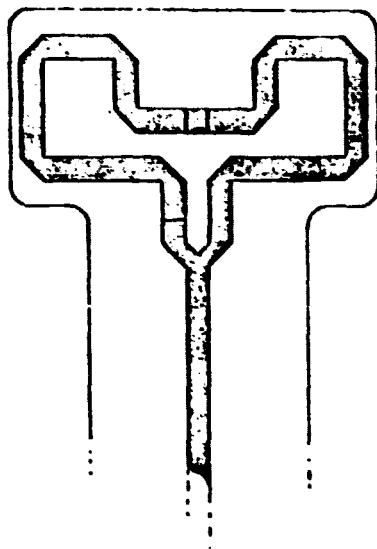3.   The separate phase comparator module has been incorporated into the two amplifier modules. This gives phase comparison for each pair of amplifiers, rather than each four amplifiers as before.

4.   A top sheet has been added to increase structural stiffness.

5.   A mounting and heat dissipation scheme is detailed for the fault load resistors.

These features are perceived to afford the following benefits.

1.   Inductive coupling of input and output circuits affords rf coupling with adequate dc isolation. The indicated materials and dimensions have been chosen to stand off up to 10 kV dc on a subarray. It is felt that this operating voltage could not be realized with the previous design.

2.   The use of the BeO substrate as the slot loading dielectric has several advantages.

        a.   The mounting of the BeO slab on the aluminum structure appears to be mechanically superior to the proposed mounting of the dielectric slab in the previous design.

        b.   The large area of the BeO slab affords adequate heat transfer to the Al structure. It is envisioned that the amplifier circuitry would be deposited directly on the BeO substrate. This would give a temperature drop of approximately 1°C between the output device and the Al radiator. However, as indicated in previous studies, the temperature drop internal to the amplifier chip between the active region and the mounting pad is greater (approximately 20°C) and that is of prime importance.

        c.   The integration of the circuitry onto the BeO and the use of transformer rf coupling obviates solder joints in the rf circuit (previously required). This should enhance reliability.

3.   The top sheet of this design has three beneficial functions: 1) it increases the effective backside thermal radiation area, 2) it provides an environmental shield for rf components mounted below, and 3) it greatly increases the moment of inertia of the assembly, and thereby increases its mechanical integrity.

4.   The fault load resistor radiator provided in this design will allow these resistors to operate at a lower temperature, thereby enhancing their reliability.

        Tables 2.2-1 through 2.2-3 give mass estimates for 3 types of cavity radiator modules for use in antenna taper steps 1 and 2, 3 and 4, and 5, respectively. Even
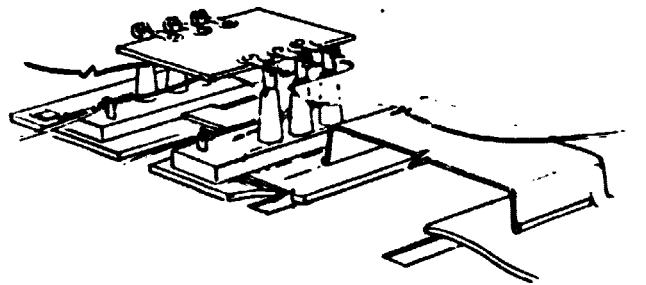
SP4-2008
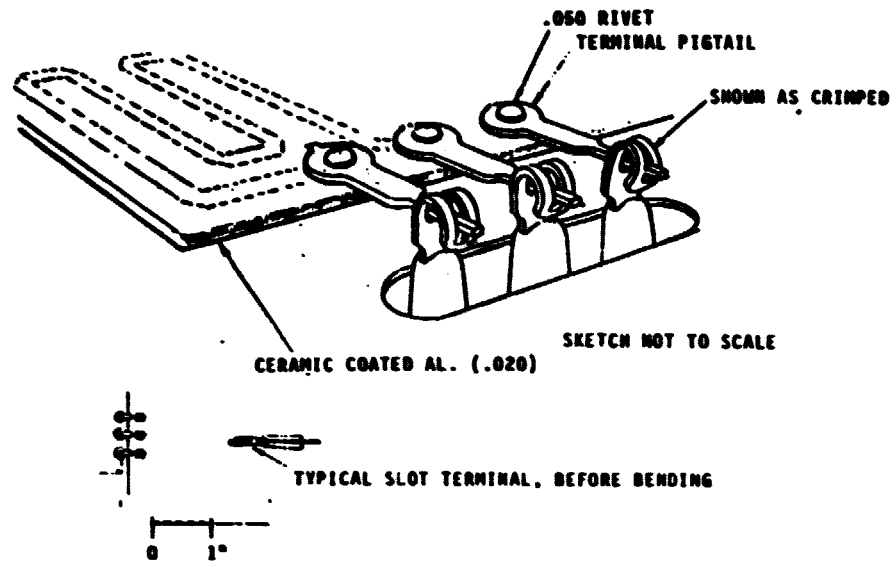
Figure 2.2-9. *Enlarged View of One Fourth of the Fault Load Resistor, Showing Crimp Connections*

SP4-3208

Figure 2.2-10. *Fault Load Resistor Configuration*

18

Table 2.2-1. Mass Statement: High Power Density 4-FET Solid State Cavity Radiator Combining Module Design

ITEM	COMMENTS	MASS (g)
FACE SHEET	$.6\lambda$ x $.6\lambda$ x $.010"$ x ρ_{A1}	= 3.70
BeO SUBSTRATE	$.5\lambda$ x $.5\lambda$ x $.040"$ x ρ_{BeO}	= 7.61
POLYSULFONE INSULATION	2 x $.5\lambda$ x $.1\lambda$ x $.015"$ x ρ_{PS}	= 1.14
AMPLIFIER MODULE (W. FAULT LOAD TOWERS)	2 x .003 m x $.1\lambda$ x .2 x (3000 kgm^{-3})	= 5.39
SHIELD CAN	$.6\lambda$ x $.6\lambda$ x $.020"$ x ρ_{A1}	= 7.40
TOP SHEET AND FAULT LOAD RESISTOR	$.6\lambda$ x $.3\lambda$ x $.01"$ x ρ_{A1}	= 1.85
PHASE DISTRIBUTION STRIPLINE	$.1\lambda$ x $.6\lambda$ x $.020"$ x ρ_{A1}	= 1.23
MODULE TOTAL		28.32 g = 5.25 kg/m²
x 64		1.81 kg
PANEL STRUCTURE		.20 kg
PANEL TOTAL		2.01 kg
x 324		651.2 kg
SUBARRAY STRUCTURE		68.3 kg
SUBARRAY ELECTRONICS		12.0 kg
SUBARRAY TOTAL		731.5 kg = 6.73 kg/m²

Table 2.2-2. Mass Statement: Reduced Power Density 4-FET Cavity Radiator Design

ITEM	COMMENTS	MASS (g)
FACE SHEET	$.6\lambda$ x $.6\lambda$ x $.0075"$ x ρ_{A1}	= 2.78
BeO SUBSTRATE	$.5\lambda$ x $.5\lambda$ x $.040"$ x ρ_{BeO}	= 7.61
POLYSULFONE INSULATION	2 x $.5\lambda$ x $.1\lambda$ x $.015"$ x ρ_{PS}	= 1.14
AMPLIFIER MODULES (W. FAULT LOAD TOWERS)	2 x .003 m x $.1\lambda$ x $.2\lambda$ x (3000 kgm^{-3})	= 5.39
SHIELD CAN	$.6\lambda$ x $.6\lambda$ x $.020"$ x ρ_{A1}	= 7.40
TOP SHEET AND FAULT LOAD RESISTOR	$.6\lambda$ x $.3\lambda$ x $.0075"$ x ρ_{A1}	= 1.39
PHASE DISTRIBUTION STRIPLINE	$.1\lambda$ x $.6\lambda$ x $.020"$ x ρ_{A1}	= 1.23
MODULE TOTAL		26.94 g = 5.00 kg/m²
x 64		1.72 kg
PANEL STRUCTURE		.20 kg
PANEL TOTAL		1.92 kg
x 324		622.1 kg
SUBARRAY STRUCTURE		68.3 kg
SUBARRAY ELECTRONICS		12.0 kg
SUBARRAY TOTAL		702.4 kg = 6.46 kg/m²

Table 2.2-3. Mass Statement: 2-FET Solid State Cavity Radiator Module Design

ITEM	COMMENTS	MASS (g)
FACE SHEET	$.6\lambda \times .6\lambda \times .0075" \times \rho_{A1}$	= 2.78
BeO SUBSTRATE	$.5\lambda \times .4\lambda \times .040" \times \rho_{BeO}$	= 6.09
POLYSULFONE INSULATION	$2 \times .5\lambda \times .75\lambda \times .015" \times \rho_{PS}$	= .86
AMPLIFIER MODULES (W. FAULT LOAD TOWERS)	$2 \times .003 \text{ m} \times .1\lambda \times .1\lambda \times (3000 \text{ kgm}^{-3})$	= 2.70
SHIELD CAN	$.6\lambda \times .6\lambda \times .020" \times \rho_{A1}$	= 7.40
TOP SHEET AND FAULT LOAD RESISTOR	$.3\lambda \times .3\lambda \times .0075" \times \rho_{A1}$	= .70
PHASE DISTRIBUTION STRIPLINE	$.1\lambda \times .6\lambda \times .020" \times \rho_{A1}$	= 1.23
MODULE TOTAL		21.76 g = 4.04 kg/m^2
X 64		1.40 kg
PANEL STRUCTURE		.20 kg
PANEL TOTAL		1.60 kg
X 324		518.4 kg
SUBARRAY STRUCTURE		68.3 kg
SUBARRAY ELECTRONICS		12.0 kg
SUBARRAY TOTAL		598.7 kg = 5.50 kg/m^2

though there is less microwave power per unit area at each successive ring the module mass can not be reduced proportionately because of various configuration overheads.

However, after step 5 this power per unit area is low enough to allow the use of the much less massive dipole radiator module configuration described on Figure 2.2-11 and Table 2.2-4. Dipole radiator antenna arrays of this type are well understood. The effective driving resistance that the dipole presents to the power amplifier may be varied to match the amplifier by changing the dipole standoff distance and spacing. This is shown on Figure 2.2-12.
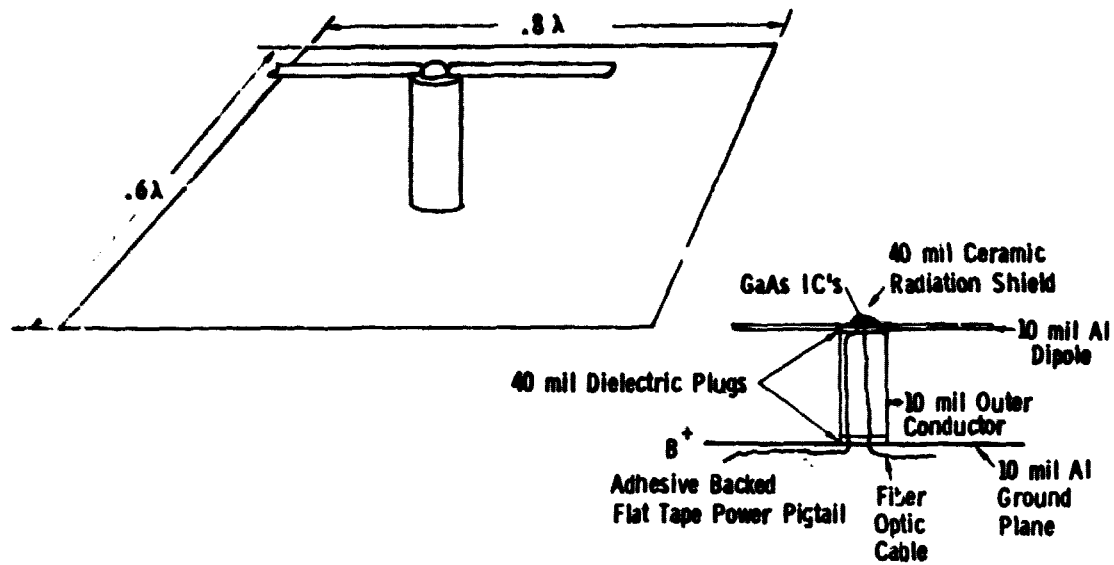
Figure 2.2-11. Solid State Dipole Radiator Module

Table 2.2-4. Dipole Radiator Module Mass Statement

.6λ x .8λ MODULE SIZE

ITEM	MASS
10 MIL A1 GROUND PLANE	4.93 g
CERAMIC SHIELD	.7 g
DIPOLE AND SUPPORT, 10 MIL A1	3.75 g
DIELECTRIC PLUG(S)	2.8 g
CHIPS, METALLIZATIONS, BONDING, ETC.	.5 g
TOTAL MODULE	12.68 g ≈ 1.76 kgm^{-2}
X 48	608.6 g
PANEL STRUCTURE	150.0 g
TOTAL PANEL	758.6 g
X 324	245.8 kg
SUBARRAY STRUCTURE	35.0 kg
SUBARRAY ELECTRONICS	12.0 kg
SUBARRAY TOTAL	292.8 kg = 2.69 kgm^{-2}

22

SPS-1304

IN A VARIABLE
SPACING DESIGN
OR EDGE EFFECT
COMPENSATED
DESIGN

$\underline{\text{LENGTH OF SLOT}}$
COMPENSATES FOR VARIABLE REACTANCE

$\underline{\text{OFFSET OF SLOT}}$
COMPENSATES FOR VARIABLE RESISTANCE

$$R = \frac{120}{\pi} \quad \frac{\sin^2(2\pi\, 2/\lambda)}{D_x D_y}$$
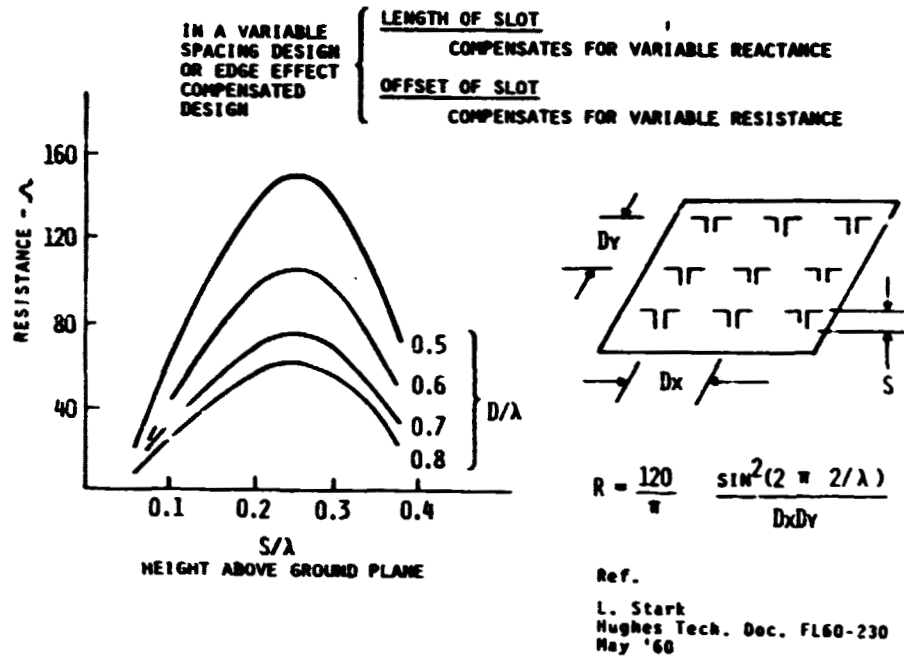
Ref.

L. Stark
Hughes Tech. Doc. FL60-230
May '60

Figure 2.2-12. Driving Resistance in Infinite Array

3.0 SOLID STATE SPS POWER BUSSING

3.1 Introduction

Because the performance of the previous (Phase II) 2.5 GW solid state SPS was greatly penalized by power bussing losses at its array output voltage of 5500 volts it was felt desirable to examine the effects of raising the buss voltage. In particular, the buss voltages were raised to give a subarray power voltage input of 8640 volts. This greatly improved system performance because of reduced I^2R losses, lower array mismatch power losses and reduced conductor mass.

3.2 Optimum Conductor Temperature Trade

The analysis of Phase II, Volume IV (Boeing document D180-25461-4) of low voltage dc power bussing losses versus temperature were repeated for the case of a delivered subarray power voltage of 8640 volts. A key factor of the analysis was the more than proportionate reduction in cell string mismatch losses as the voltage was increased (see Figure 3.2-1. Then, using the flat perpendicular edge strip buss string relationship shown on Figure 3.2-2, conductor sizing and costing was accomplished for the cases of conductor temperatures of 0, 25, 50 and 100°C.

The result, shown in Table 3.2-1 and Figure 3.2-3, indicates rather flat minima as a function of conductor temperature. As expected, the cost minimum at 40°C is at a lower temperature than the mass minimum at 50°C.

3.3 Baseline Solid State SPS Power Bussing Description

The cost minimum at 40°C was picked as the array conductor operating temperature, giving a required cell string voltage of very close to 10 KV. The resulting total system efficiencies are shown on Table 3.2-2.

A satellite of this size can easily be adapted from the 5 GW Klystron reference system satellite with a length of 9 bays and a width of 8 bays to deliver 4200 MW to the transmitting antenna subarrays. At the voltage desired, the cell strings would go out longitudinally to the edge of their bay and then return. Their current would be collected on 9 pairs of busses whose combined widths are as shown on Figure 3.2-4.

Note the very large conductor equivalent width of 256.5 m at the rotary joint "neck" of the satellite. This necessitated a redesign of the rotary joint region from the Klystron reference system configuration, with a larger diameter rotary joint and some local conductors that were necessarily thicker than the collecting busses on the solar array portions of the satellite. Figure 3.2-5 shows a view of the bare structure of the main satellite up to the mechanical rotary joint. Four of the beams telescope to allow the rotary joint to be assembled from the deck of the construction base with subsequent deployment into the operational position after construction is complete. Figure 3.2-6 shows the layout of the 9 pairs of busses that converge on the electrical rotary joint. Figure 3.2-7 shows both interfaces of the mechanical rotary joint. On the antenna side this is 6 actively controlled linear actuators that provide a soft mechanical connection. The electrical rotary joint, constructed from prefabricated quadrants, is fed from the sheet busses by pigtails as shown on Figure 3.2-8.

After crossing the rotary joint and a flex cable across the soft active elevation joint to the transmitting antenna, the 18 main busses are distributed into nine transmitting antenna power buss rings at the main switchyard. The transmitting antenna subarray

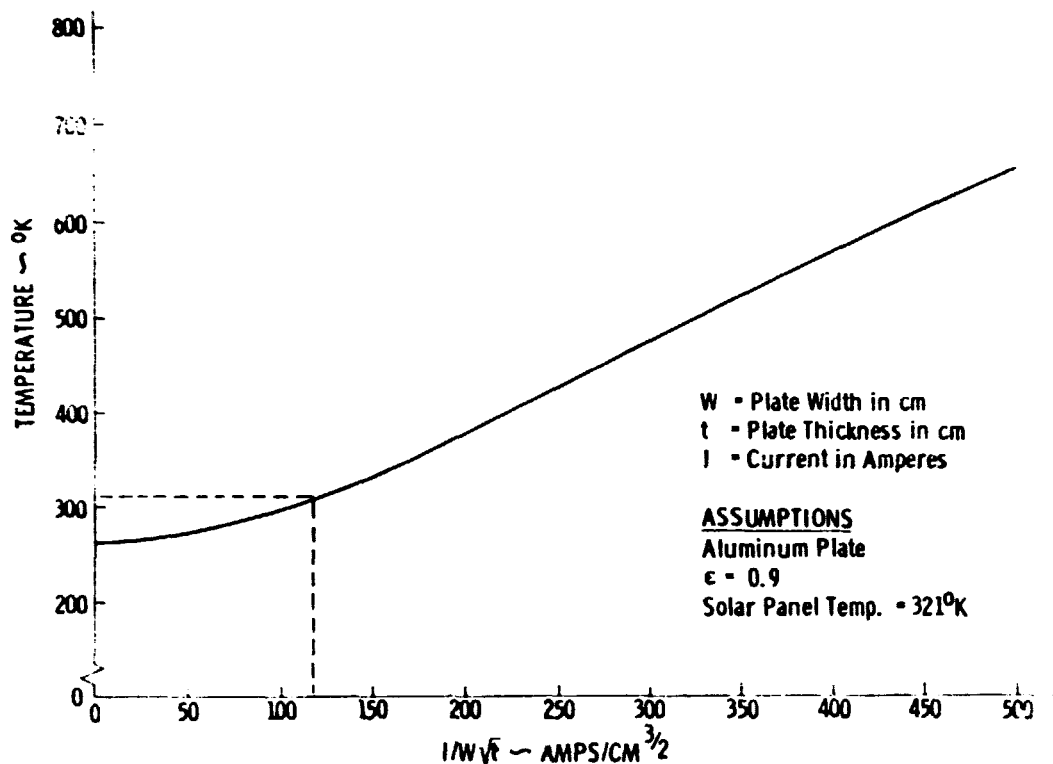**2.5 GW SOLID STATE SPS CONFIGURATION**
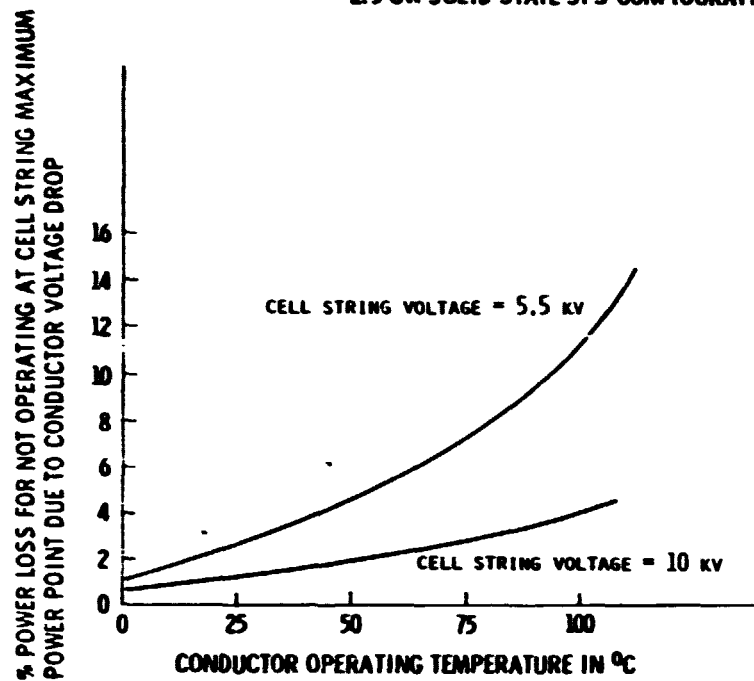
Figure 3.2-1. Array Mismatch Losses

Figure 3.2-2: SPS

25

Table 3.2-1. Revised Solid State SPS Power Distribution System Parameters As A Function of Temperature

	MASS/COST (Metric Tons/$M)				POWER LOSS (Megawatts)			
Conductor Temperature (°C)	0	25	50	100	0	25	50	100
Non-P_{max} Power Loss	-	-	-	-	56.1	84.1	112.6	302.?
Power Busses ($37 kg^{-1})	4517.4/167.2	2630.6/97.3	1997.5/73.9	1585.2/59.3	251.6	522.4	642.5	1245.?
Array Power (Megawatts)	4507.9	4806.5	4955.1	5747.1	307.7	606.5	755.1	1547.?
Array Area (km² @ 179 w m^{-2})	25.00	26.85	27.68	32.11				
Array Mass/Cost .425 kg m^{-2}, $40 m^{-2}	10683.3/1005.5	11412.0/1074.1	11764.9/1107.2	13645.3/1284.3				
Switchgear (.0273 kg kw^{-1}; 6.53 $ kw^{-1})	123.1/29.4	126.8/31.4	125.2/32.4	133.3/37.5				
Number of Bays (Smeared @ 69.34 MW/Bay)	65.0	69.3	71.5	82.9				
Bay Structural Mass/Cost (Smeared @ 32.3 T/Bay, 66$ kg^{-1})	2097.2/138.5	2240.5/147.9	2309.2/152.4	2678.6/176.8				
Total Mass/Component Cost	17421.0/1340.6	16409.9/1350.7	16196.8/1365.9	18042.4/1557.9				
Transportation & Constr. Cost ($75 kg^{-1})	1306.6	1230.7	1214.8	1353.1				
Total Cost Involved in Tradeoff	2647.2	2980.4	2580.7	2911.0				
Cell String Voltage (V)	9273	9888	10193	11823				
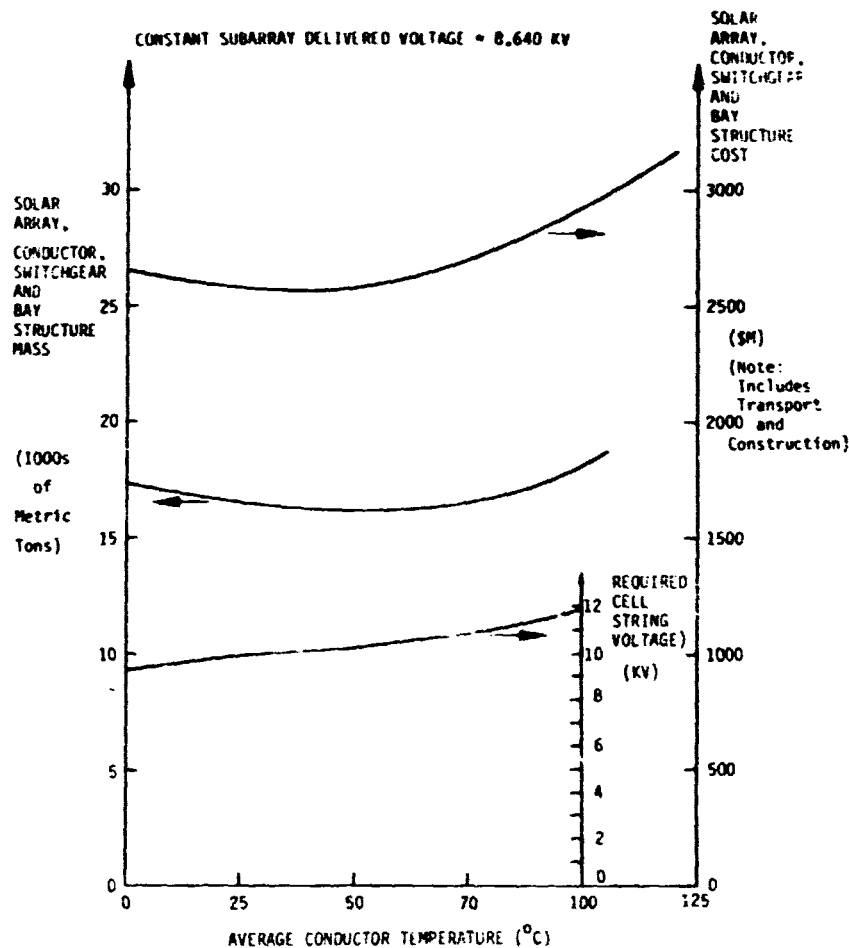
Figure 3.2-3. Cost and Mass Trades

Table 3.2-2. Solid State SPS Efficiency & Sizing

ITEM	EFFICIENCY	MEGAWATTS	
Array Mismatch			
Array Mismatch	.975	5033	Ideal Array Output
Main Bus I^2R	.854	4907	
Antenna Distr	.985	4191	Total Antenna Input
DC-RF Conversion	.8	4128	
Waveguide I^2R	N/A	3303	Total RF Radiated Power
Ideal Beam	.965	3303	
Inter-Subarray Losses	.976	3187	
Intra-Subarray Losses	N/A	3110	
Atmosphere Loss	.98	3110	
Intercept	.95	3048	
Rectenna RF-DC	.89	2896	Incident on Rectenna
Grid Interface	.97	2577	
	.497	2500 Net to Grid	

TOTAL ARRAY OUTPUT   5033 MW
TOTAL SOLAR ARRAY AREA = 28.1 km²
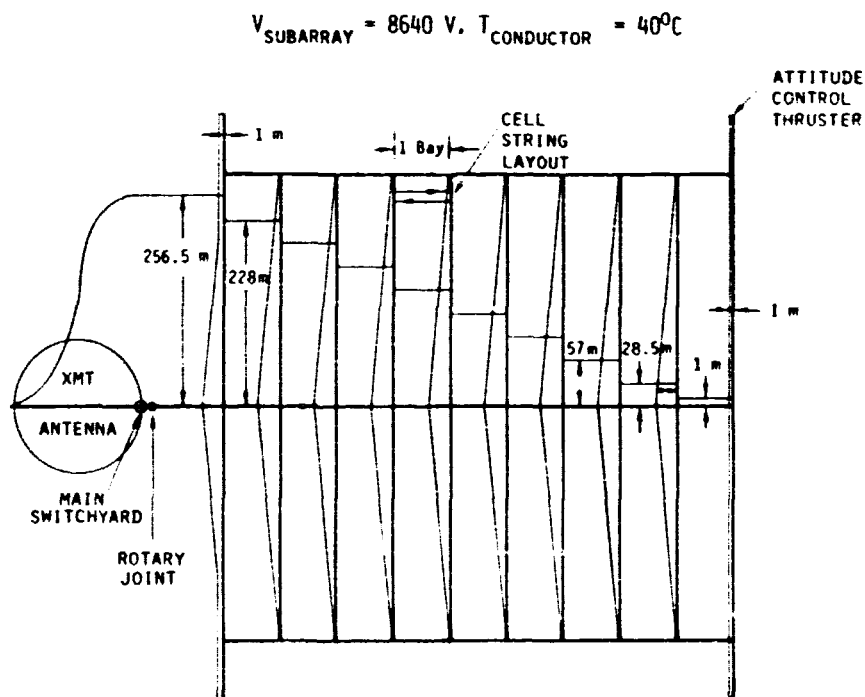
$V_{SUBARRAY}$ = 8640 V, $T_{CONDUCTOR}$ = 40°C

Figure 3.2-4. 2.5 GW Solid State SPS Main Bussing Arrangement
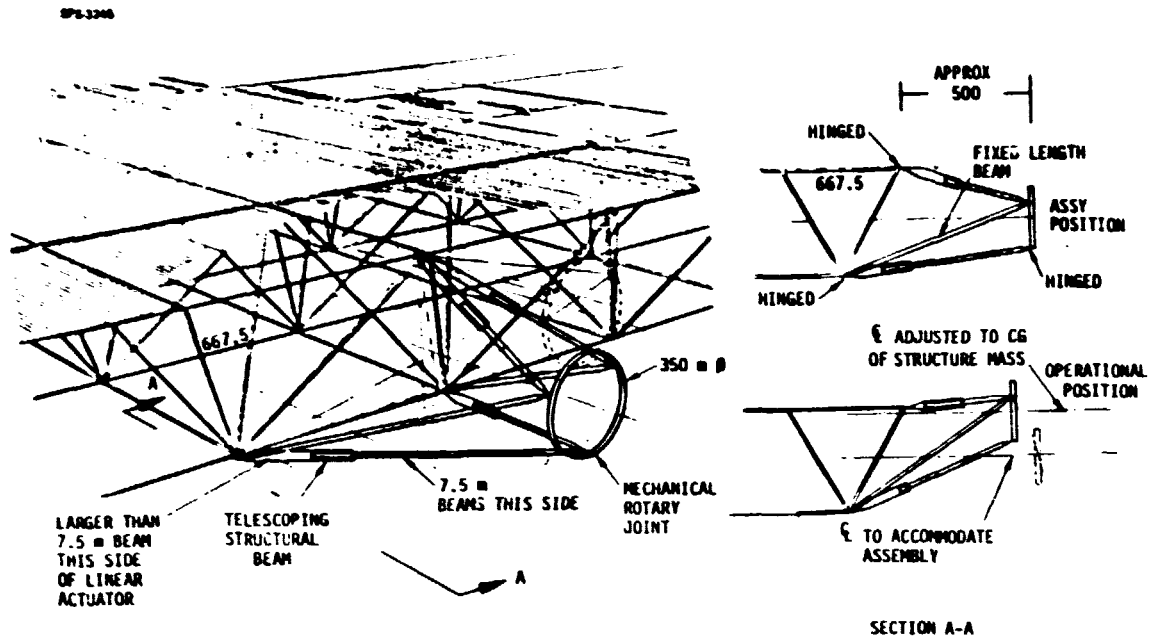
Figure 3.2-5. Interface System Structure
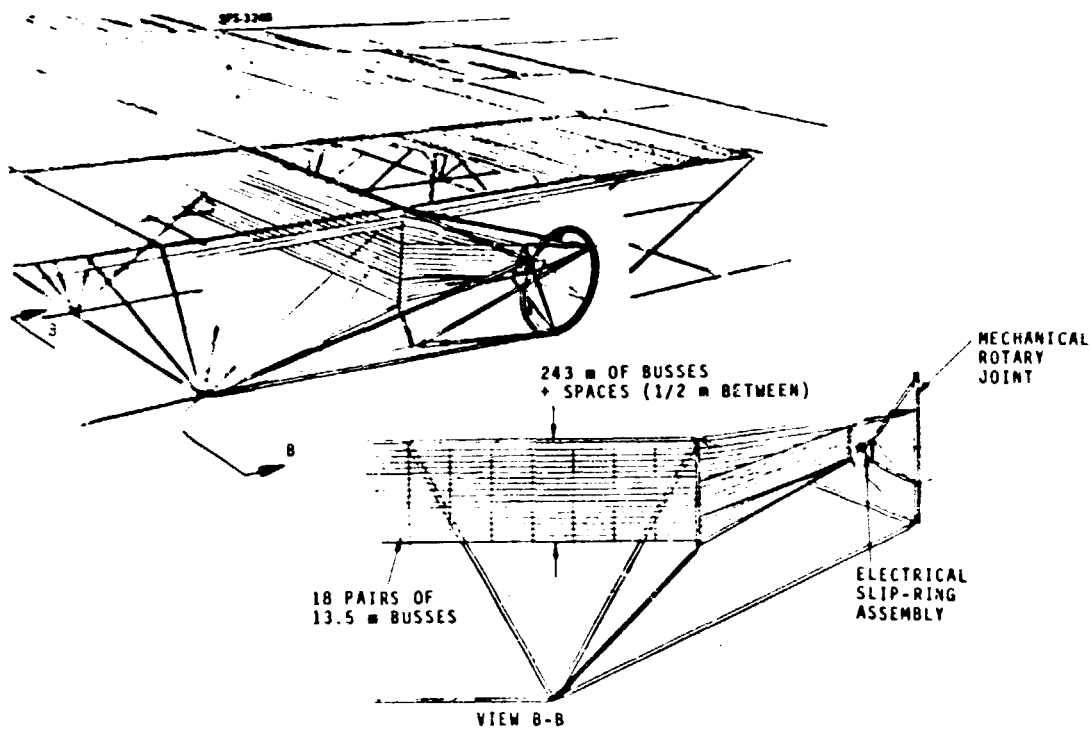
Figure 3.2-6. Interface System Busses

MECHANICAL
ROTARY JOINT
(THIS IS FIXED)

THIS STRUCTURE ROTATES

ATTACHED TO BOGEY'S

LINEAR ACTUATOR
(TYPICAL)

LINKAGE (6 PCS)

ELECTRICAL
SLIP-RING
ASSEMBLY

BOGEY'S
(6 PCS)

ANTENNA
PRIMARY
STRUCTURE
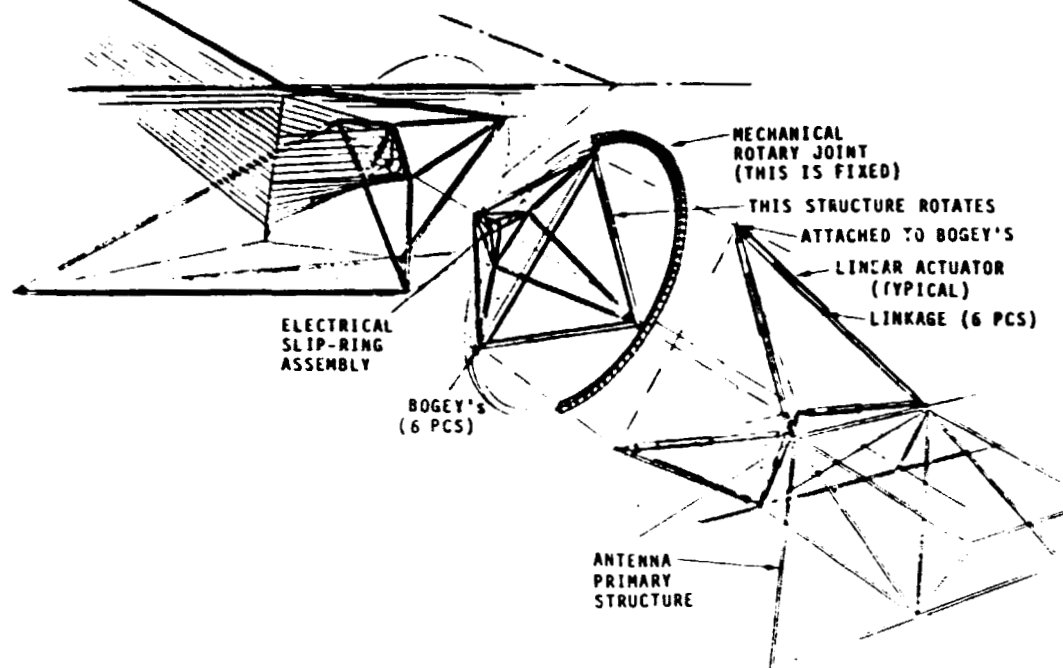
Figure 3.2-7. Interface System Mechanical Rotary Joint and Actuator

BUS EXPANSION LOOP

PIGTAIL LEAD
TO SLIP-RING
(ROUTING AND
MECHANICAL
SUPPORT NOT SHOWN)

ELECTRICAL
SLIP-RING
ASSEMBLY
(APPROX 20 m Ø)
(SHIP IN QUADRANTS)
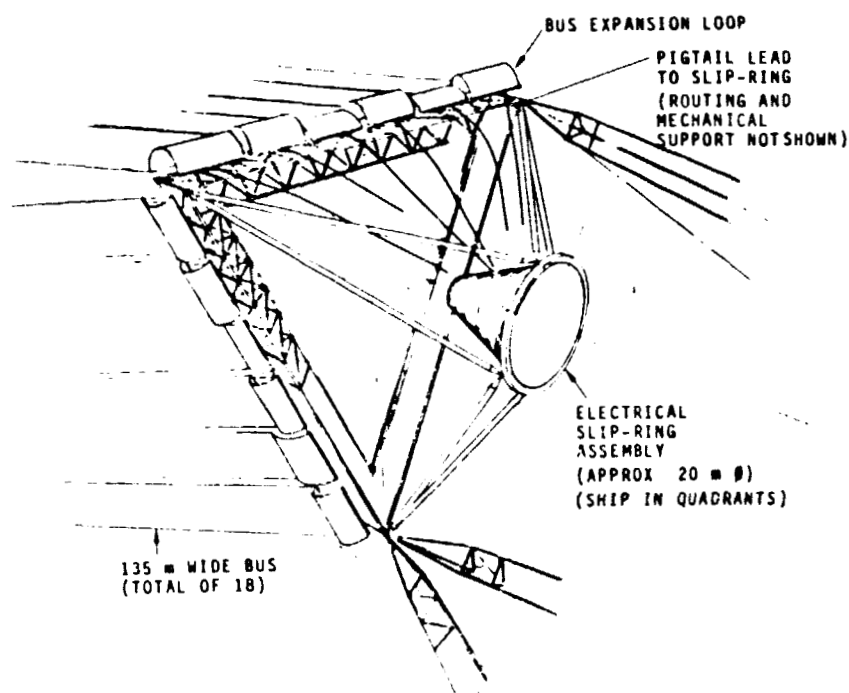
135 m WIDE BUS
(TOTAL OF 18)

Figure 3.2-8. Interface System Electrical Rotary Joint

quantization scheme assumed for this analysis is described on Table III and shown on Figure 3.2-9a. The transmitting antenna main power busses shown on Figure 3.2-9b run perpendicularly along the bottom edge of the transmitting antenna primary structure. Their power is distributed "above" along the back side of the transmitting array structure by small flat feeder busses that run laterally at opposite edges of adjacent subarrays. Using 1 mm aluminum strip, the main busses are up to 28.5 meters wide per pair, while the feeders range up to half a meter in width.
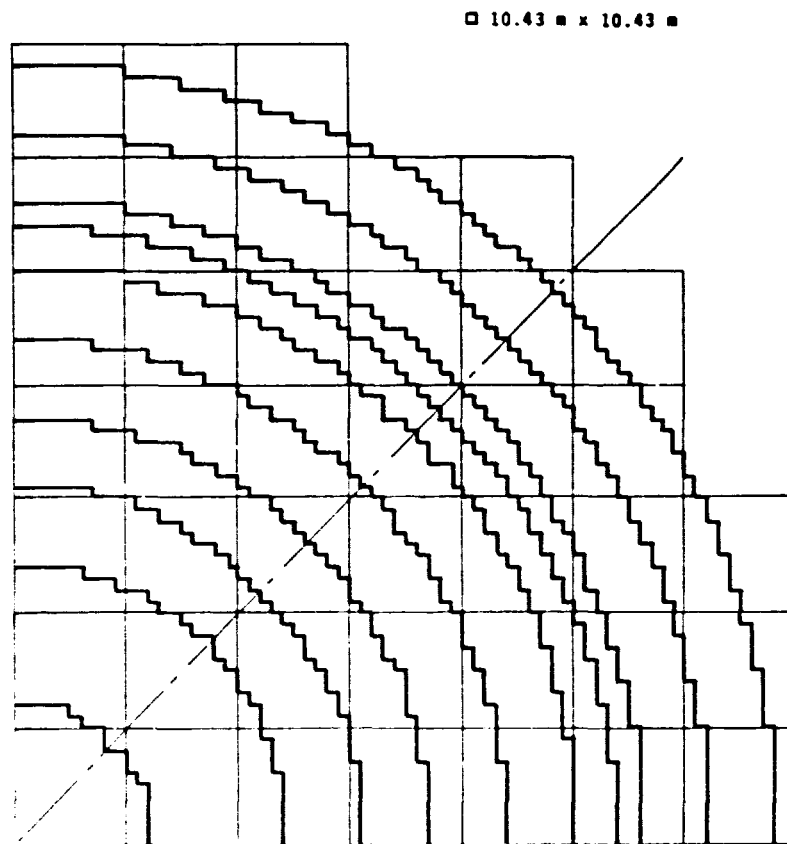
☐ 10.43 ■ x 10.43 ■

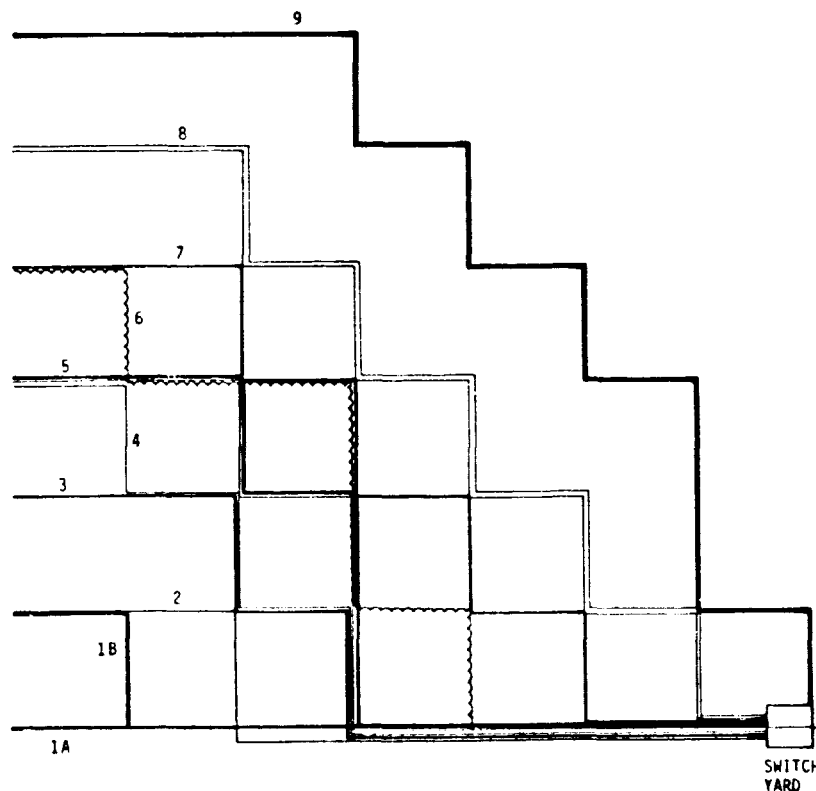*Figure 3.2-9a. 2.5 GW Solid State SPS Transmitting Antenna 9.54 db Gaussian Step Quantization*

Figure 3.2-9b. 2.5 GW Solid State SPS Transmitting Antenna Main Buss Configuration

4 - SOLID STATE SPS CONSTRUCTION

The construction methods used to assemble the 2500 MW Solid State Solar Power Satellite (SPS) are very similar to those described for assembling the 5000 MW reference klystron SPS concept (D180-25461-3). The GEO construction base and its operations were updated, as needed, to meet the peculiar requirements of the Solid State SPS design. Wherever possible, the same groundrules and constraints have been followed.

The reference SPS GEO Construction Base (D180-25461-2) is required to assemble one 5 GW reference satellite every six months, or produce 10 GW system capacity each year for 30 years. This, and other major groundrules and constraints for the operation of GEO base systems, are shown in Figure 4-1. For example, to avoid free-flying construction facilities and/or assembly methods, the base is required to provide contiguous facilities for assembling all SPS system elements. As a GEO operational base, the 4 Bay End Builder is also required to support the maintenance and repair of operational SPS systems. Therefore, the GEO base must be capable of docking and unloading orbital transport vehicles and implementing other essential work support and crew support functions. Essential operational areas of the base include command and control modules, crew habitats, cargo handling and distribution network, subassembly factories, base attitude control, base electrical power, base maintenance, etc. GEO base operation timelines, in turn, are based upon two 10 hour shifts per day and rely upon normal IVA assembly methods. These requirements are extracted from the Phase 2 study reports (D180-25461-3/4) and guide the definition of all other requirements.

The Phase 2 Solar Power Satellite (SPS) construction method is illustrated in Figure 4-2. The 5000 MW reference satellite is assembled entirely in geosynchronous earth orbit (GEO) by the 4 Bay end Builder Construction Base. This GEO construction base supports the emerging satellite during all phases of construction. The satellite 8 bay-wide energy conversion system is constructed in two successive passes on one side of the base, while the microwave antenna is assembled on the other side of the base. During each construction pass, the GEO base builds one-half of the energy conversion system, a 4 bay-wide strip by 16 bays long, which contains

32

- CONSTRUCT ONE 5 GW SPS WITHIN 6 MONTHS ±5% (OR PRODUCE 10 GW CAPACITY/YEAR)

- USE CONTIGUOUS FACILITIES TO ASSEMBLE SATELLITE ELEMENTS

- SUPPORT MAINTENANCE OF OPERATIONAL SPS SYSTEMS

- DOCK, OFFLOAD & SERVICE POTV, CARGO TUG & OTV

- PROVIDE ESSENTIAL WORK FACILITIES & CREW SUPPORT FACILITIES

- TWO 10 HR SHIFTS/DAY @ 75% EFFICIENCY, 6 DAYS/WEEK

- BASELINE IVA OPERATIONS — EVA EMERGENCY LIMITED

0847-011W

Figure 4-1 SPS GEO Construction — Major Groundrules & Constraints

ACTIVATE GEO BASE

FIRST CONSTRUCTION PASS

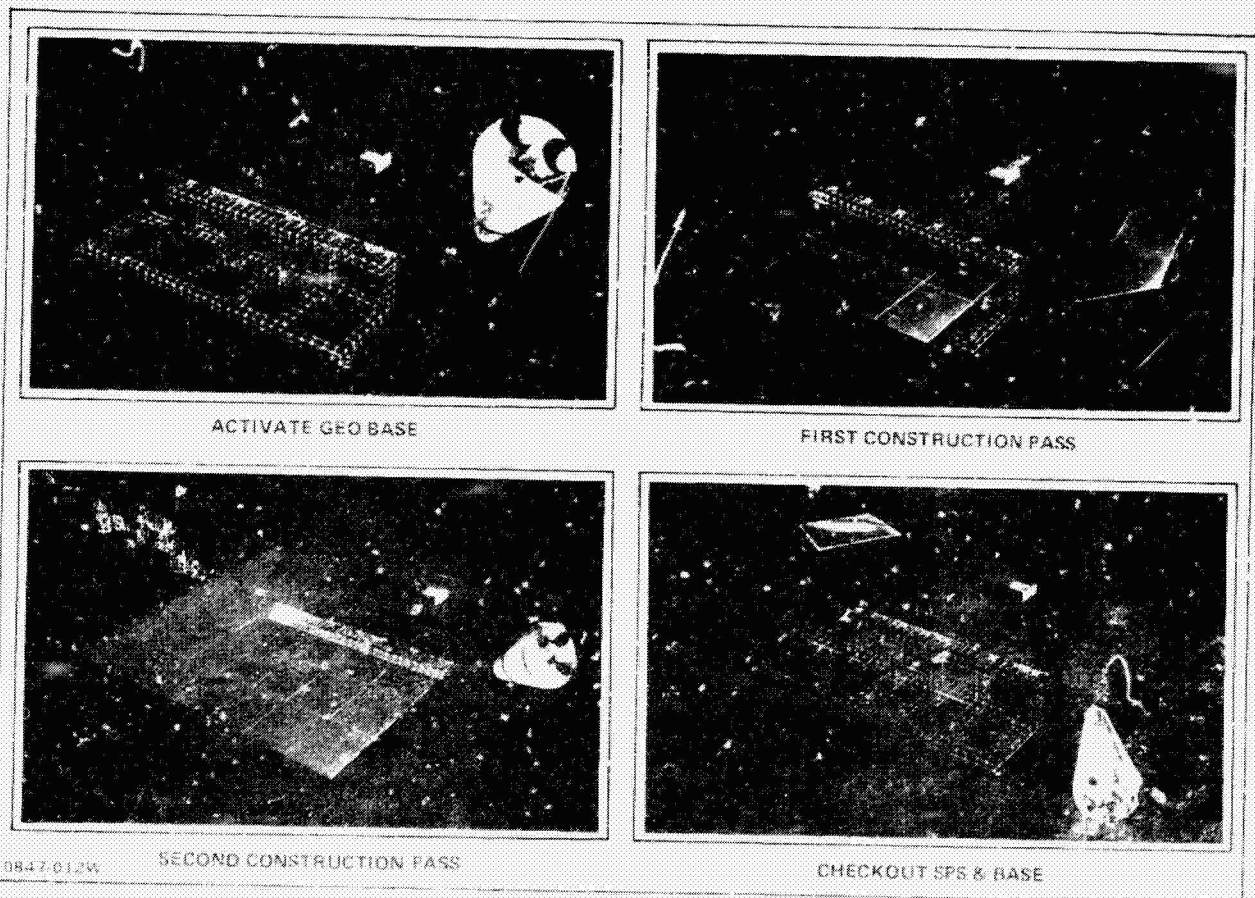SECOND CONSTRUCTION PASS

CHECKOUT SPS & BASE

0847-012W

Figure 4-2 SPS 4 Bay End Builder Construction

the appropriate subsystems. The satellite power transmission antenna is simultaneously built-up by assembling one row at a time until the 11 row planform is completed. At the end of the second pass, the base is then indexed sideways to mate the antenna with the center line of the energy conversion system. After final test and checkout, the base separates from the satellite and is transferred to the next orbital position for SPS construction.

As presently defined, the energy conversion system of the Solid State SPS is similar to the one used on the reference SPS (i.e., 8 bays wide but not as long). The solid state power transmission antenna however, follows the reference structural configuration but is larger in diameter (1.42 km vs 1.0 km). In addition, the reference antenna support yoke is replaced by a smaller cantilever support system. The major impact to the reference GEO base is, therefore, restricted to the antenna building platform and its facilities. Figure 4-3 shows the solid state SPS construction base and highlights the antenna construction system which is described more fully below.

Figure 4-4 provides a top level comparison of the Solid State Construction Base with the baseline GEO Construction Base. It shows the GEO base for Solid State SPS construction to be of comparable size and weight with respect to the Phase 2 reference base. However, even though the Solid State Construction Base requires a larger crew, it does not achieve the same level of annual productivity as the reference base (i.e., 8.65 GW/yr vs 10 GW/yr). The unit cost and annual cost of the Solid State Construction Base are 10% higher than the Phase 2 reference.

The rationale for the loss in annual productivity due to the solid state SPS concept is discussed further below. The following paragraphs describe the analysis performed on solid state satellite construction operations and the modifications required for the GEO construction base.
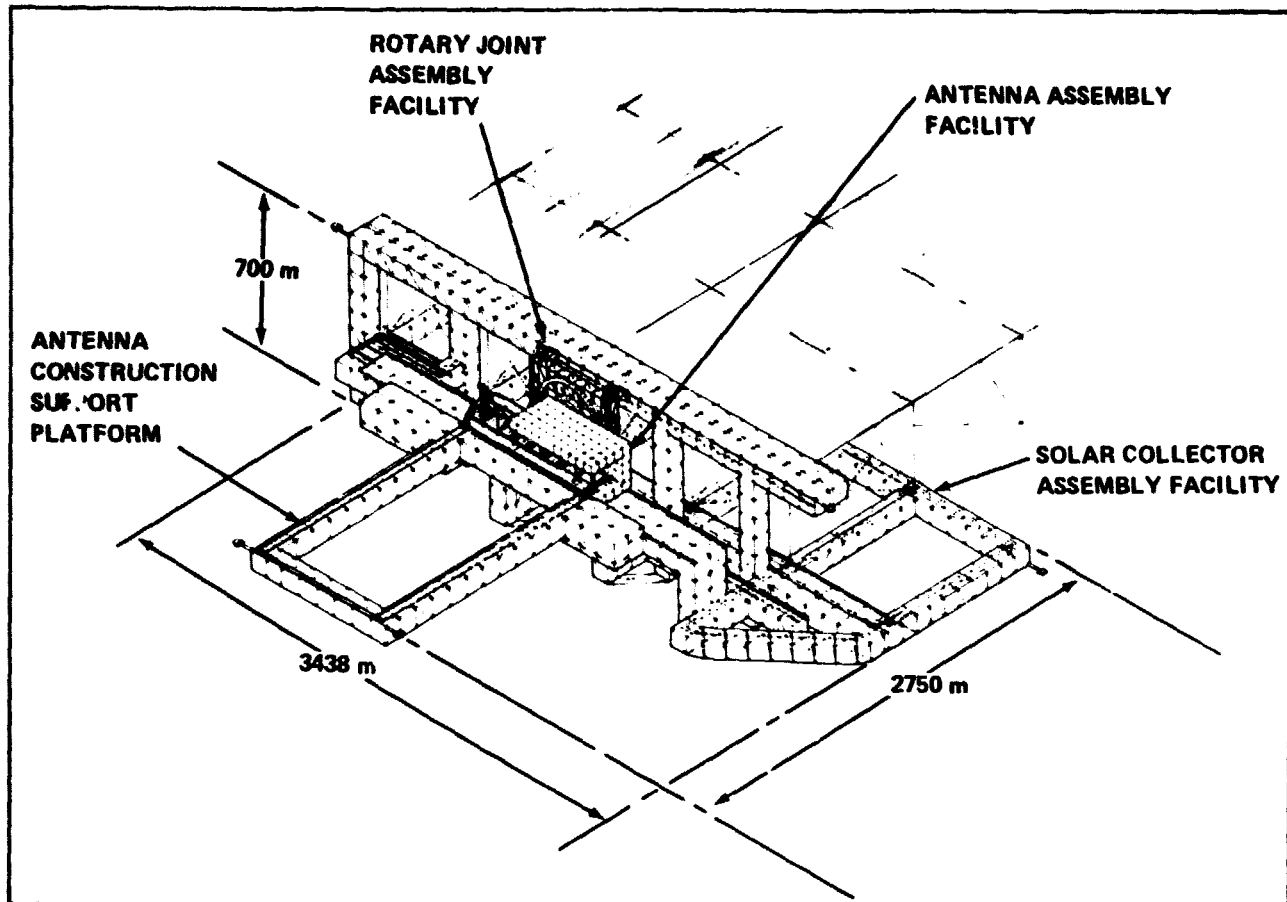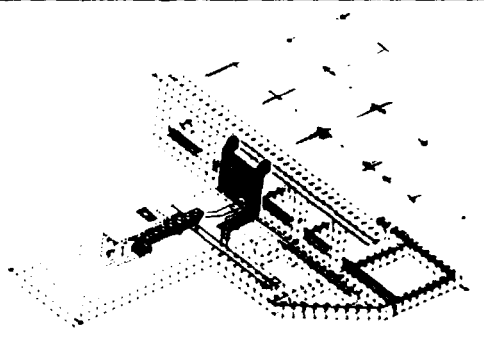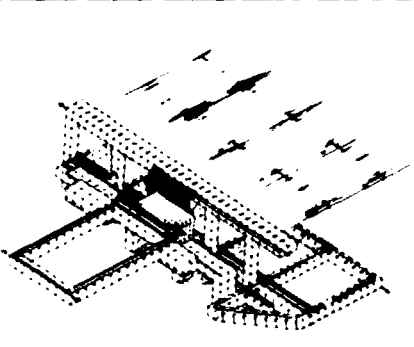
Figure 4-3 Solid State SPS Construction Base

	BASELINE	SOLID-STATE
● SPS PRODUCTION RATE	10 GW/YR	8.65 GW/YR
● BASE UNIT COST, 1979$	$9.01B	$10.21B
● BASE ANNUAL COST	$1.30 B/YR	$ 1.43B/YR
● MASS, MT	6656	6678
● CONSTRUCTION CREW	444	491

0847-014W

Figure 4-4 SPS Construction Base Comparison — Baseline vs Solid State

35

4.1 SOLID STATE SATELLITE CONSTRUCTION REQUIREMENTS

Figure 4-5 summarizes the requirements and issues concerned with construction of the 2500 MW Solid State SPS. This satellite is to be constructed entirely in GEO, with assembly similar to the 5000 MW reference satellite. To facilitate comparison with the reference SPS program scenario, the smaller capacity solid state SPS will have to be produced at a faster rate. That is, to meet the reference program goal of 10 GW annual capacity growth, one 2500 MW Solid State SPS will have to be fully assembled and checked out every 90 days.

The solid state satellite has a single antenna located at one end of the 8 x 11 bay photovoltaic energy conversion system. The microwave antenna is designed with the reference pentahedral primary structure, whereas the energy conversion system uses the reference hexahedral structure. The interface system retains the reference rotary joint design with its solar array support structure. However, the reference antenna support yoke is replaced by an end mounted linear actuator.

To achieve SPS microwave power transmission performance requirements, both solid state and reference klystron antenna concepts must be constructed to meet similar flatness design goals (i.e., 2 arc minutes rms with a maximum of 3 arc minutes). Hence, to cover all aspects of the solid state SPS construction process, a broad range of technology issues (which are beyond the scope of this study) must be addressed. For example, as the solid state SPS system matures, the satellite construction approach must be re-examined for the energy conversion, power transmission, and interface systems. In addition, the structural assembly methods should be well understood to the level of beam fabrication, handling and joining. Techniques for installing the major subsystems (i.e., solar arrays, buses and subarrays) must be further developed and the requirements for construction equipments need further refinement. In addition, the structural dynamic, thermodynamic and control interactions between the base and the satellite should be investigated and defined. Other areas to be examined include methods for berthing or mating of large system elements, techniques for in-process inspection and repair, and concepts for implementing satellite final test and checkout.

4.1.1 Satellite Construction Timelines & Analysis

Timelines comparing the solid state SPS with the 5000 MW reference satellite are shown in Figure 4-6. Both timelines follow the same construction approach; that is where the energy system conversion assembly is timed for simultaneous completion and mating with the satellite's power transmission and interface systems. The 4 Bay End
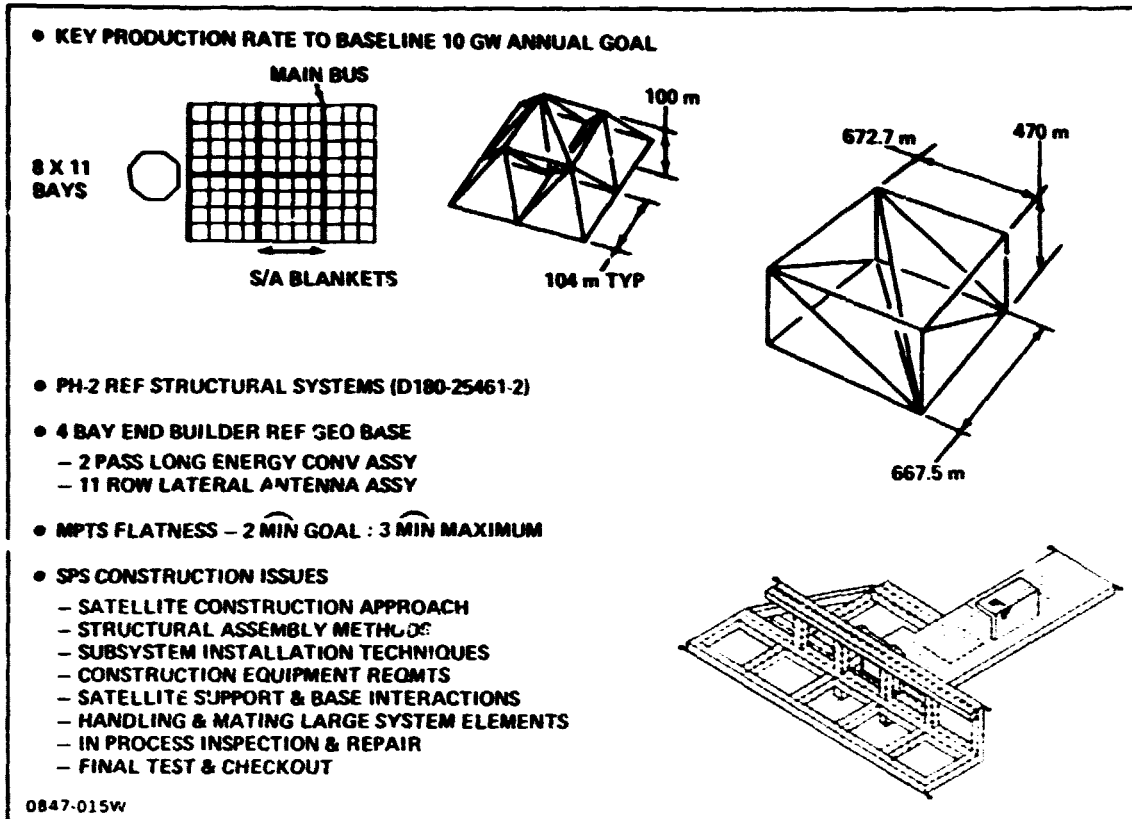
- KEY PRODUCTION RATE TO BASELINE 10 GW ANNUAL GOAL

MAIN BUS

8 X 11 BAYS

S/A BLANKETS

100 m

104 m TYP

672.7 m   470 m

667.5 m

- PH-2 REF STRUCTURAL SYSTEMS (D180-25461-2)

- 4 BAY END BUILDER REF GEO BASE
  - 2 PASS LONG ENERGY CONV ASSY
  - 11 ROW LATERAL ANTENNA ASSY

- MPTS FLATNESS – 2 MIN GOAL : 3 MIN MAXIMUM

- SPS CONSTRUCTION ISSUES
  - SATELLITE CONSTRUCTION APPROACH
  - STRUCTURAL ASSEMBLY METHODS
  - SUBSYSTEM INSTALLATION TECHNIQUES
  - CONSTRUCTION EQUIPMENT REQMTS
  - SATELLITE SUPPORT & BASE INTERACTIONS
  - HANDLING & MATING LARGE SYSTEM ELEMENTS
  - IN PROCESS INSPECTION & REPAIR
  - FINAL TEST & CHECKOUT

0847-015W

Figure 4-5 Solid State SPS Construction Requirements & Issues

	DAYS 0 20 40 60 80 100 120 140 160 180
ASSEMBLE ENERGY CONVERSION SYS	74 (LONG INDEX @ 0.5 mpm) 71
REINDEX BASE	1.5
ASSEMBLE INTERFACE SYS (YOKE)	10
ASSEMBLE POWER TRANSMISSION SYS	140
MATE ASSEMBLED SYSTEMS	5 GW BASELINE WITH KLYSTRONS 4
FINAL TEST & CHECKOUT	20 IOC 180.5 DAYS

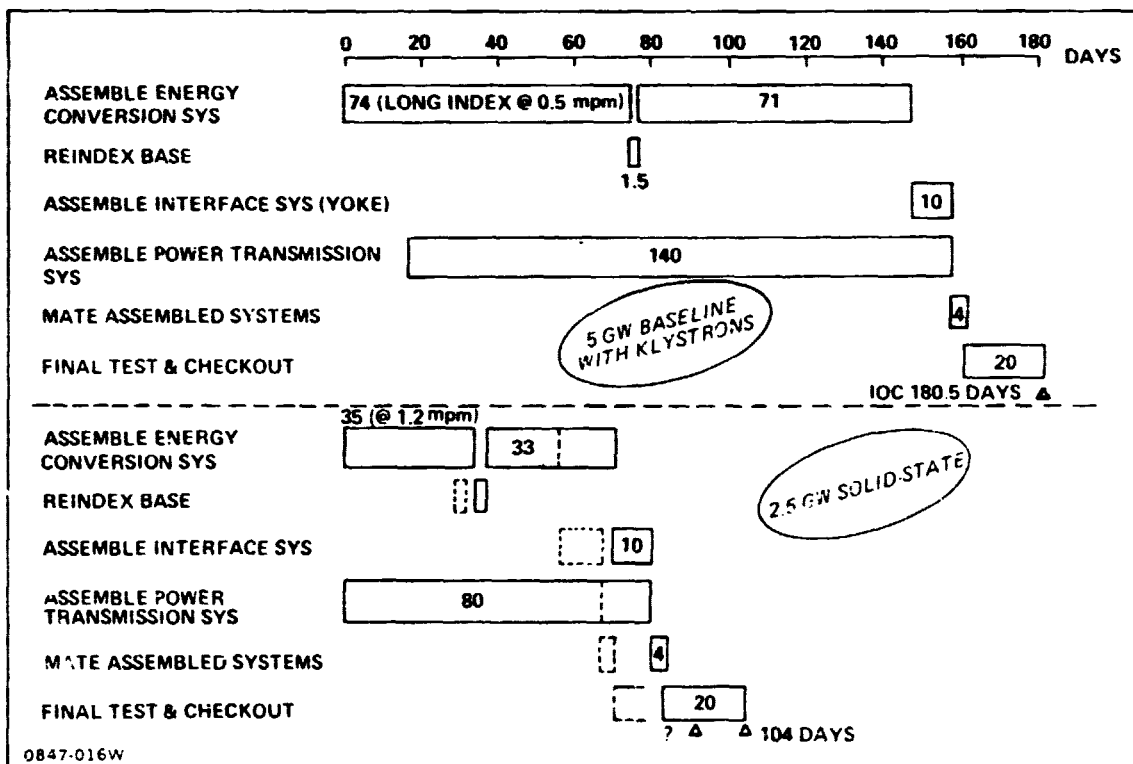|	
ASSEMBLE ENERGY CONVERSION SYS	35 (@ 1.2 mpm) 33
REINDEX BASE	
ASSEMBLE INTERFACE SYS	10
ASSEMBLE POWER TRANSMISSION SYS	80
MATE ASSEMBLED SYSTEMS	2.5 GW SOLID-STATE 4
FINAL TEST & CHECKOUT	20 ? △ △ 104 DAYS

0847-016W

Figure 4-6 SPS GEO Construction Timelines – 5 GW Baseline & 2.5 GW Solid State

Builder also assembles the solid state 8 x 11 bay energy conversion system during two successive passes, as previously defined. However, the production rate to complete final tests and checkout of the solid state SPS is slower than the reference SPS with klystrons, which is fully constructed and checked in GEO in six months. The production rate for the reference system is 27.7 MW/day. In order to match this production rate, the solid state SPS would have to be completed in one-half the time (i.e., 90 days) which, at this juncture, appears to fall short of the 10 GW annual production goal. The present design and construction approach used for the solid state SPS has slowed the production rate to 24.03 MW/day or 104 days to IOC.

Considering the inherent production capability of the 4 Bay End Builder Construction Base, Figure 4-7 shows how the total satellite construction time can be altered by either changing the fabrication rate for continuous longitudinal beams, reducing the length (i.e. number of rows) of the energy conversion system, or both. For example, the baseline SPS, which has a 16 row energy conversion system, is constructed in 180 days by limiting synchronized longitudinal beam fabrication to 0.5 meters per minute. By increasing the beam fabrication rate to 3 meters per minute, the entire SPS (including yoke assembly, systems mating, test and checkout) would be constructed in 140 days. A similar production advantage can be achieved with the shorter solid state energy conversion system, which is only 11 rows long. However, increasing the operating rate of the longitudinal beam builders is not sufficient to achieve the solid state SPS construction goal of either 90 or 104 days. To achieve these goals, additional cherry pickers must be provided to speed up the installation of solar array blankets. Hence, the solar collector assembly facility on the reference GEO base can be revised, as required, to meet either construction goal for the solid state SPS concept. The time critical construction operation, therefore, lies with assembly of the solid state antenna.

Operations analysis sequence for construction of the solid state antenna is shown in Figure 4-8. During Phase 3, major construction operations were analyzed from the top down, as was done previously for the reference system. Construction follows the same sequence as the reference system. A breakdown of assembly operations for the power transmission system is shown by the abbreviated flow illustrated on the lower half of the figure. This assembly activity includes the fabrication and assembly of the first row of primary and secondary structures (function 3.2.1). It also includes the parallel installation and inspection of other subsystems during first row construction. These subsystems include installation of RF subarrays (function 3.2.2), power
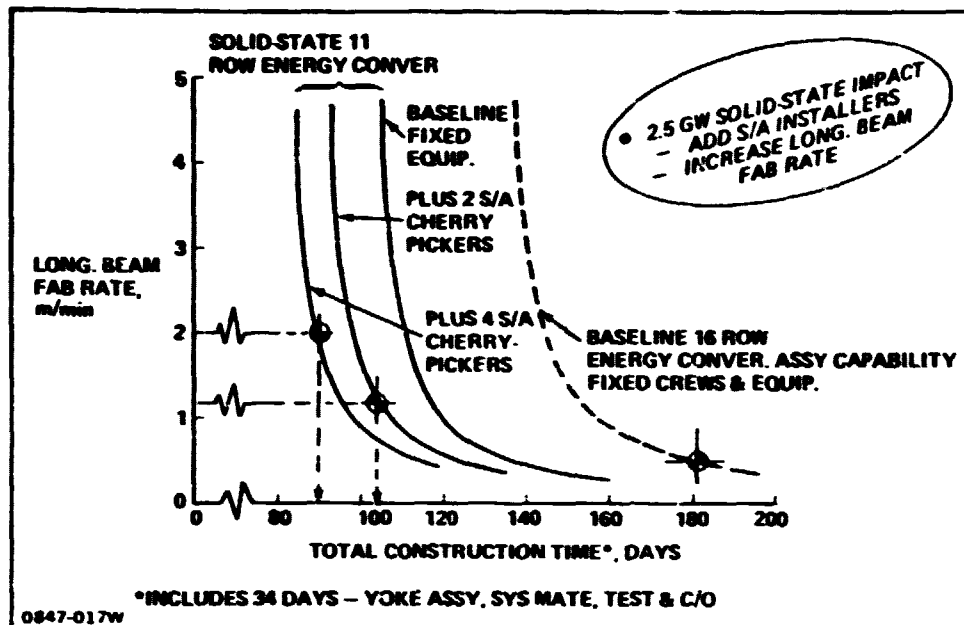
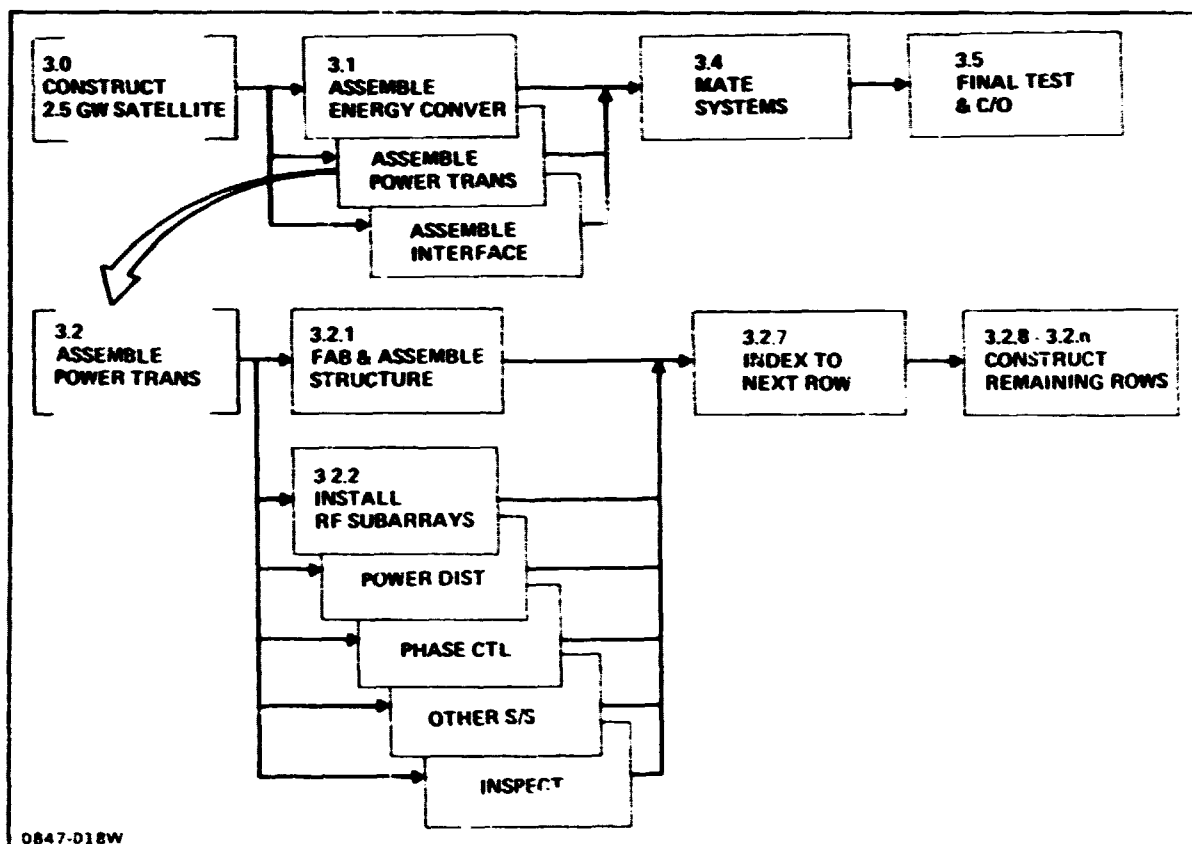Figure 4-7 GEO Base — Energy Conversion Production Capability

Figure 4-8 Satellite Power Transmission Construction Operations Analysis

distribution, phase control, etc. When first row construction is complete, the antenna is indexed away (function 3.2.7) to allow the second row to be added. The remaining rows of the antenna are constructed in a like manner.

4.1.2 Antenna Construction Operations

The structural design for the SPS power transmission antenna has evolved, as shown in Figure 4-9, from the Phase 1 A-frame structure to the reference pentahedral structure defined at the end of Phase 2. The Phase 2 reference antenna construction approach, however, was not updated for this change. Thus the reference antenna construction method still reflects the Phase 1 design concept, which is important when comparing the effect of solid state construction requirements.

In Phase 1, the antenna provided a transmitting area, 1 km in diameter, made from 98 bays of A-frame primary structure. Each bay had 10 triangular beams, 7.5 m deep, produced in space by beam machines operating at 5 m/min. Secondary structure, mounted to the primary structure, supported energy transmitting equipment. There were eighty-eight 104 m^2 bays of this deployable tetrahedral secondary structure. At the end of Phase 2, the 1 km diameter reference antenna was changed to a more efficient pentahedral primary structure having 88 bays. Each bay had 9 or 11 members, dependent on whether it required closing beams or not, which were 1.5 m deep beams. Construction of this structure was never analyzed, therefore no beam production rate is shown. An egg crate secondary structure was defined to support RF subarray equipment on 88 bays. The solid state SPS system in Phase 3 requires an antenna whose area increases to 1420 m diameter, effectively twice that of Phase 1 and 2. Primary structure uses the same pentahedron bays as defined in the Phase 2 reference system description (D180-25461-2). Fabrication of the 1.5 m deep triangular beams is limited to a beam production rate of about 1 meter per minute. Being larger in area, 172 bays of 104 m^2 egg crate secondary structure are required to support transmitting equipment.

Antenna Construction Options - Considering the solid state antenna, three alternate methods were considered for its construction. These options are sketched in Figure 4-10 which includes the Phase II baseline as a reference. The sketches are to the same scale, thus indicating the relative size of each antenna build area. The 1 km diameter 5 GW baseline is constructed by progressive buildup of its 11 row planform. The antenna is assembled one row at a time, as it is indexed back and forth through the fixed location antenna construction facility. As a result, the antenna must be supported during this process on a platform at least twice as large as the antenna is

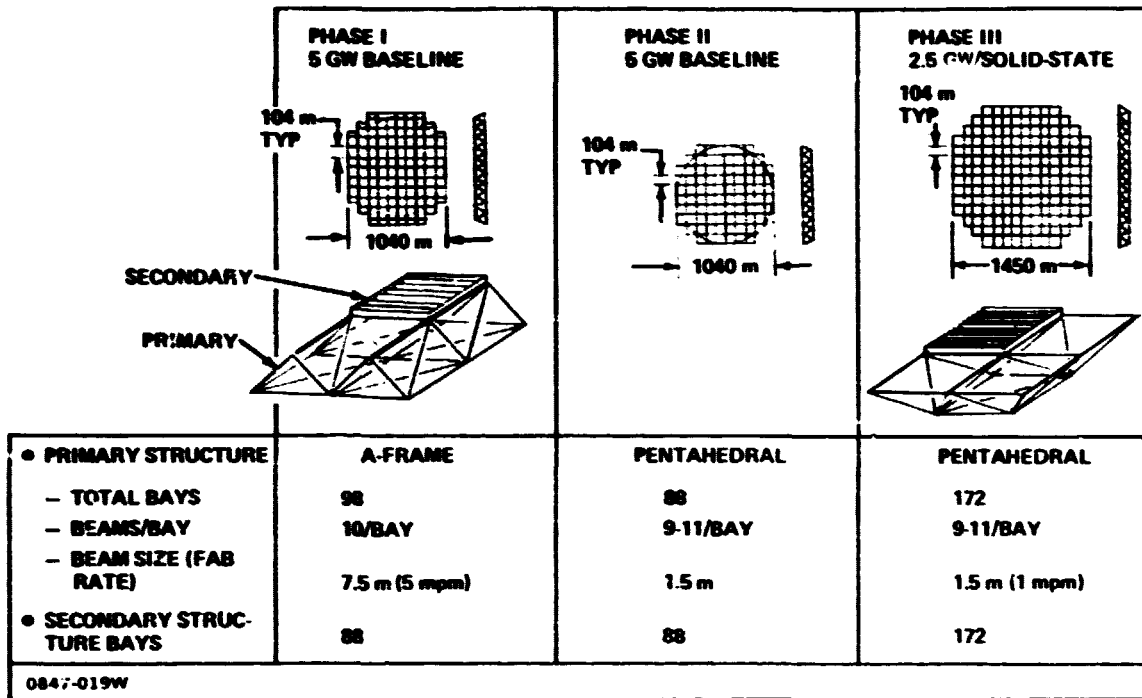| • PRIMARY STRUCTURE	A-FRAME	PENTAHEDRAL	PENTAHEDRAL
— TOTAL BAYS	98	88	172
— BEAMS/BAY	10/BAY	9-11/BAY	9-11/BAY
— BEAM SIZE (FAB RATE)	7.5 m (5 mpm)	1.5 m	1.5 m (1 mpm)
• SECONDARY STRUC-TURE BAYS	88	88	172

0847-019W

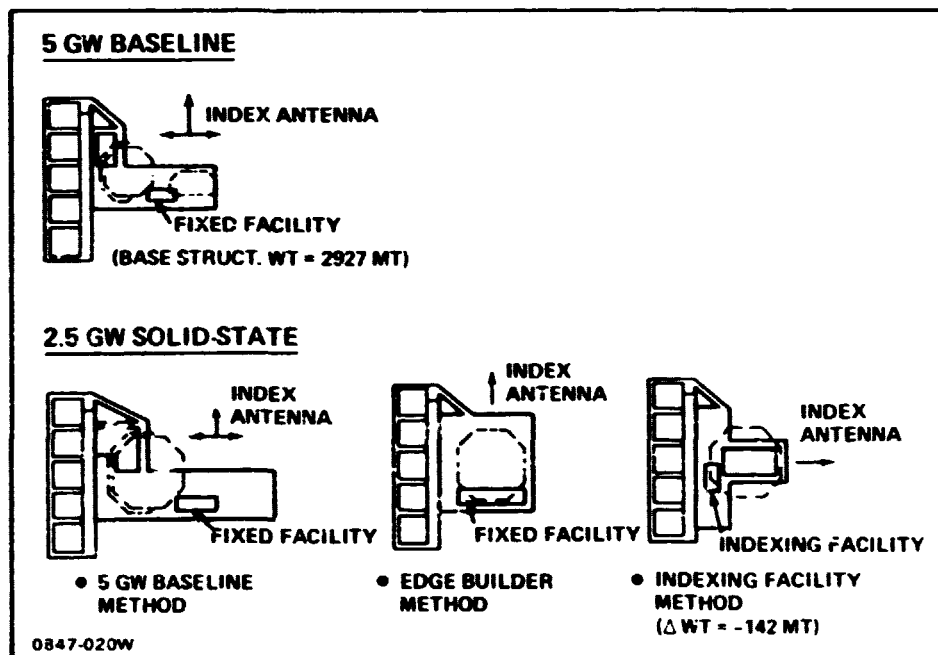Figure 4-9 SPS Baseline & Solid State Antenna Concepts

Figure 4-10 Antenna Construction Options

41

wide. The area of the 1.4 km diameter, 2.5 GW solid state antenna is nearly twice that of the 1 km diameter reference antenna. Hence, if the reference antenna construction approach is simply adapted to the solid state antenna requirement, the large antenna support platform would simply grow in proportion. As a consequence, other assembly approaches were considered to reduce the overall size of the antenna construction area. The first option uses the 5 GW baseline method to build the new antenna on a platform area approximately 65% greater than the 5 GW baseline area. This method caters for parallel construction of a yoke support for the antenna, as well as for the current cantilever support baselined for these options.

The second construction method is an edge builder in which the antenna indexes in one direction only. The construction facility is still of fixed location but is now much longer, since it must cover the width of the antenna to provide many machines for building all longitudinal beams simultaneously. Area for antenna construction is about 25% less than that for the first option but needs the longer facility for the increased number of beam machines. An antenna yoke support could be built on this facility but it would be a sequence operation which extends the timeline.

The third option retains the unidirection indexing of the antenna (Option 2) but relocates the small construction facility of Option 1 and allows it to move laterally to cover the width of the antenna. This is made possible by the introduction of cantilever support for the antenna in place of the yoke support. Construction area is minimum for this method and is, in fact, less than the 5 GW baseline area, even though the antenna is larger. This is reflected in the reduced weight for the base. Should a yoke support for the antenna be reintroduced, it will require added platform area, more facilities, and will extend the timeline. This third option was selected for preliminary design work to derive weights and costs.

Antenna Construction Sequence - Using this method of antenna construction, the overall assembly sequence is shown in Figure 4-11. It is built in rows of repeatable bays and first, the facility indexes across the construction base to fabricate and assemble the first row as it goes. It then indexes back along the track while, at the same time, the completed row indexes forward for one row width. The second row is now built onto the first row by the indexing facility on its second construction pass. This process is repeated until the antenna is completed. Taking a more detailed look at the sequence as it builds the first rows, the facility starts construction by building primary structure for the first bay of the first row. The facility then indexes for one bay length, then builds primary structure for the second bay while, at the same time, installing
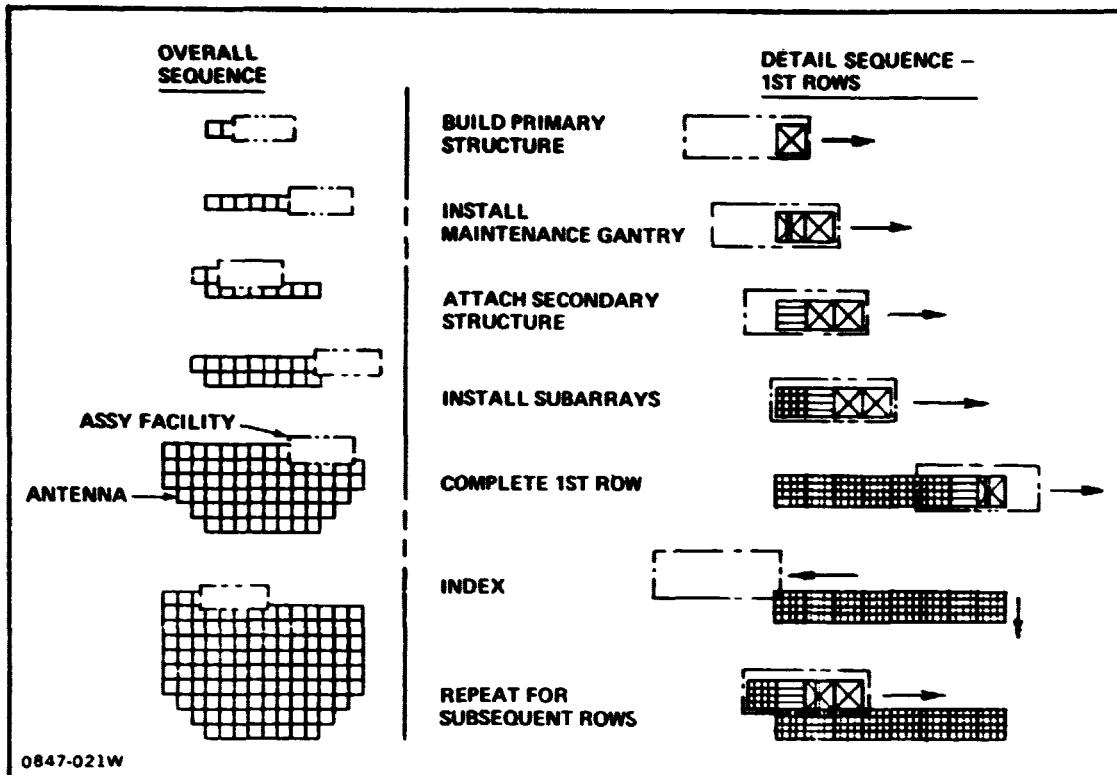
42

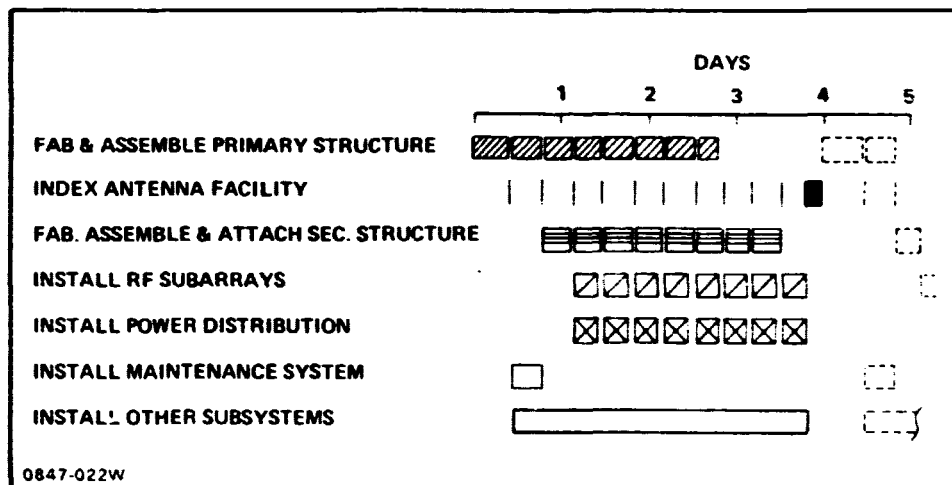Figure 4-11 Solid State Antenna Construction Sequence

Figure 4-12 2.5 GW Solid State Power Transmission System Assembly —
1st Row Timeline

43

maintenance equipment in the first bay. Following another one bay index of the facility, the third bay primary structure is built while secondary structure is assembled to the first bay primary structure in parallel. Another one bay index of the facility is followed by construction of the fourth bay primary structure while, at the same time, secondary structure is added to the second bay and subarrays installed on the first bay secondary structure. This process continues to complete the first row. It should be ncted that maintenance gantries are installed only on the first and last bays of this and all subsequent rows. Thus, two parallel maintenance operations can be performed along each row. At completion of the first row, the facility indexes back along its track while, at the same time, the completed row is indexed forward for one bay width. The sequence is now repeated for the second and subsequent rows to completion of the antenna build.

Antenna Assembly Times - The timeline for assembling the 1st row is shown in Figure 4-12. As previously described, the antenna facility builds the structure in progressive steps, and sequentially installs the required subsystems. There are eight primary pentahedral structural bays in the 1st row of construction. As each primary pentahedral bay is built, the antenna facility moves sideways to allow the next pentahedral bay to be added. Maintenance equipment is installed in the first structural bay before the secondary structure is attached. Hence the sequential installation of RF subarrays and power distribution subsystems parallels assembly of the 4th structural bay at the start of Day 2. This one day lag in subsystem installation is common to each row of antenna construction operations.

Construction time for the overall antenna is discussed in Figure 4-13. The 2.5 GW solid state antenna configuration contains 172 pentahedral bays which are arranged in rows of 8, 10, 12 and 14 bays per row. Time allowed to fully assemble the 14 rows of structure (primary and secondary) and install the required subsystems (RF subarrays, power distribution, etc) is shown. As each row is constructed, there is a one day lag in the sequential installation of subsystem hardware. The cumulative effect of this sequential process results in a 14 day delay in the total antenna construction time that may be used for either structural assembly or subsystem assembly. Therefore, only 66 days are available for dedicated assembly operations from the total construction time scheduled (80 days). In light of the 14 day constraint, it is questionable that any further reduction can be made in construction time without impacting the assembly facility, construction equipment, and related work crews. If
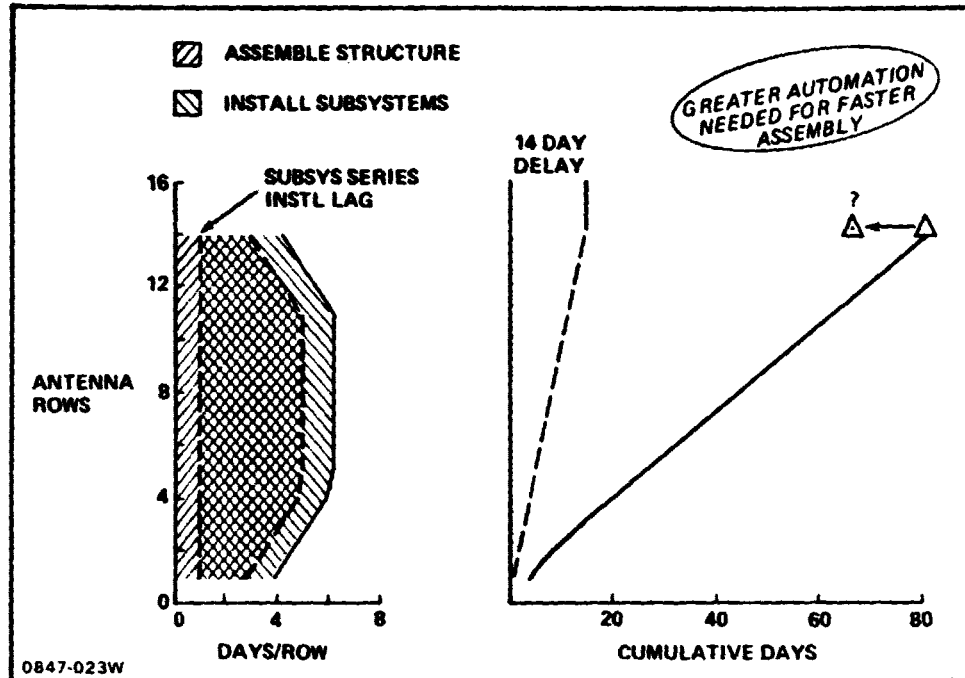
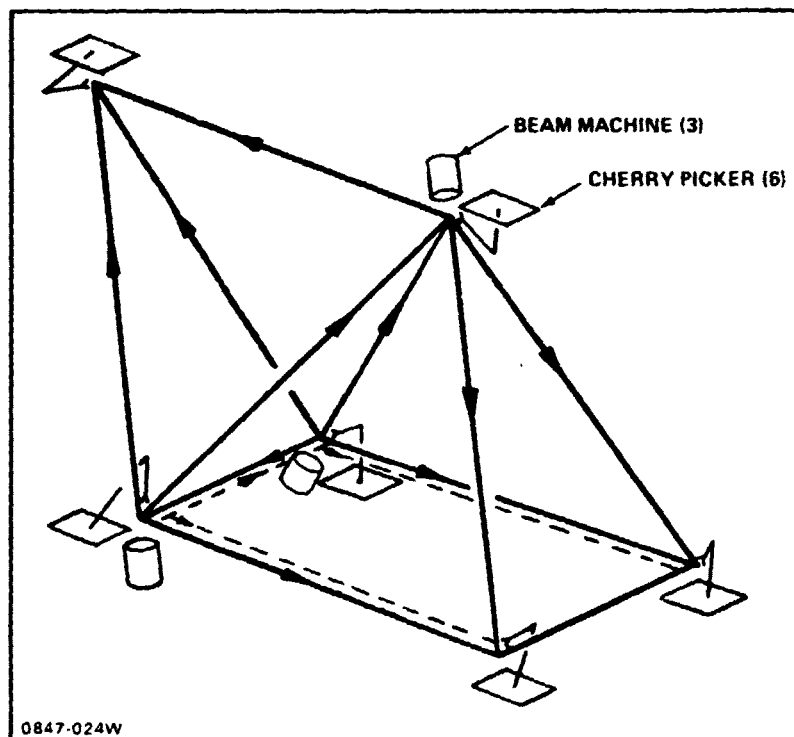**Figure 4-13 Solid State Antenna Construction Time**

**Figure 4-14 Antenna Primary Structure — Fabrication & Assembly
(1st Bay, 1st Row)**

faster antenna construction times are needed, it is recommended that the assembly sequence be re-examined with an eye toward implementing a greater degree of automation.

Primary Structure Fabrication and Assembly - Equipment types and quantities for building the antenna within the prescribed timeline are dictated by baseline construction scenarios. Considering the first row of the primary structure, Figure 4-14 shows that three beam machines and six cherry pickers will build all structural elements. Except for the first structural bay, each beam builder substation fabricates 3 beams in the required orientation and location. During assembly of the first bay in each row, 4 or 5 beams may be fabricated from these fixed beam builder substations. As shown, the outboard edge member is transferred to its assembly location by cherry pickers, after being produced by a beam machine located on the same level. The other beams in the structure are produced and located by pointing the pivot mounted beam machines in the required direction. Cherry pickers, located at node points, then align the beams and join them. An arrow on each beam member shows its direction of fabrication and indicates the beam machine which produced it.

Requirements for segmented beam design and automated beam building operations affect the assembly rates achievable for the antenna primary structure. For example, automated fabrication of the segmented beams for the pentahedral structure requires that four basic operations be performed, as shown in Figure 4-15. A typical beam building cycle includes about 30 minutes for handling each 104 m long beam. This time is over and above beam fabrication time and allows for alignment of the beam builder and attaching end fittings. The actual fabrication time is a function of beam length and batten spacing. Achievable composite beam fabrication rates are shown in the lower left corner of the figure for different beam batten spacings and beam cap framing rates. (These data were developed by Grumman in support of its Phase 1 SPS studies for Boeing (D180-25037-2)). For the required batten spacing of 1.5 m, a fabrication rate of 1.7 m/minute was selected since the curve quickly becomes asymptotic above this rate. Using the foregoing data and a production rate of 75%, primary structure requires at least 62 days to be assembled.

Secondary Structure Assembly Requirements - Primary structure is an assembly of pentahedral bays, each of which presents an open surface 104 m x 104 m. For each of these bays, a secondary structure is necessary to support 100 subarrays. Figure 4-16 shows an egg crate structure assembled from 2.5 m deep beams which are spaced to support the 10.4 m-wide subarrays and provide lateral stability at 20.8 m intervals.
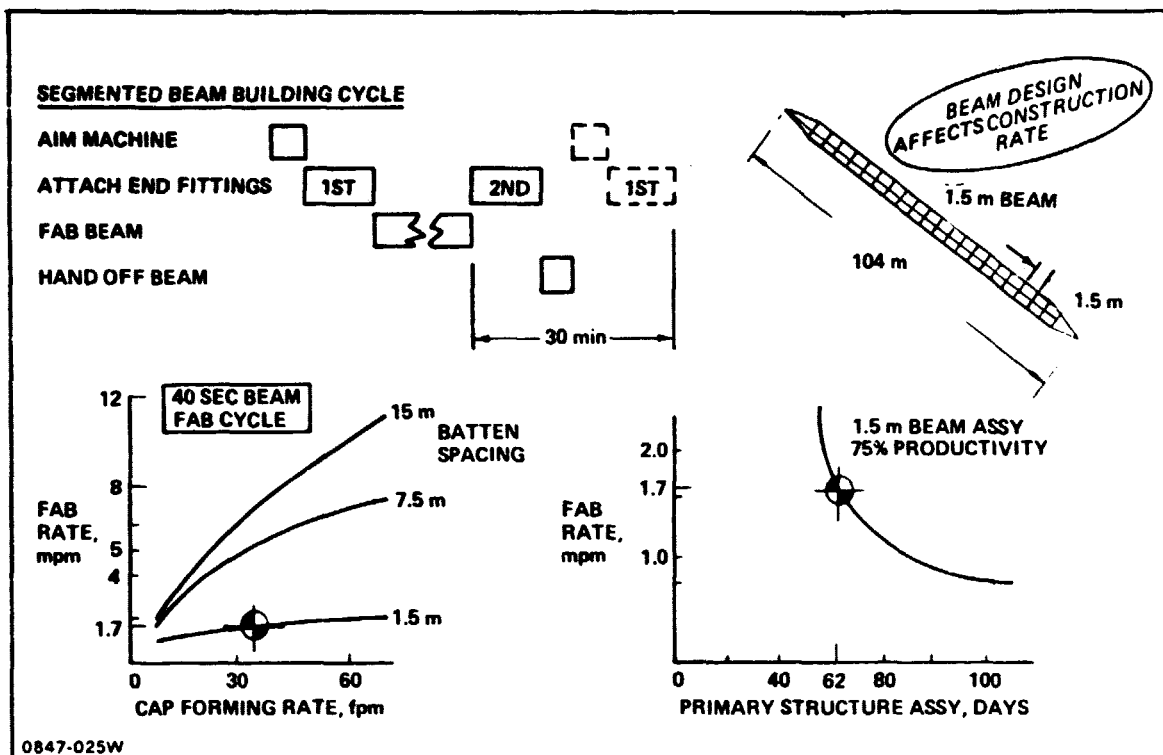
SEGMENTED BEAM BUILDING CYCLE

AIM MACHINE

ATTACH END FITTINGS

FAB BEAM

HAND OFF BEAM

BEAM DESIGN AFFECTS CONSTRUCTION RATE

1.5 m BEAM

104 m

1.5 m

30 min

40 SEC BEAM FAB CYCLE

15 m BATTEN SPACING

7.5 m

1.5 m

FAB RATE, mpm

CAP FORMING RATE, fpm

1.5 m BEAM ASSY 75% PRODUCTIVITY

FAB RATE, mpm

PRIMARY STRUCTURE ASSY, DAYS

0847-025W

Figure 4-15 Antenna Primary Structure Fabrication Requirements

JOINT FITTING

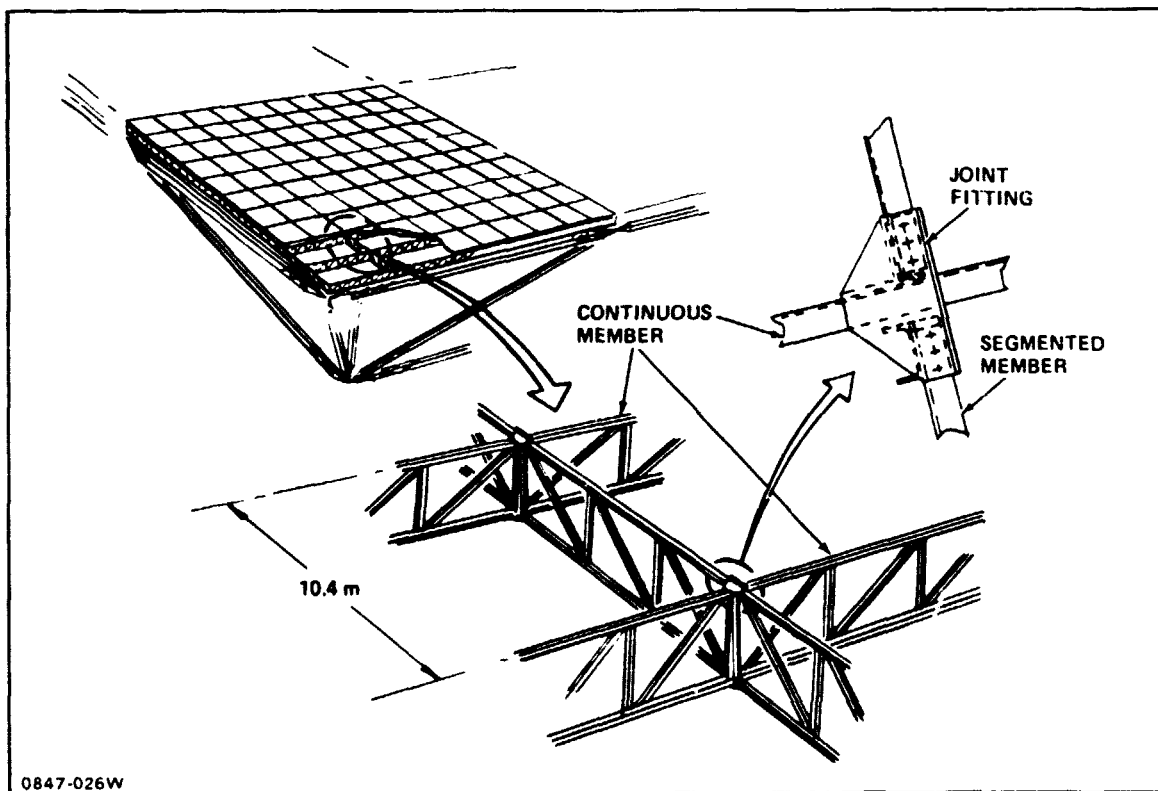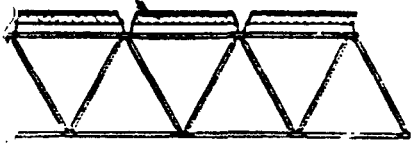CONTINUOUS MEMBER
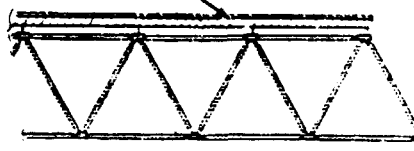
SEGMENTED MEMBER

10.4 m

0847-026W

Figure 4-16 Secondary Structure Assembly Requirements

47

The longitudinal and lateral beams are joined to form a grid having 50 cells (10.4 m x 20.8 m).

It can be built as segmented structure which covers one bay of the primary structure, or it can be built as a continuous structure covering the whole antenna. Figure 4-17 summarizes some advantages and disadvantages of the options. A segmented structure is easier to assemble, handle and install since it can be built in the 104 m^2 units, then individually mounted at three points to the primary structure, thus minimizing effects of primary structure operational distortions. A disadvantage is that, being separate squares, closing members are necessary and these add to the total beam length and antenna mass. Continuous secondary structure adds to antenna overall stiffness, which helps to minimize subarray flatness distortions during operation. Installation to the primary structure is more complex since it would be built in sections, which are then attached to the primary structure and to each other by moment carrying joints. The segmented secondary structure approach is the preferred option since it simplifies construction.

Having selected separate, 104 m^2 units for the secondary structure, the four options shown in Figure 4-18 were considered for fabrication and assembly of the 2.5 m-deep beams. They may be prefabricated on the ground for high density, nestable space transport or produced in space by automated beam machines. One option is to assemble the unit completely from 10.4 m-long beams. This would be done by a facility weaving across a support bed assembling in series as it goes. Many joints must be made to assemble two, three and four beams at a time. The second option is to build from 20.8 m-long beams. This involves a similar operation to the 10.4 m beams assembly, but reduces the number and complexity of the assembly joints. Third and fourth options use the end builder principle by producing synchronized continuous beams in one direction, jointed by segmented beams to form the egg crate structure. In one case, 11 beam machines fabricate continuous beams which are interjoined by sixty 10.4 m beams. The other case used 6 beam machines to produce continuous beams interjoined by fifty-five 20.8 m beams.

The four assembly options (10.4 m or 20.8 m beam buildup and 6 or 11 beam autofab) are compared in Figure 4-19 in terms of their structural assembly method, total assembly time, required construction equipment, construction base impact and number of crew operators per shift.

	SEGMENTED SECONDARY STRUCTURE	CONTINUOUS SECONDARY STRUCTURE
ADVANTAGE	• SIMPLER ASSY & INSTALLATION • MINIMIZES EFFECTS OF PRIMARY STRUCTURE DISTORTIONS	• ADDS TO ANTENNA STIFFNESS
DISADVANTAGE	• ADDITIONAL BEAM LENGTH	• MORE DIFFICULT ASSY & INSTALLATION • SHARES PRIMARY STRUCTURE DISTORTIONS

0847-027W

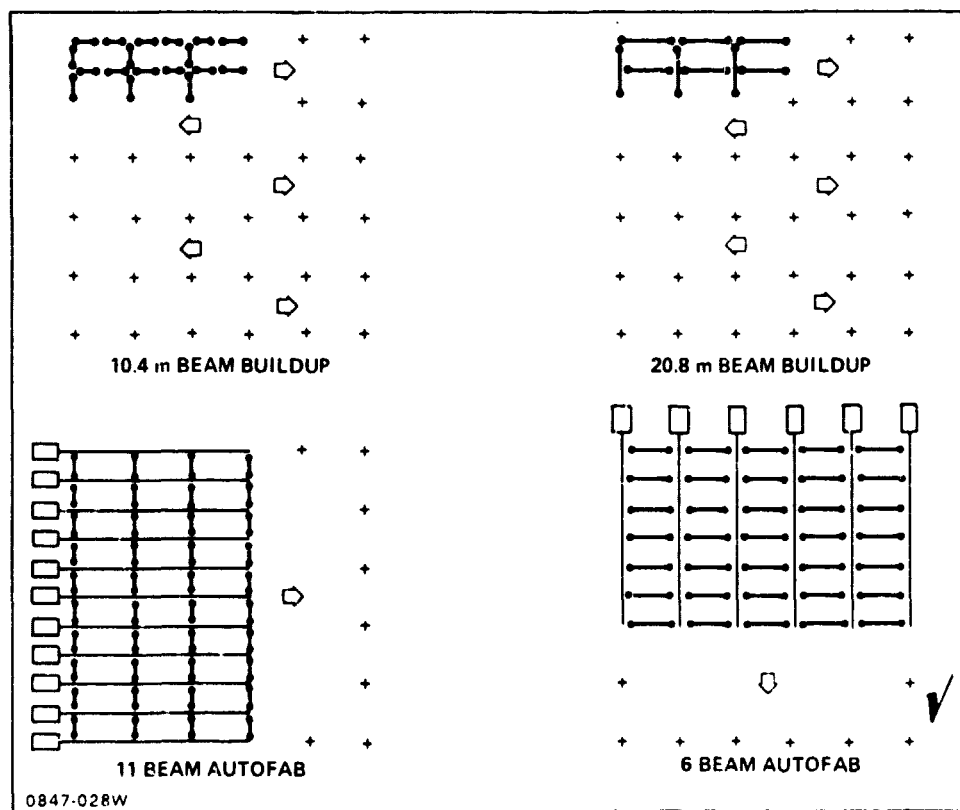Figure 4-17 Secondary Structure Installation Concepts

10.4 m BEAM BUILDUP   20.8 m BEAM BUILDUP

11 BEAM AUTOFAB   6 BEAM AUTOFAB

0847-028W

Figure 4-18 Secondary Structure Assembly Options

	10.4 m BEAM BUILDUP	20.8 m BEAM BUILDUP	11 BEAM AUTOFAB	6 BEAM AUTOFAB
ASSEMBLY METHOD	SERIES BAY-TO-BAY	SERIES BAY-TO-BAY	SYNCHRONIZED FRAME-TO FRAME	SYNCHRONIZED FRAME-TO-FRAME
ASSEMBLY TIME, MIN	930	720	225	305
CONSTRUCTION EQUIPMENT	100 m GANTRY 2 BEAM DISPENS (10 m LAT & LONG) JOINERS	100 m GANTRY 2 BEAM DISPENS (20 m LAT & LONG) JOINERS	11 BEAM BUILDERS 10 BEAM DISPENS (10 m LAT) JOINERS	6 BEAM BUILDERS 5 BEAM DISPENS (20 m LAT) JOINERS
BASE IMPACT	MOBILE SUBSTA SUPPORT	MOBILE SUBSTA SUPPORT	FIXED SUBSTA UTILITIES	FIXED SUBSTA UTILITIES
CREW OPERATORS	8	6	4	4

PRIMARY STRUCTURE ASSEMBLY LIMITATION = 308 MIN   (PREFERRED)

0847-029W

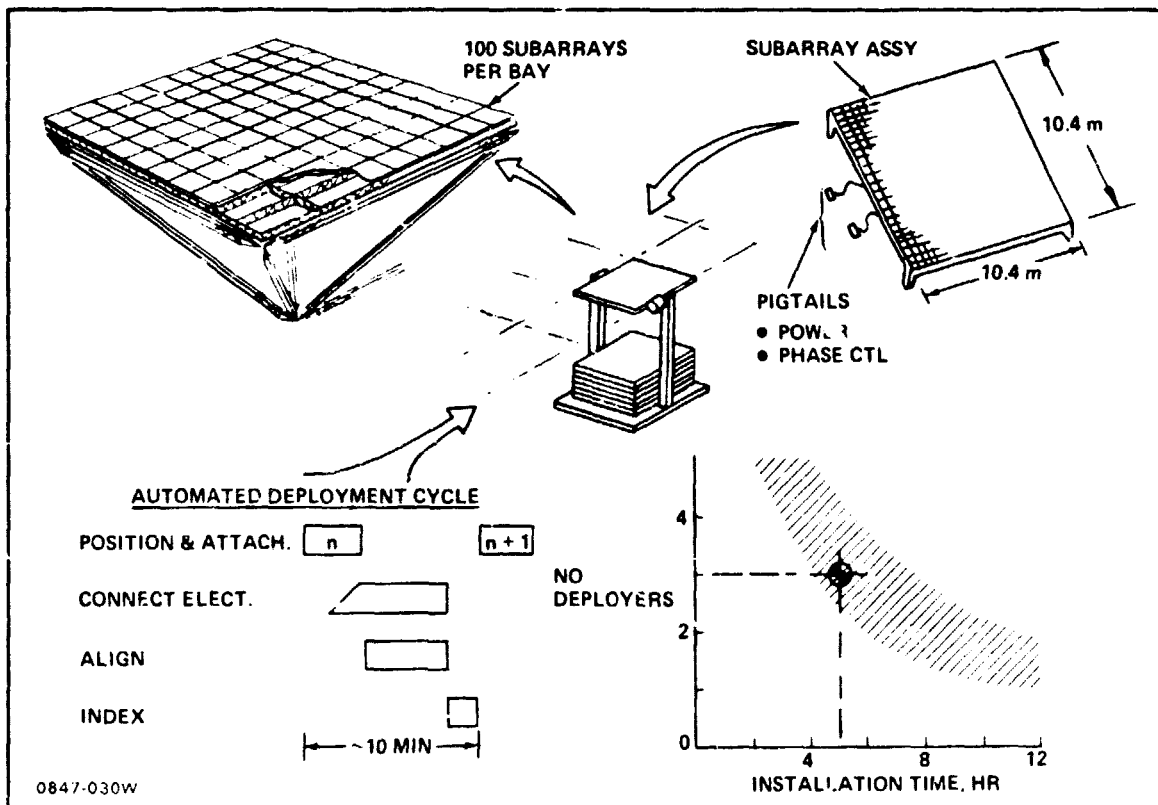Figure 4-19 Secondary Structure Assembly Options Comparison

Figure 4-20 Solid State Subarray Installation Requirements

As previously noted the secondary structure must be completed and installed in parallel with the assembly of preceding primary structure. Due to the primary structure assembly time limit (308 minutes) only the two autofab methods can meet this requirement. Both methods require four crew operators and have the same impact on the base. The discriminator is, therefore, the number of beam machines and dispensers. This leads to the six beam autofab method as the preferred option.

<u>Installation of Subarrays and Other Subsystems</u> – Mounting 10.4 m^2 preassembled solid state subarrays to this secondary structure requires mechanical and electrical connections. Figure 4-20 presents requirements for subarray installation and shows an automated deployer which takes a subarray installation and shows an automated deployer structure that makes the connections. The 10 minutes deployment time estimated for automatically dispensing and installing each subarray is based on the equipment concepts defined in Boeing's earlier System Definition Study (D180-24071-1).

At least three deployers are needed to meet this requirement. The number of deployers needed for the subarrays is a function of the installation time, which must match the time allotted to the building of the primary structure.

The phase control wiring harness (or perhaps fiber optics harness) is installed on the secondary structure as it is being assembled. The interbay phase control network is connected as secondary structure unit is attached to the primary structure. The phase control interconnection between the subarrays and the harness is accomplished as part of the subarray installation operation.

The antenna power bus is installed similar to the reference antenna construction operation.

4.2 SOLID STATE SPS CONSTRUCTION BASE

The GEO construction base for the solid state SPS concept is shown in Figure 4-21. This base is 3.44 km wide x 2.75 km long x 0.7 km deep, whereas the reference base measures 3.65 km long. Configuration of this solid-state SPS Construction Base closely follows the reference GEO base described in the Phase 2 study. For example, the energy conversion system is built in the same solar collector assembly facility, while the rotary joint is assembled on a facility very similar to that of the previous base.

The main differences are in the antenna construction facility. It is smaller in area than that on the reference base, since the construction method can now be simplified due to the change in support of the antenna from the rotary joint. Instead of a fixed antenna assembly facility and bilateral indexing of the growing antenna, the antenna assembly facility now indexes laterally across the antenna platform as it builds the antenna in rows. The platform is a frame of open truss members which provides tracks along which the antenna indexes as it is built. Facilities for mating the antenna to the rotary joint are similar to those in the Phase 2 Study. It is positioned high in the facility to produce the antenna with its c.g. closely aligned with that of the solar collector, thus minimizing control penalties during SPS operations.

4.2.1 Antenna Construction Facilities

Figure 4-22 illustrates the antenna construction operation and shows where the rotary joint is assembled. The antenna is built in one direction, bay by bay, with an assembly facility which indexes across the base. As the antenna is progressively built, the completed rows are indexed outboard and the assembly facility tracks back to start building the next row. The antenna assembly facility and the rotary joint assembly facility are able to operate independently and index across the base as needed. The rotary joint, which provides electrical and mechanical interface between energy conversion and power transmission systems, is built in parallel. Figures 4-23 and 4-24 show how the partially constructed antenna might be supported during this construction operation.

Antenna Assembly Facility - A more detailed look at the antenna assembly facility is presented in Figure 4-25. It covers four bays of the antenna primary structure and builds in one direction only. At one end, the facility builds primary structure on the lower and upper levels. Maintenance gantries are installed in the next lower facility, followed by fabrication and installation of the secondary structure to the primary structure. In the last lower level facility, subarrays are installed on the secondary

ANTENNA CONSTRUCTION SEQUENCE
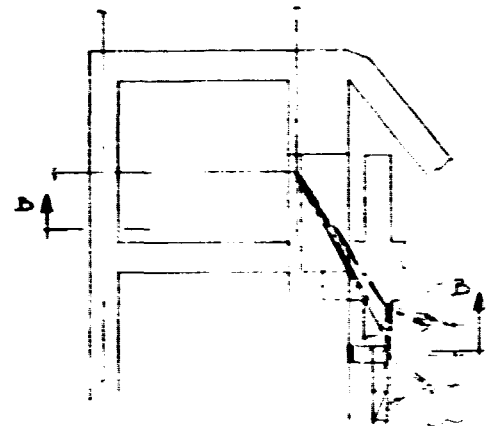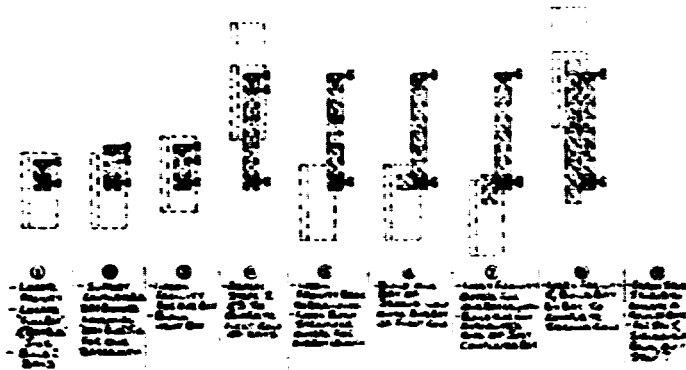
START OF INSTAL'N OF
SOLAR COLLECTOR/ROTARY JOINT
INTERFACE STRUCTURE
(REMAINING STRUCTURE INSTALLED
AS FINAL ERGN; PHASE 2, AND 3)/

SECTION B-B

Base Level

Antenna Support Level

Antenna Construction Facility
Track Level
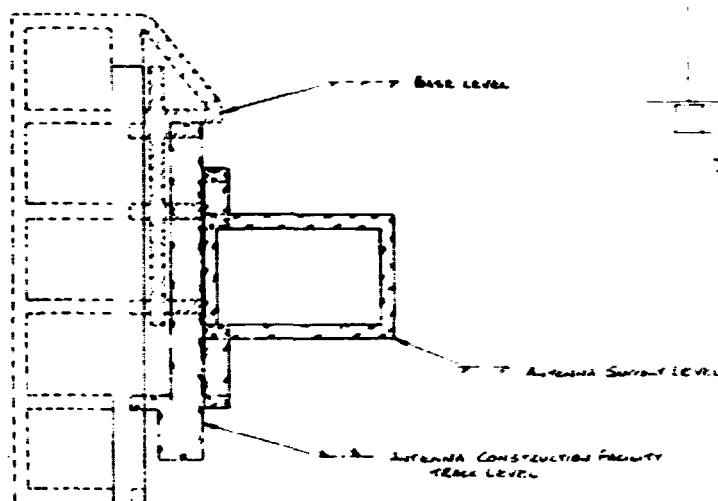
SKETCH SHOWING BOUNDARIES
OF ANTENNA CONSTRUCTION LEVELS

PRIMARY STRUCT
ASSY
PRIMARY STRUCT
ASSY
POWER DISTRIB
INSTL'N

PRIMARY STRUCT
ASSY
MAINTENANCE
GANTRY
INSTL'N
SECONDARY
STRUCT ASSY
& INSTL'N
SUBARRAY
INSTL'N
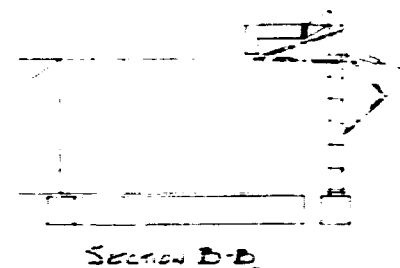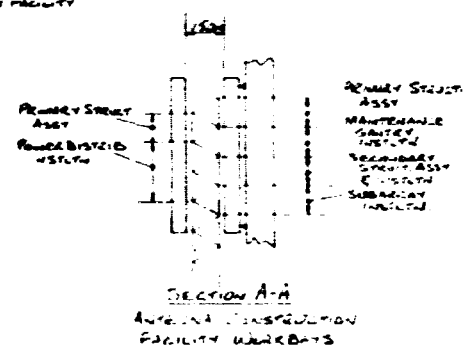
SECTION A-A
ANTENNA CONSTRUCTION
FACILITY WORKBAYS

ORIGINAL PAGE IS
OF POOR QUALITY
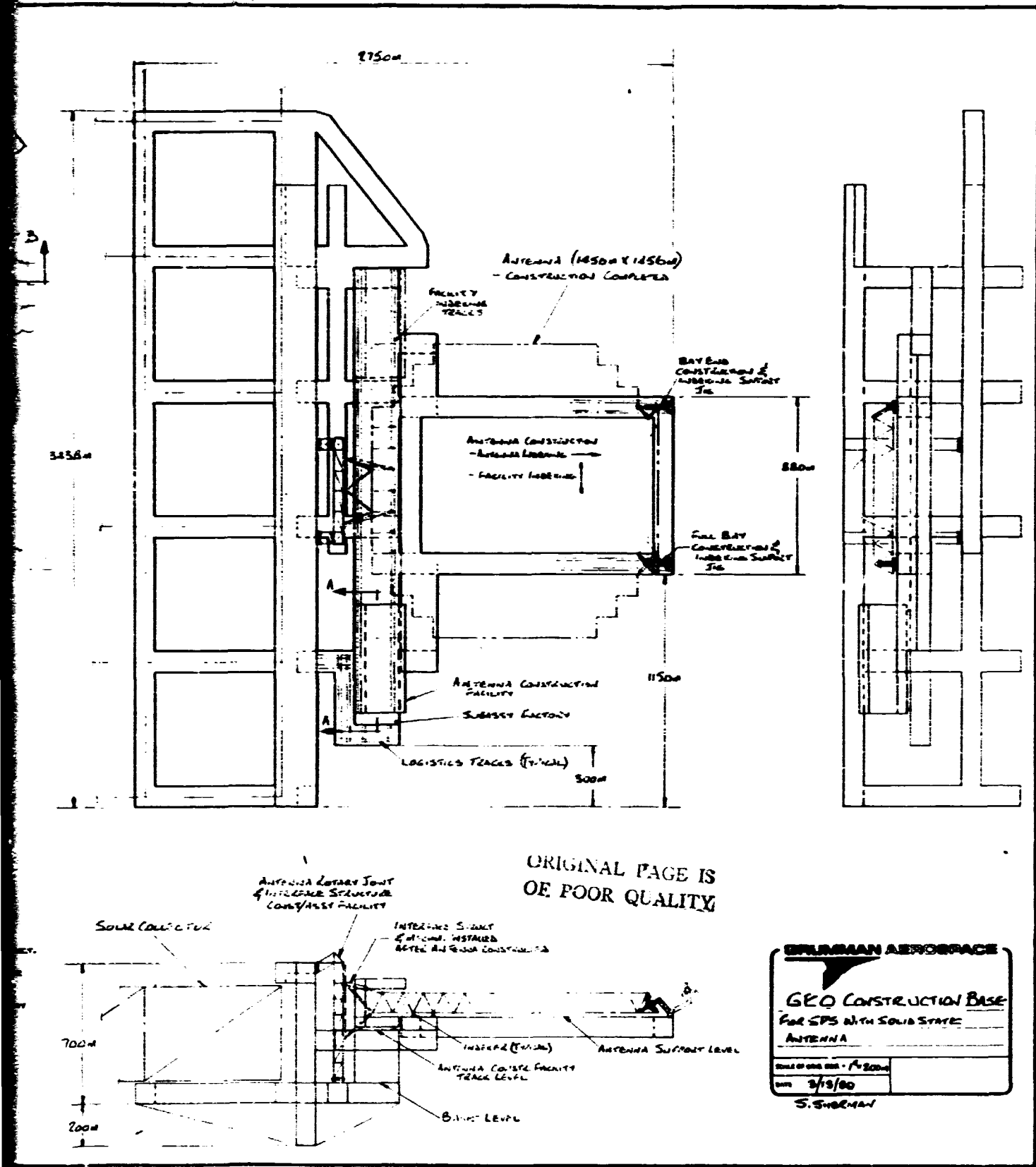
Figure 4-21 GEO Construction Base for SPS with Solid State Antenna

53

- BUILD FIRST ROW OF ANTENNA BY INDEXING ASSEMBLY FACILITY
- START ROTARY JOINT CONSTRUCTION IN PARALLEL

0847-032W

- CONTINUE ANTENNA BUILD, ROW-BY-ROW, TO COMPLETION
  - INDEX ASSY FACILITY FOR EACH ROW
  - INDEX ANTENNA OUTB'D AS EACH ROW IS COMPLETED
- CONTINUE ROTARY JOINT CONSTRUCTION TO COMPLETION
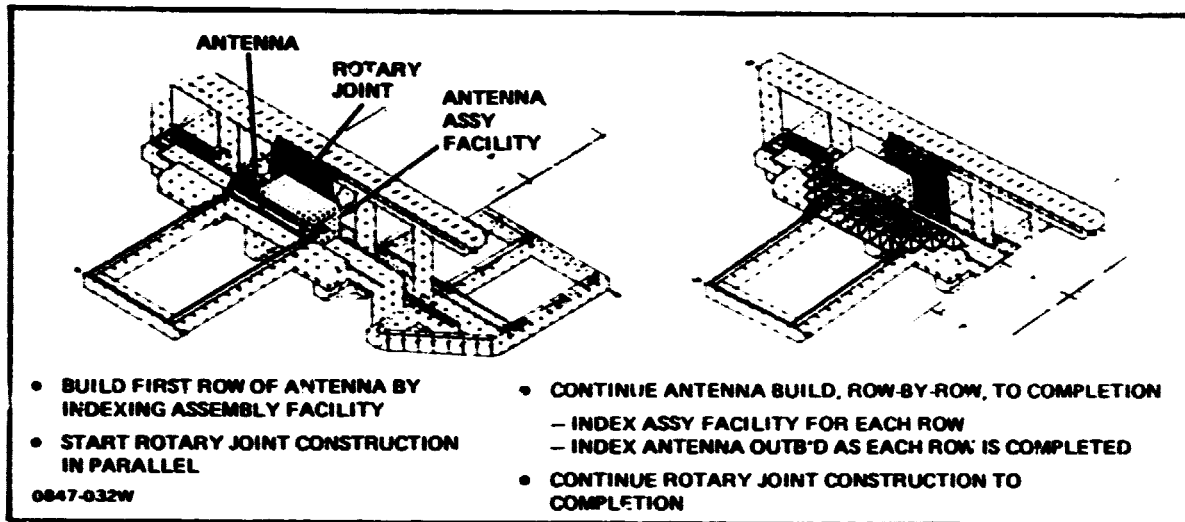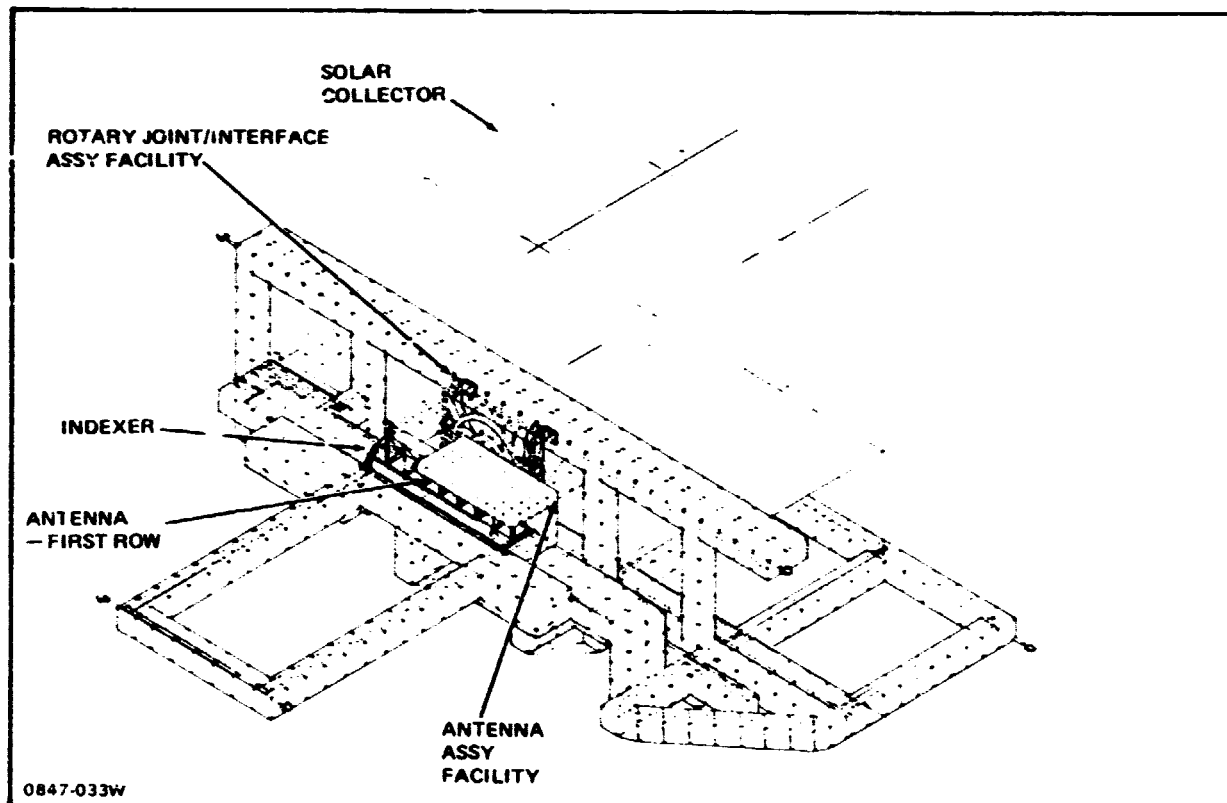
Figure 4-22   Antenna Construction Operations

Figure 4-23   Antenna First Row Build

54

structure. At the corresponding upper level power distribution busses and switch gear are installed. Primary structure fabrication and assembly operations are shown in Figure 4-14. The assembly station for secondary structure is shown in some detail in Figure 4-26.

This station is located in the antenna assembly facility which indexes across the base to build the antenna in successive rows. Here, secondary structure is fabricated, assembled and installed.

The secondary structure assembly station is 140 m x 118 m x 25 m in size. A large bed, sized for the 104 m per side structure unit, provides a flat surface for its assembly. This assembly station operates like a mini end builder which operates six beam machines to fabricate continuous longidutinal, two-dimensional 2.5 m beams in unison. At the same time, two similar beam machines located at an upper level produce 20.3 m beams. These segmented beams are collected by the Lateral Member Installation gantry for assembly to the continuous beams. Continuous beam fabrication proceeds in 10.4 m steps to accommodate synchronized lateral member attachment operations. The gantry, with five 20.8 m beams mounted on it, positions and joins these beams to the continuous longitudinal beams. The gantry then returns to its original position to collect five more short beams. As this process is repeated, the assembled structure is indexed outboard across the bed. Indexers guide the leading edge of the structure to maintain the required geometry and provide structural support. On completion of this 104 m^2 unit structure, two elevating cross-beams lift and support the secondary structure for its attachment to the primary structure positioned overhead. Subarrays installation to the secondary structure is performed by three tracking facilities, each of which carries a store of 10.4 m^2 subarrays for successive installation on the secondary structure. Figure 4-20 includes a sketch of this type of facility.

Antenna Flatness and Support - To achieve the required SPS microwave power transmission performance, the solid state antenna must be constructed to meet similar flatness requirements to those defined for the reference klystron antenna. The basic alignment requirement for the subarray surface is ±3 arc minutes in the operating environment. This includes all manufacturing errors, all static and dynamic movement due to construction flight attitude loads, and all related thermal distortions. A recent study on achievable flatness in a Large Microwave Power Antenna (NASA-15423) recommended a design goal of 2.00 arc minutes rms for the subarray slope error. This 2.00 design slope error was budgeted between manufacturing tolerance (1.50), maneuvering tolerance (1.10), thermal allowance (0.70) and attitude control system
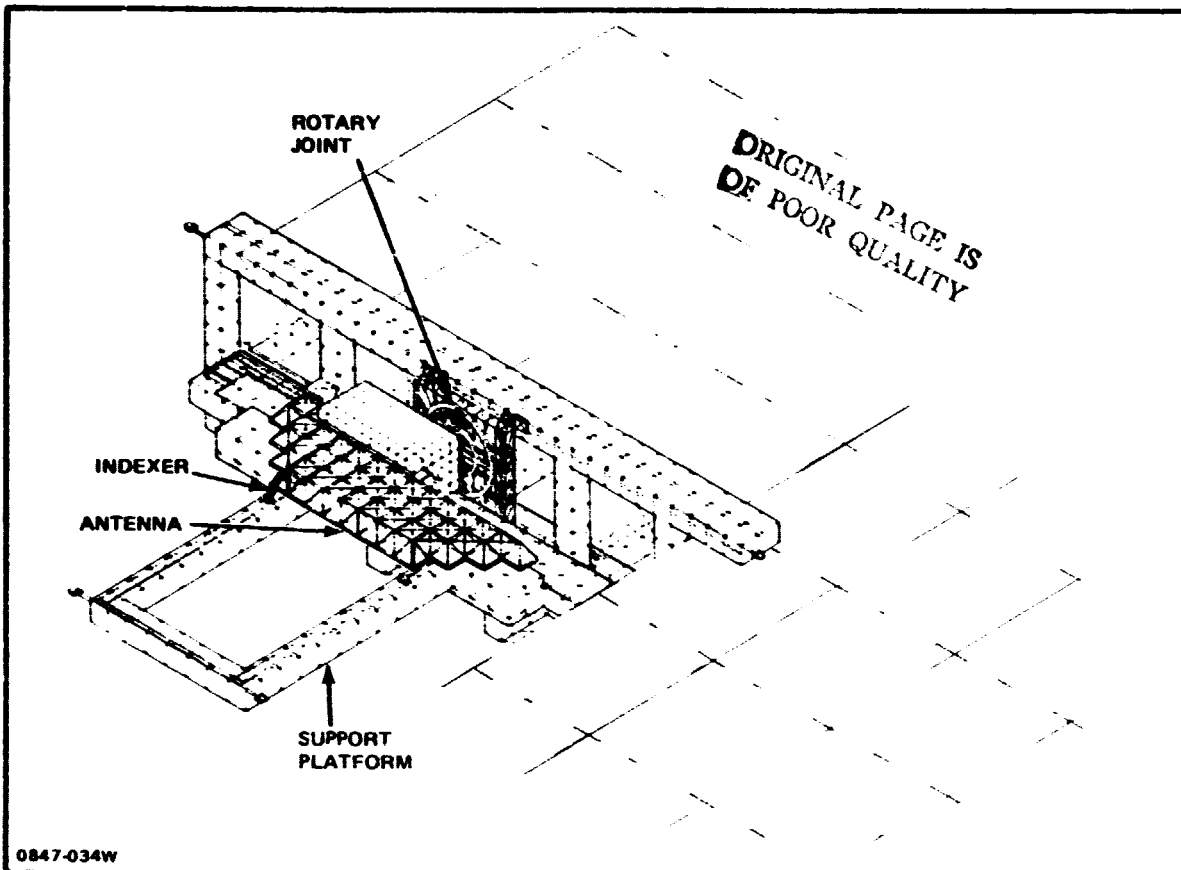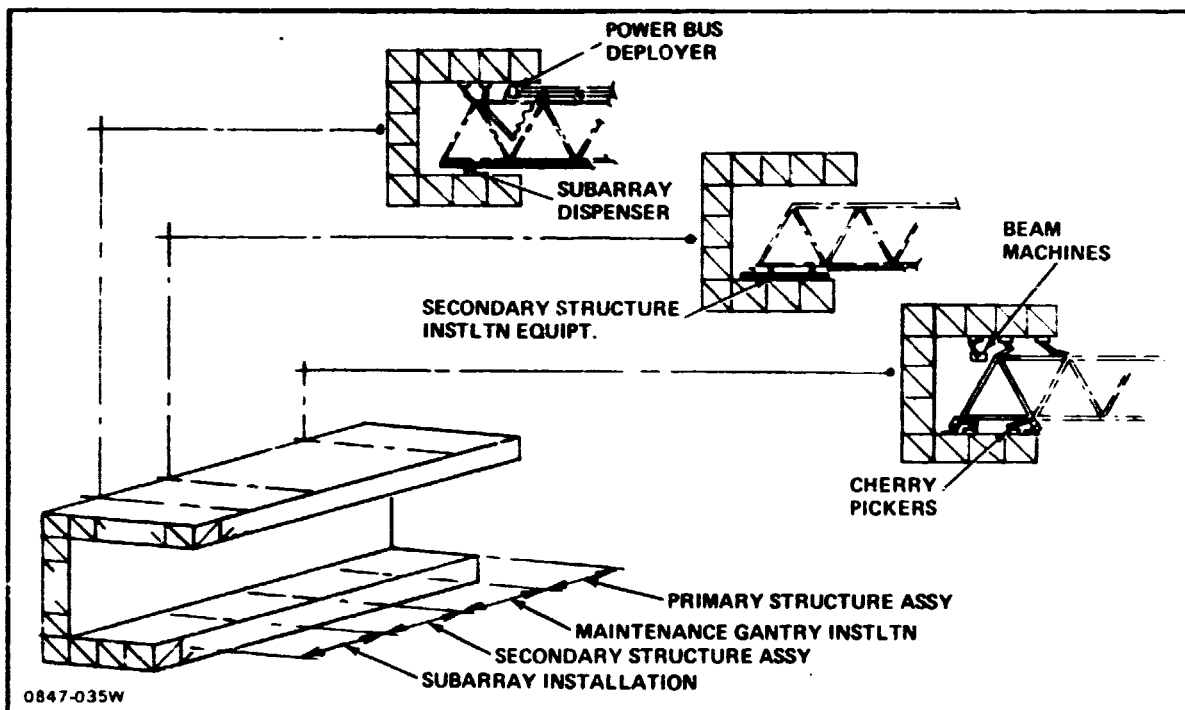
Figure 4-24 Antenna Buildup Row by Row

Figure 4-25 Solid State Antenna Assembly Facility

.

(0.00). Attitude control errors only become important for the completed SPS when line-of-sight pointing accuracy must be maintained. At that point any built-in manufacturing bias should be detectable and correctable by electronic beam offset techniques.

Figure 4-27 lists sources of misalignment which may occur during construction and offers possible solutions.

During space assembly, the antenna is supported by indexers which run on a flatbed outrigger structure. Deviations from flatness of the bed will be reflected in the flatness of antenna structure. Other sources of misalignment during fabrication are tolerances of the structural beam lengths and of assembly jigs. A proposed solution for this problem is to locate Electro Optical Distance Measuring Equipment on the base and optical reflectors at suitable points on the emerging antenna. The equipment will sense misalignments and call for adjustments of structure beam lengths to compensate. Firing of attitude control thrusters will impose inertia forces on the antenna, resulting in distortion of its structure. These distortions can be minimized by the number of indexers tying the antenna to the stiffer base. Thermal distortion effects, due to differing thermal coefficients for dissimlar materials and to thermal expansion variation with sun/shade changes, require careful materials selection and a constant attitude to the sun.

While plausible techniques have been identified to meet the antenna flatness requirement, a great deal of additional analysis and technology development work remains to be accomplished before we can be confident in the achievable flatness. For example, future dynamic analysis of the satellite construction process should investigate the effect of base interactions on the surface flatness of the emerging antenna.

Rotary Joint/Interface Assembly - As in the reference approach, the rotary joint and antenna are simultaneously built in their facilities. When the power transmission system is fully constructed, the antenna assembly facility is moved away and the rotary joint/interface assembly facility is positioned to build and attach the interface end-mounted linear actuator support structure. The electrical bus is fed across this structure to connect the rotary joint slip ring with the antenna systems.

Final mating of the rotary joint/antenna assembly with the solar collector is accomplished, similar to the reference approach, as shown in Figure 4-28. First the base is indexed to the solar collector antenna support strut pickups, then the antenna assembly is indexed to align with the collector and the rotary joint facility is
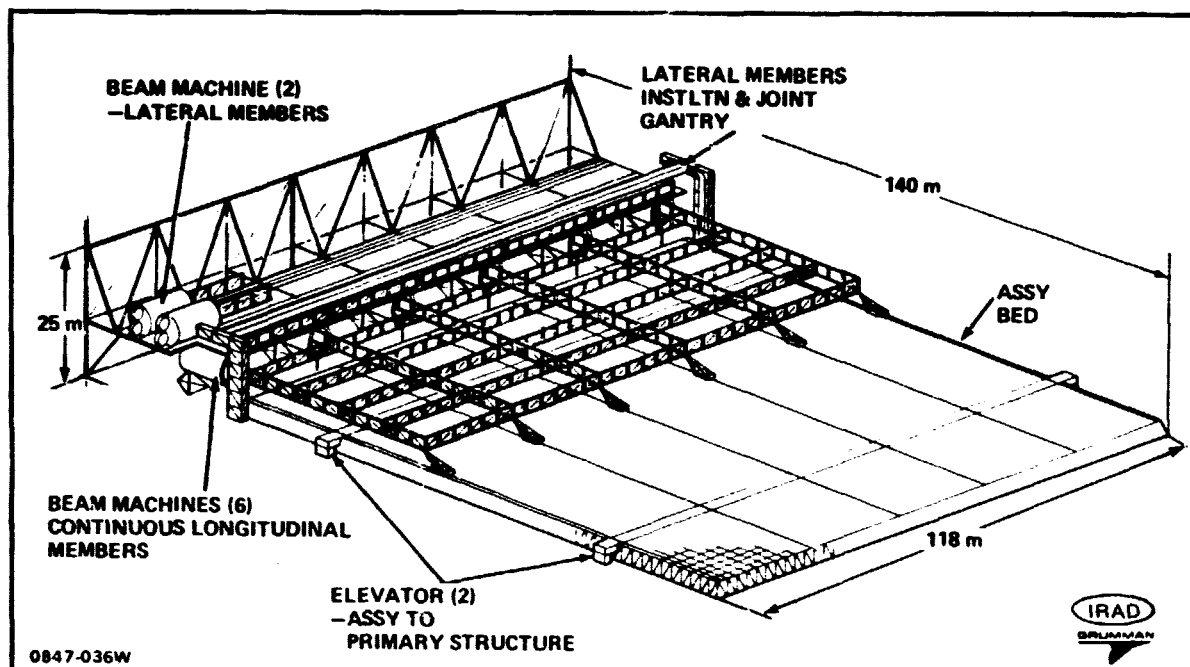
Figure 4-26 Secondary Structure Assembly Station

MISALIGNMENT SOURCES

- FABRICATION
  - STRUCTURE ELEMENT TOLERANCES
  - ASSY JIGS TOLERANCES
  - INDEXING BED FLATNESS

- CONTROL FORCES
  - INERTIAS RESULTING FROM BASE ATTITUDE CONTROL IMPULSES

- THERMAL EFFECTS
  - DISSIMILAR MATERIALS
  - BASE SHADOWING
  - LIGHT/DARK CYCLING

CANDIDATE SOLUTIONS

- ELECTRO OPTICAL ALIGNMENT SENSING

- LENGTH ADJUSTMENT ON STRUCTURE ELEMENTS

- SUFFICIENT INDEXING TIEDOWNS

- MAINTAIN CONSTANT ATTITUDE TO SUN
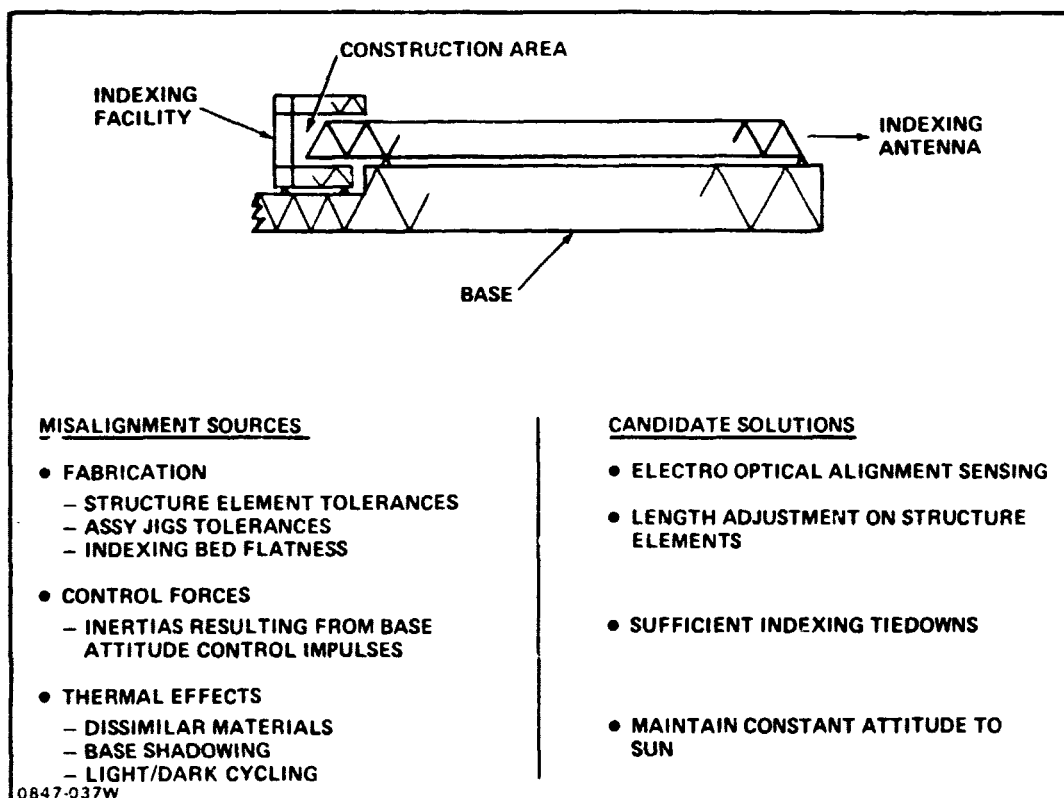
Figure 4-27 Antenna Flatness & Support Considerations

positioned. Two mobile 7.5 m beam builder substations, mounted on the joint facility, initiate fabrication of the outboard support struts. These stations align the beam fabrication with the collector-pickup point areas where cherry pickers mounted on the collector facility wait to capture and attach the fabricated struts to the collector attach fittings. The joint facility mobile cherry picker perform this same operation in attaching the strut end to the rotary joint pickup fitting. This procedure is repeated until all five outboard struts are installed. Next the base is re-indexed and the joint facility is repositioned to fabricate and install the four center struts. After the struts have been installed the solar collector power buses are routed along and attached to these struts and final power bus hook-up is made between antenna and collector. With the power bus installation completed, the base and yoke facility are again relocated to align with the five remaining strut pickups and the operations are repeated for the fabrication and installation of these antenna support struts. The remaining operations are those for final satellite checkout. Figures 4-29 and 4-30 illustrate the stowed position of the antenna assembly facility during the final systems mating operation. These figures also illustrate the lateral indexing required between the antenna and the base, and between the base and the satellite energy conversion system.

4.2.2 Construction Equipment

Construction equipments for building the solid state antenna are similar to those for building the baseline, but they differ in sizes and quantities. Figure 4-31 identifies these changes. Redesigned primary structure affects numbers and sizes of beam builders. The heavy increase in the number of cherry pickers is due to the shorter time available to build each SPS when striving for a production goal of 10 GW per year. Due to the lower operating voltage of the solid state system, the power bus in the energy conversion system is much wider (250 m vs 75 m) and thus requires more bus deployers. As a result, the total equipment used for constructing the Solid State SPS is heavier than the reference equipment listing (481.1 MT vs 460 MT). It also requires a higher investment cost to begin construction operations ($2251M vs $1800M).

4.2.3 Net Impact of Solid State SPS on GEO Base

Comparison of the estimates on GEO base structure, mass and cost are shown in Figure 4-32 for the reference SPS and for the solid state option. The major difference between these 4 Bay End Builder construction bases lies in the geometry, arrangement and support of their respective antenna construction platforms. While these platforms are located at different levels on each base, they are both attached to the support

- INSTALL ANTENNA/ROTARY JOINT INTERFACES
- INDEX BASE TO SOLAR COLLECTOR PICKUP
- INDEX ANTENNA TO ALIGN WITH COLLECTOR
- POSITION ROTARY JOINT FACILITY TO FAB & INSTALL ONE SET OF SUPPORT STRUTS

- RE-INDEX BASE & REPOSITION ROTARY JOINT FACILITY TO FABRICATE & INSTALL REMAINING SUPPORT STRUTS
- INSTALL POWER BUS.
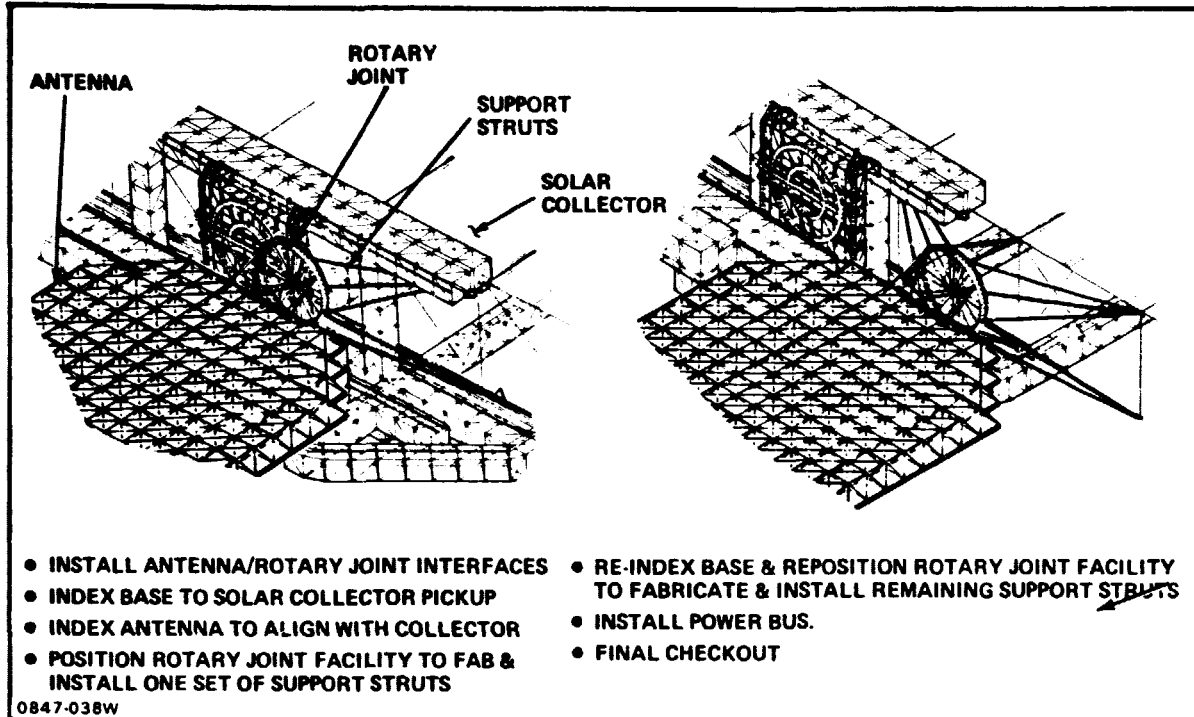- FINAL CHECKOUT

0847-038W

Figure 4-28 Final Systems Mating Operation

0847-039W
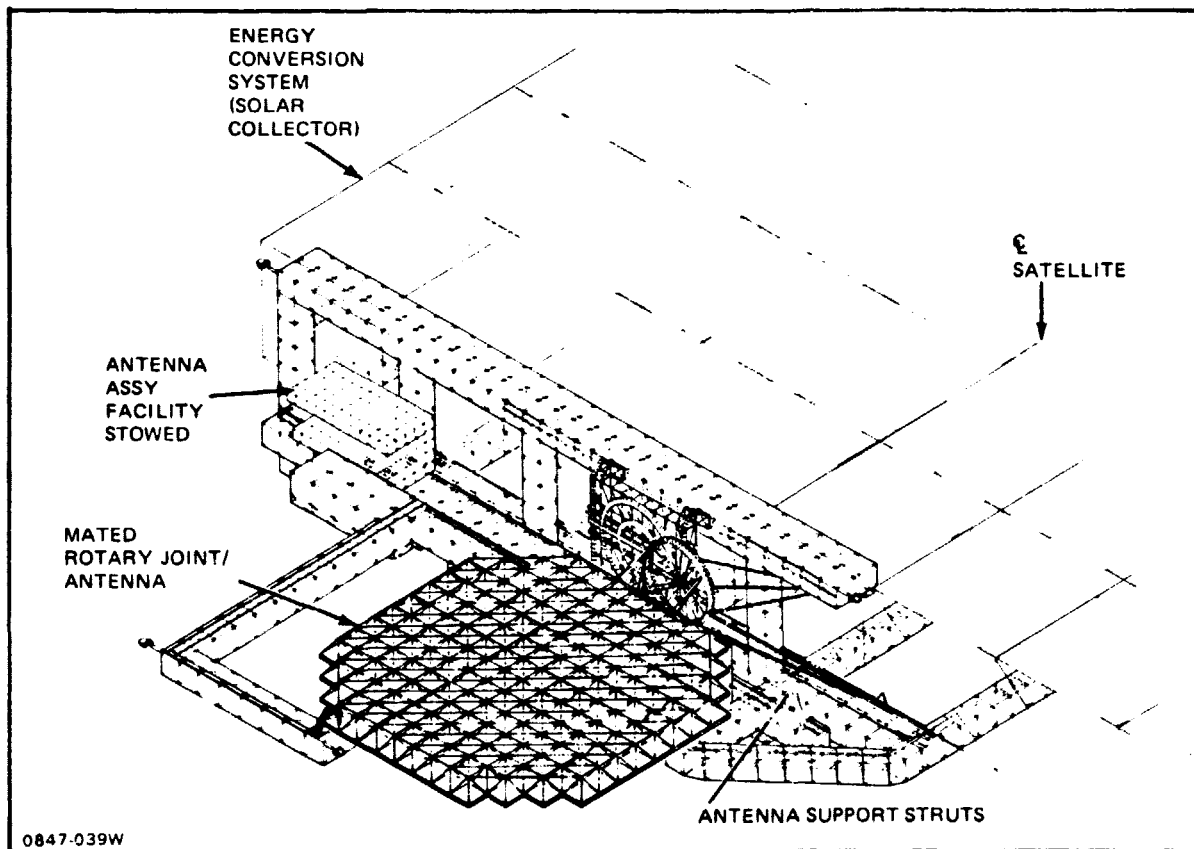
Figure 4-29 Final Systems Mating
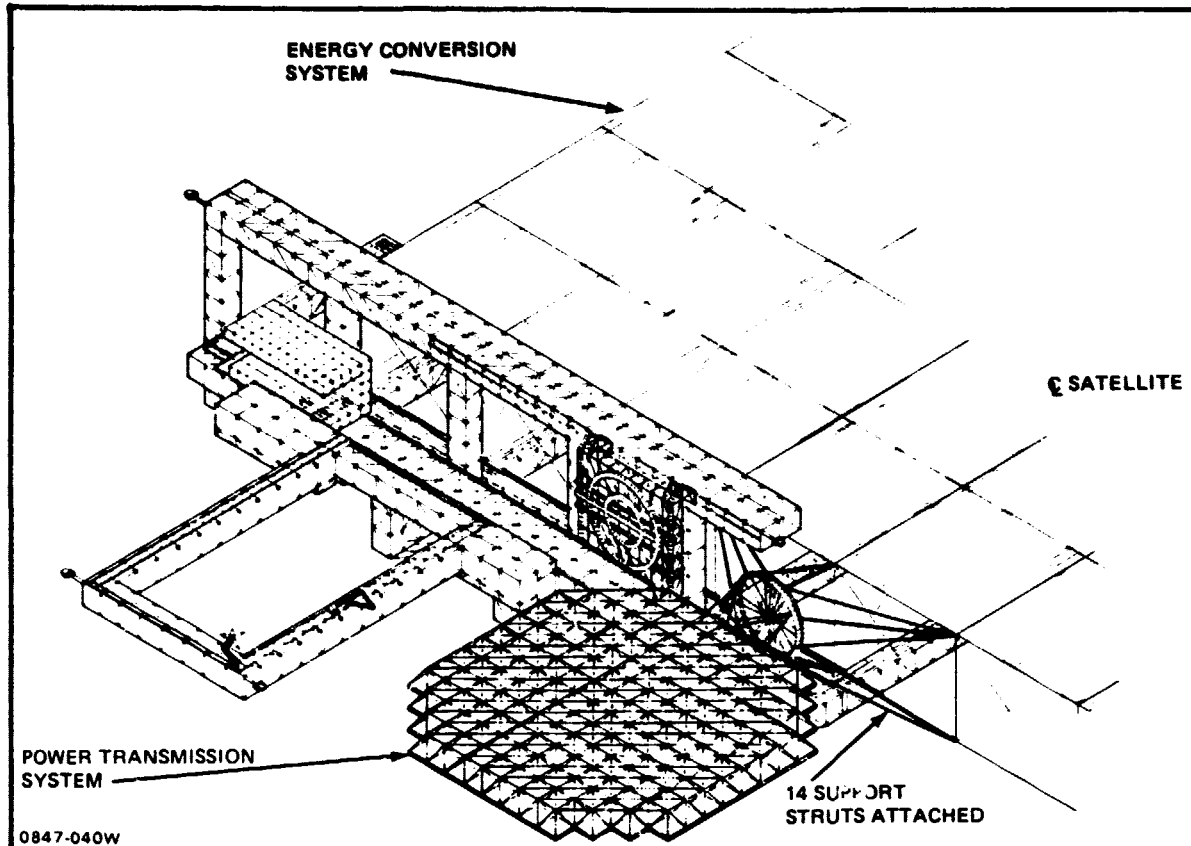
Figure 4-30 Satellite Systems Mated

EQUIPMENT	5 GW BASELINE	2.5 GW SOLID-STATE	RATIONALE
• BEAM BUILDERS			
1.5 m MOBILE MANNED	–	3	PH-2 VS PH-1 DEFN
7.5 m MOBILE MANNED	2	–	
• CHERRY PICKERS			
30 m	–	17	MPTS ASSY & SOLAR ARRAY
90 m	2	–	
120 m	2	–	
150 m	–	1	
250 m	1	–	
• INDEXERS			
45 m ⎫	–	5	
130 m ⎬ SINGLE SUPPORT	6	–	
230 m ⎭	2	–	
20 m ⎫ MULTI SUPPORT	–	2	ASSY FACILITY
70 m ⎭	–	2	INDEX REQ
BUS DEPLOYERS			
– ENERGY CONV BUS	1	3	LOWER VOLTAGE REQ
– ANTENNA BUS	1	1	
ANTENNA DEPLOYMENT PLATFORM	1	–	
SECONDARY STRUC ASSY SUBSTA		1	
SUBARRAY DEPLOYERS		3	

Δ MASS = +21.1 MT
Δ COST = $+451M

Figure 4-31 Solid State SPS Construction Equipment Comparison

structure shared by the rotary joint assembly facility. At this stage of concept development, the solid state SPS construction base is somewhat lighter than the reference GEO base. The alternate solid state antenna construction platform could also be modified to build the smaller reference antenna (1.0 km vs 1.4 km diameter). If that were done, the modified reference base would then be lighter than the solid state construction base shown.

The impact of Solid State SPS construction on the reference GEO base mass, cost and productivity, is shown in Figure 4-33. Reference base work facilities were revised primarily for the solid state antenna construction operation. Due to the alternate antenna construction approach, less structure is needed for the base. However, to strive for the 10 GW annual production goal, additional construction equipment and operating crews are needed. It is estimated that reference construction crew (444) must be increased by 47 people, which necessitates an additional 17 m dia habitat. The net effect increases the initial mass of the reference base by 122 MT. Investment cost and annual operations costs also increase as shown. For the solid state SPS construction base defined, it was not practical to accelerate the antenna assembly operation further to complete construction in less than 1 . days. Consequently, productivity of the solid state SPS construction base is 86.5% of the reference. It is possible, however, that another more highly automated antenna facility could have built the entire solid state satellite in the desired time. This remains as an area for future study.
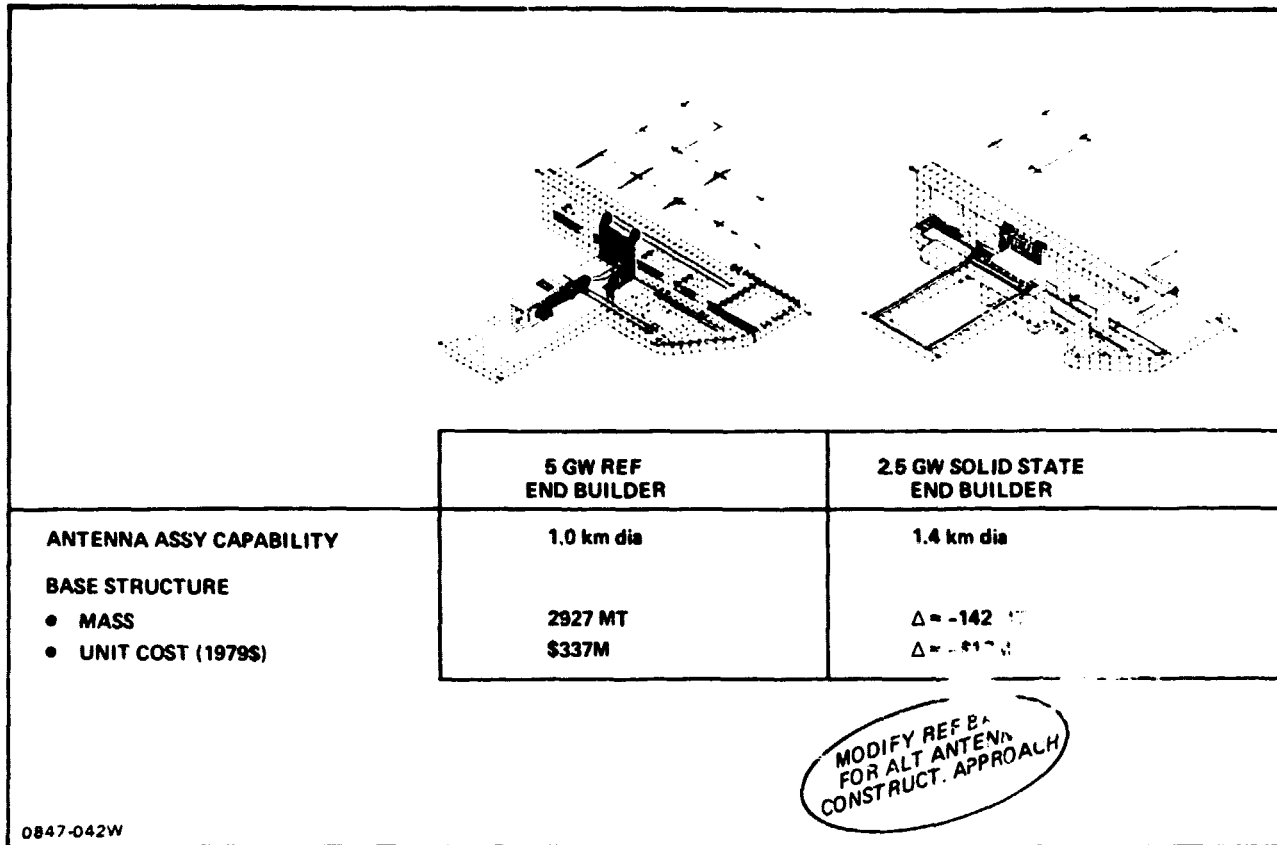
	5 GW REF END BUILDER	2.5 GW SOLID STATE END BUILDER
ANTENNA ASSY CAPABILITY	1.0 km dia	1.4 km dia
BASE STRUCTURE		
● MASS	2927 MT	Δ = -142
● UNIT COST (1979$)	$337M	Δ = -$1

MODIFY REF B
FOR ALT ANTENN
CONSTRUCT. APPROACH

0847-042W

Figure 4-32 Solid State SPS GEO Base Structure Comparison

BASE PRODUCTIVITY
- SOLID STATE SPS = 8.65 GW/YR
- REFERENCE SPS = 10 GW/YR

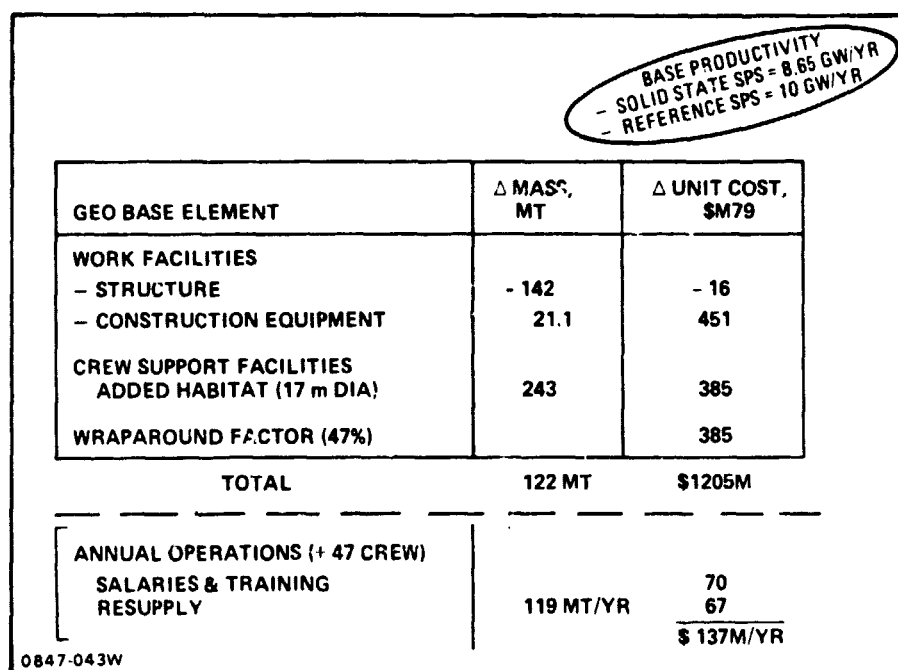| GEO BASE ELEMENT	Δ MASS, MT	Δ UNIT COST, $M79
WORK FACILITIES		
– STRUCTURE	- 142	- 16
– CONSTRUCTION EQUIPMENT	21.1	451
CREW SUPPORT FACILITIES ADDED HABITAT (17 m DIA)	243	385
WRAPAROUND FACTOR (47%)		385
TOTAL	122 MT	$1205M
ANNUAL OPERATIONS (+ 47 CREW) SALARIES & TRAINING RESUPPLY	119 MT/YR	70 67 $ 137M/YR

0847-043W

Figure 4-33 Solid State SPS Construction Base Impacts

5.0 OPERATIONAL FACTORS

The solid-state SPS system exhibits a number of operational differences compared to the reference system. These are summarized in Figure 5-1. Most are minor. Because the power per rectenna is halved, twice the number of rectennas are needed to deliver the same total power. Each rectenna site, however, uses only slightly more than half as much land as is required for the reference rectenna. The total land use is about the same, but it is used in more, smaller parcels.

Differences in space operations are modest and derive mainly from the somewhat greater SPS mass and construction effort per megawatt for the solid-state system. Note that the estimated maintenance requirements are much less. This is because the maintenance effort for the reference system is largely Klystron replacement. The estimated reliability of the solid-state transmitter is roughly an order of magnitude greater than for the reference transmitter.
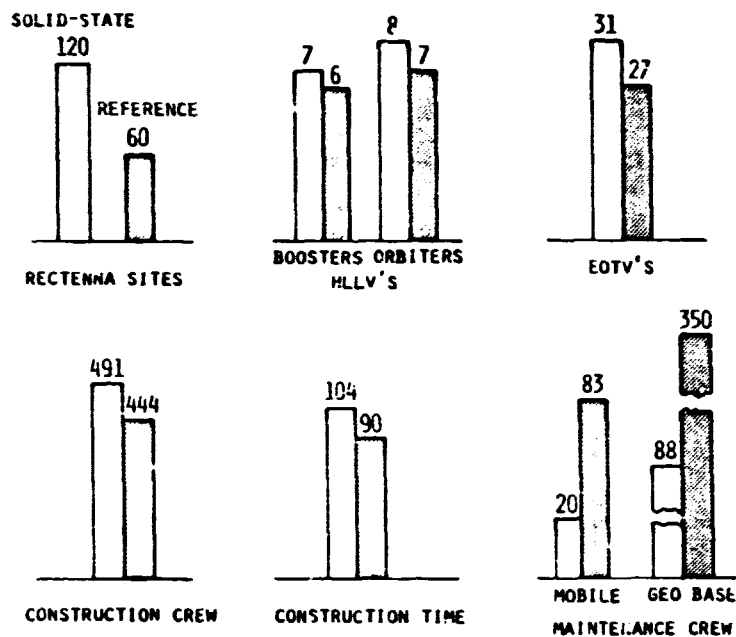
Figure 5-1 Solid State SPS Operational Factors

64

6.0 NEW TECHNOLOGY REQUIREMENTS

The main research and development items unique to the solid state SPS are:

o   Efficient dc-rf amplifiers (efficiency over .8);

o   A high-voltage module or a high-voltage series/parallel module arrangement;

o   Mass production and manufacturing techniques for the above modules and amplifiers;

o   Very well characterized failure and wear out properties of solid state dc-rf power amplification devices.

With the exception of the characterization of failure and wear out properties of the solid state amplifiers, all the above R and D items are already included in the SPS Phase II Record Planning and Interim Report (Boeing Document D180-25381-1). It is recommended that this final item be incorporated in future revisions of this document.

7.0 2.5 GW SOLID STATE SPS SUMMARY

7.1 Masses and Costs

Table 7.1-1 shows the masses and costs estimated for the Phase III solid state SPS. Figures 7.1-1 and 7.1-2 provide mass and cost comparisons with the 5 GW klystron reference satellite and the Phase II solid state SPS. Note that the main improvement over the Phase II results is due to the smaller solar array required by the more efficient 8.64 kv electrical conductors used in Phase III. The other substantial change, the cavity combining antenna radiator module configuration and overall module mass growths affected the microwave transmitting antenna matter and costs slightly (circa 10%) upward.

The resulting recurring costs for a 2.5 GW solid state SPS are shown on Table 7.1-2. These show a small reduction in cost from Phase II because of the mass and size reduction in the overall satellite.

7.2 Device Operating Temperature as an Operational Issue

While a solid state SPS can apparently be designed to have very low operational component failure rates, economics does dictate that the devices be operated at as high an RF power level (and herefor at as high a temperature) as possible. As Figure 7.2-1 illustrates, mean time to failure of solid state devices of a strongly decreasing function with temperature. This implies that the operational characteristics of this system are such that it is less robust with regard to overload operation above nominal power ratings, because a short time of overload operation can reduce the total lifetime of the system appreciably. Much the same effect might be expected regarding charged particle radiation damage - i.e., a few bad events might take the system down.

It is likely that an operational strategy of monitoring device failures closely, using statistical analysis to spot failure trends early, taking advantage of detailed DC-RF conversion device characterization and applying corrective actions when necessary can be successfully formulated. In some sense the requirement for this is sophisticated monitoring the price one pays for the reduced solid state system maintenance costs vis-a-versa the klystron reference system.

7.3 Sandwich Configuration Analysis

The analysis here, done in Phase II, explains why a conventional solid state SPS is favored. A new and fundamentally different power satellite design, the "solid state sandwich" has been introduced by workers at MSFC. (See Figure 7.3-1). The basic idea behind the design is to put DC-microwave conversion elements and solar cells on opposite sides of the same surface, and use optical reflectors to satisfy illumination geometry requirements.

The greatest advantage of the sandwich design is that the close proximity of the generation of DC electrical power (by solar cells) and its conversion to microwaves (by the DC-RF convertors, assumed to be solid state) allows power bussing low voltages without excessive conductor loss. Also, the electrical rotary joint in conventional power satellite designs is eliminated, although other mechanical joints are still necessary. In the event that effects of plasmas on high voltage surfaces on reference SPS designs turn out to be intractible, sandwich satellites may offer a way out.

SPS-3040	MASS (MT)	ESTIMATING BASIS	(COST $M)
L.1 SPS	30,301		3,890
L.1.1 ENERGY CONVERSION	17,037		1,662
L.1.1.1 STRUCTURE	2,333	Detailed Estimate	225
L.1.1.2 CONCENTRATORS	(0)	Not Required	(0)
L.1.1.3 SOLAR BLANKETS	12,027	Scaled from Reference	1,131
L.1.1.4 POWER DISTRIB.	2,250	Detailed Estimate	116
L.1.1.5 THERMAL CONTROL	(0)	Allocated to Subsystems	(0)
L.1.1.6 MAINTENANCE	427	Scaled from Reference	190
L.1.2 POWER TRANSMISSION	7,296		1,289
L.1.2.1 STRUCTURE	460	Scaled from Reference	38
L.1.2.2 TRANSMITTER SUBARRAYS	6,673.0	Detailed Estimate	1,097
L.1.2.3 POWER DISTR. & COND.	631.0	Scaled from L.1.1.4	70
L.1.2.4 PHASE DISTR.	25	Scaled from Reference	51
L.1.2.5 MAINTENANCE	20	Docking Ports Only	20
L.1.2.6 ANTENNA MECH. POINTING	118	Scaled by Mass x Area	13
L.1.3 INFO MGMT & CONTROL	145	Scaled from Ref.	73
L.1.4 ATT. CONT. & STA. KP.	146	Scaled From Ref	13
L.1.5 COMMUNICATIONS	0.2	Same as Ref.	8
L.1.6 INTERFACE	113	Est. Based on Simplification	46.3
L.1.7 GROWTH & CONTINGY.	5,464	Same % as Reference	701

Figure 7.1-1. Phase III Solid State SPS Mass & Cost Summary
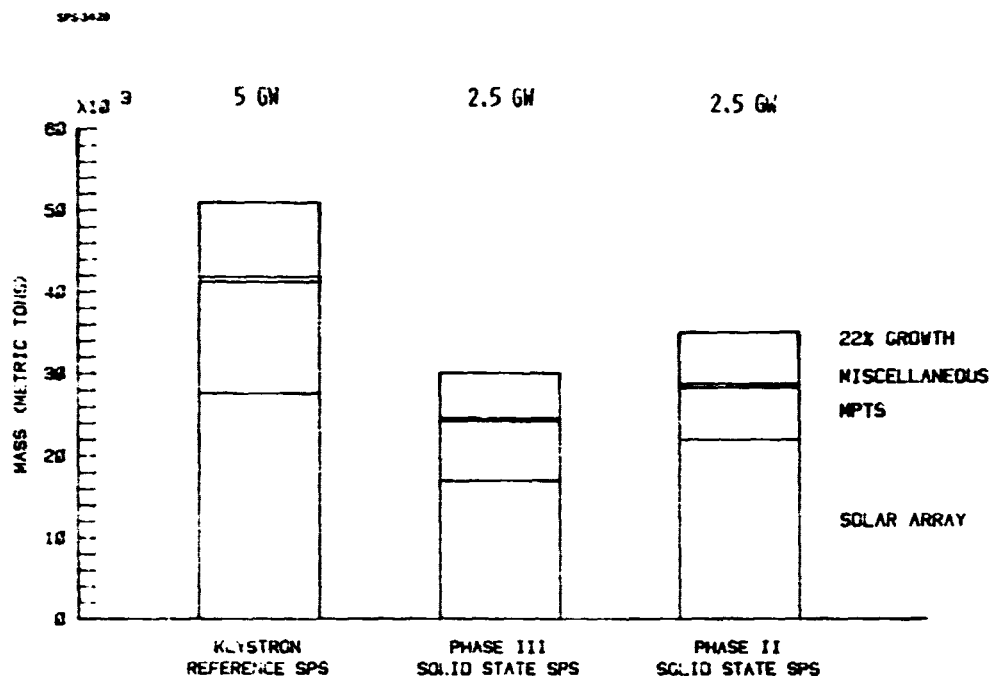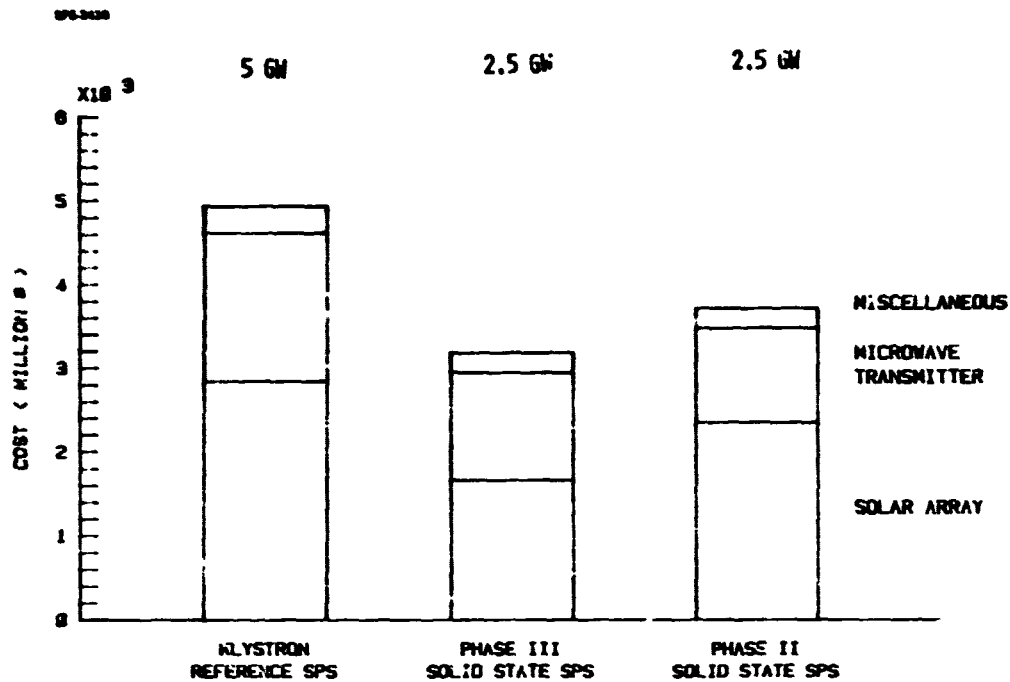

Figure 7.1-1. SPS Mass Comparisons

Figure 7.1-2. SPS Cost Comparisons

Table 7.1-2. Phase III 2.5 GW Solid State Satellite System Recurring Costs

ITEM	COST ($M)
SATELLITE	3,189
LESS IMPLICIT AMORTIZATION	280
	2,909
CONSTRUCTION AND SUPPORT	587
SPACE TRANSPORTATION	1,855
GROUND TRANSPORTATION	20
RECTENNA	1,290
MISSION CONTROL	10
MGMT AND INTEGRATION	385
MASS GROWTH (17% Net Hardware)	495
TOTAL DIRECT OUTLAY	7,551
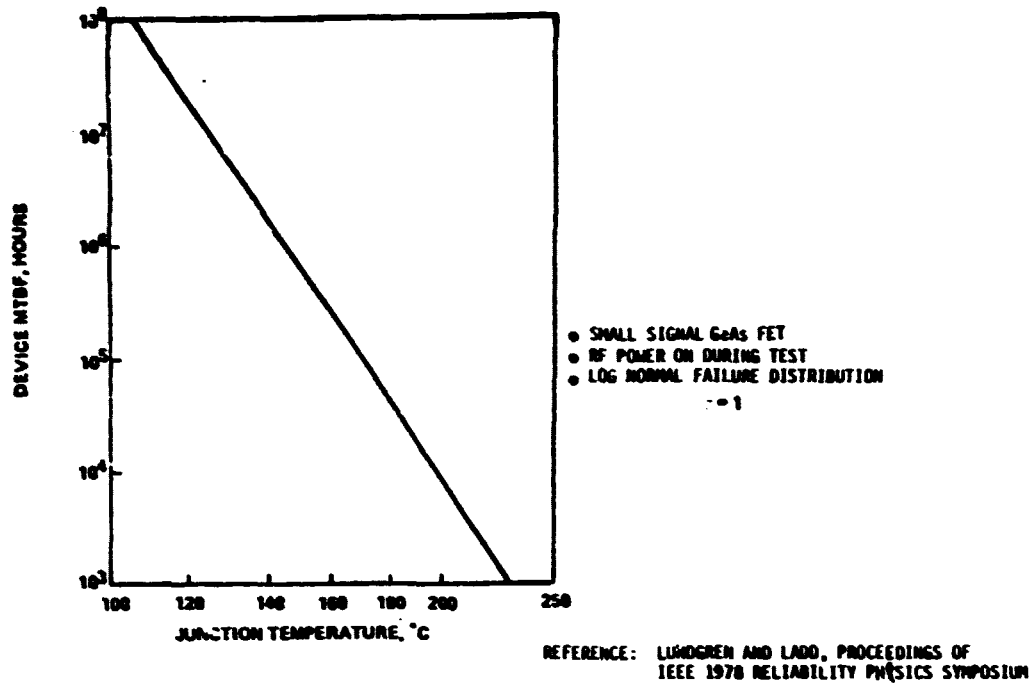
Figure 7.2-1. Solid State Device Lifetime

ADVANTAGES
- ELIMINATES POWER DISTRIBUTION & PROCESSING (AT LEAST MOST OF IT)
- ELIMINATES HIGH VOLTAGES
- ELIMINATES ELECTRICAL ROTARY JOINT
- MAY BE ADAPTABLE TO LARGE APERTURE, LOW POWER SYSTEMS

PROBLEMS
- THERMALLY-CONSTRAINED DESIGN
- HOW TO IMPLEMENT ILLUMINATION TAPER?
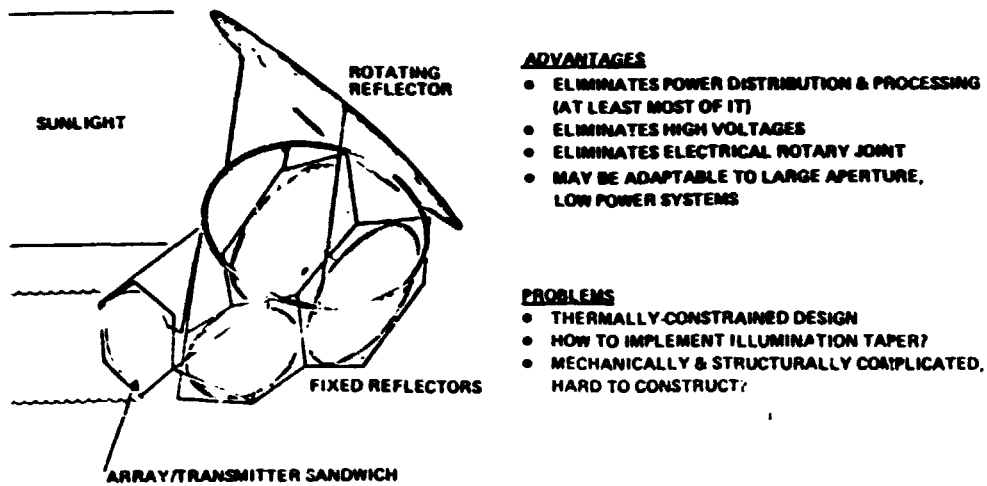- MECHANICALLY & STRUCTURALLY COMPLICATED, HARD TO CONSTRUCT?

Figure 7.3-1. The Solar Cell Solid-State Sandwich SPS Concept

The placing of solar cells and DC-RF convertors in the intimate proximity implicit in sandwich power satellite designs increases normal thermal constraints on RF power density. The reason for this is that the maximum microwave power output per unit area, $(P/A)_{RF}$ from a surface able to dissipate heat per unit area, $(\dot{Q}/A)$, is related to its power conversion efficiency, e, by the oft - seen equation:

$$(P/A)_{RF} = e \, (1-e)^{-1} \, (\dot{Q}/A).$$

In a conventional power satellite (with separate transmitting antenna and solar array) is the DC-RF conversion efficiency, which is expected to have typical values of around 8. On a sandwich power satellite, however, e is the product of the DC-RF conversion efficiency and the solar cell efficiency, given values of less than .2 with present cells. Thus, if the achievable $(\dot{Q}/A)$ is the same for both a sandwich and a conventional power satellite, the sandwich's peak $(P/A)_{RF}$ would be over a factor of 16 lower than the conventional design's. When this difference is integrated into a system design, large aperture (circa 2 km diameter), lower power (1GW), designs result. These designs have a large relative fraction of transmitting array per unit RF power with a severe (x3) attendant cost penalty. The designer's basic goal is to reduce this with either low-cost aperture area (as being proposed by RCA) or by using system design and configuration "tricks" which use the aperture more effectively.

Figure 7.3-2 shows cost per unit installed grid power, delivered power and true concentration ratio as a function of temperature, as given by the initial parametric analysis reported in Appendix 1 of Phase II Monthly Progress Report 2. The satellite configuration for this analysis was a sandwich with uniform power taper and conventional GaAs or Si solar cells illuminated by a full solar spectrum.

Figure 7.3-2a shows that silicon cells are ruled out for sandwich use due to their efficiency degradation with temperature, resulting in costs over $10,000/kw$_e$. Sandwich satellites with GaAs cells retain more performance but need to operate at high temperatures to match conventional satellite costs. Feasibility of such high temperature operations seems unlikely but needs further investigation.

If one sandwich layer can operate at higher temperatures than the other layer, insulating properly may minimize thermal output while maintaining design temperatures. While insulation may be the correct thing to do to minimize performance of a sandwich satellite design, the possible performance gains are limited for the following 3 reasons.

1. Solar cells are typically made of the same semiconductor materials as solid state DC - microwave devices and thus should suffer from roughly the same fundamental failure mechanisms. For GaAs FETs lifetime goes down roughly a factor of 10 every 25°C. However, at 125°C it takes 75°C to double the radiated thermal power per unit area.

2. Placing solar cells and DC - microwave devices on opposite sides of the same plane cuts the available thermal radiating surface in half relative to separate arrays.

3. Insulation inevitably adds to system assembly complexity, mass and, most importantly, cost. One of the most attractive possible features of a sandwich design - the integration of solar array with transmitting array into a single trivially deployable unit, may now be lost.

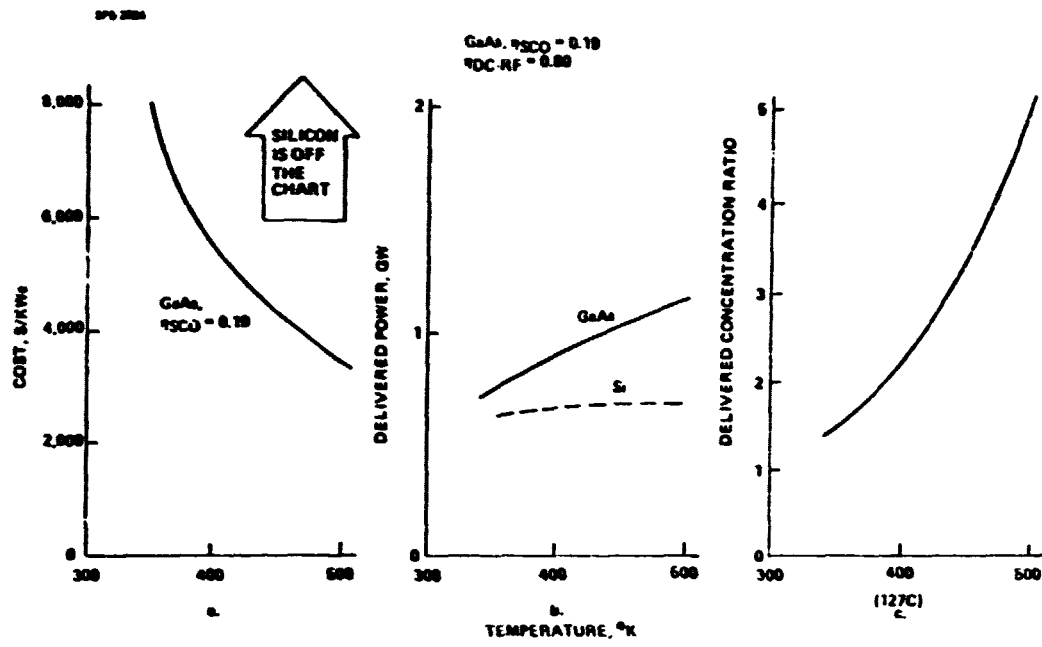Further investigation of the insulating option is needed, however, to quantify these objections.

Figure 7.3-2. Performance vs Sandwich Temperature

If selective reflectors are used to illuminate the solar cells on the sandwich with only light that they may efficiently convert, solar cell efficiency may approach the ratio of junction voltage to band gap voltage. This parameter is typically near .5, so $1/(1-e)$ approaches 1. This value is down from $1/(1-e) = 4$ for a conventional satellite design, but may nevertheless make for a solar power satellite with costs per unit installed power roughly equivalent to the reference klystron type satellites.

Figure 7.3-3a shows cost and concentration ratio as a function of solar cell efficiency for both a selective concentrator satellite and a probably unrealistic, low cost multiple bandgap solar cell. The resulting satellite geometry for the selectively concentrating satellite is shown on Figure 7.3-3b. In the analysis structural mass fraction changes for such drastic configuration stretches were not explicity addressed. However, reflector masses and costs per unit have a structural penalty added to them to allow simple first-order parametric analysis.

For environmental and microwave safety reasons all realistic power satellite system designs have some degree of transmitting array power taper. Sandwich satellites will not be an exception to this rule. Two options for the implementation of power taper are either conducting power radially inward in the sandwich plane . either shaping or cutting small holes in the reflectors. Both will raise costs an as . unevaluated amount.

Figure 7.3-4 shows initial power conductor mass, thickness and radial current for a reference 10-step Gaussian taper and indicates that voltages in the kilovolt range, (substantially higher than 30 volts), are desirable for reasonable masses and costs. This is distressing in that it detracts from what may be the main advantage of a sandwich satellite - purely local power flow and power control at low voltages. The other option, power taper via reflectors, may be easier to implement. In either case, it is worth noting that for cases where the product of the aperture diameters is well over 10 km there are antenna patterns which meet the first side lobe constraint (24.6 db down) and yet have a significantly greater average/peak power ratio than the reference 10-step Gaussian taper.

7.4 Conclusion

A 2.5 GW ground output solar power satellite of conventional configuration has been designed and analysed. It appears to be feasible with a slightly greater specific mass than the klystron reference SPS design.
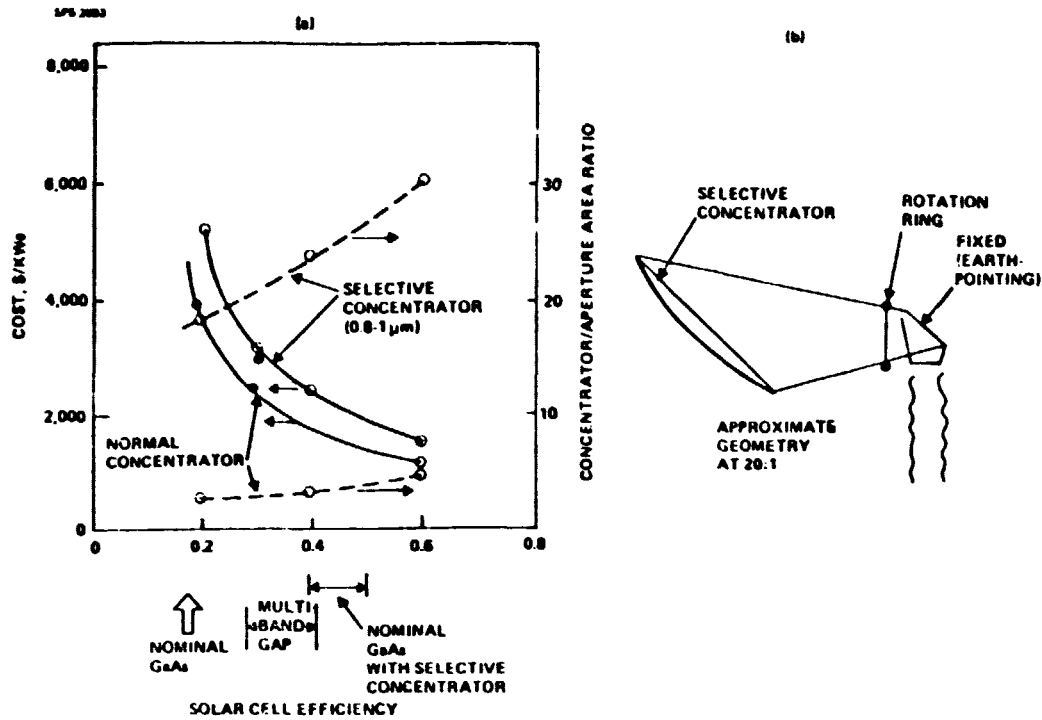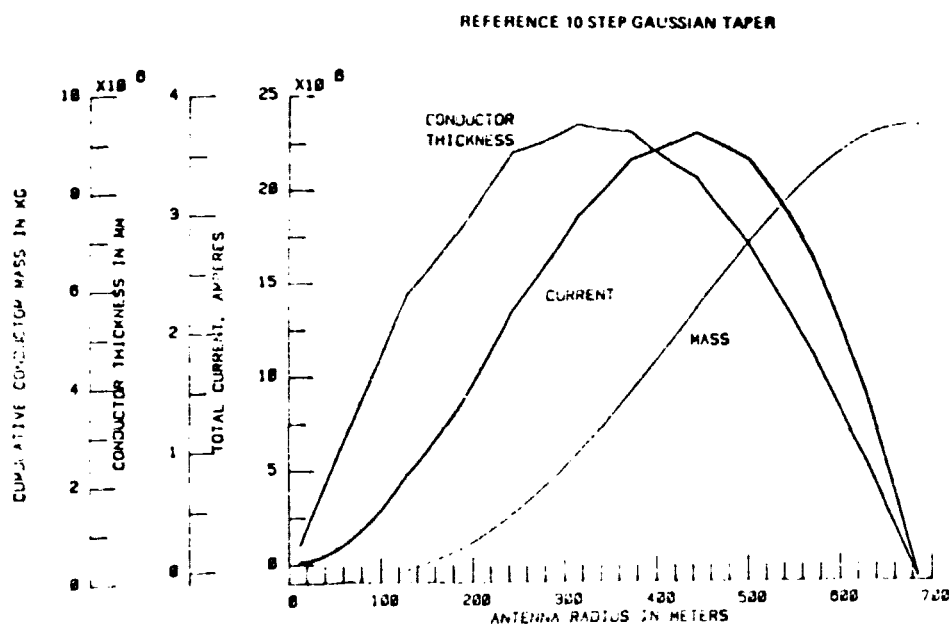
Figure 7.3-3. Performance vs Solar Cell Efficiency

Figure 7.3-4. 30 Volt Power Conduction Results